ANALYSIS OF STARTING PERFORMANCE OF AN INVERTER FED INDUCTION MOTOR

By

Ashikur Rahman Bhuiya

A thesis

Submitted to the department of Electrical and Electronic Engineering
in partial fulfillment of the requirements for the degree

of

MASTER OF SCIENCE IN ELECTRICAL AND ELECTRONIC ENGINEERING

BANGLADESH UNIVERSITY OF ENGINEERING AND TECHNOLOGY,
DHAKA

SEPTEMBER, 1994

Declaration

I hereby declare that this work has not been submitted elsewhere for the award of any degree or diploma or for publication.

6/9/94

Ashikur Rahman Bhuiya

The thesis titled "ANALYSIS OF STARTING PERFORMANCE OF AN INVERTER FED INDUCTION MOTOR" submitted by Ashikur Rahman Bhuiya Roll No. 901331P, session '88-89 to the Electrical and Electronic Engineering Department of B.U.E.T. has been accepted as satisfactory for partial fulfilment of the requirements for the degree of Master of Science in Engineering (Electrical and Electronic).

Board of Examineres

1. Dr. M. A. Choudhury
   Associate Professor
   Department of EEE
   B.U.E.T., Dhaka 1000
   Chairman *(Supervisor)* m a choudhury 6.9.94

2. Dr. Syed Fazl-i Rahman
   Professor and Head
   Department of EEE
   B.U.E.T., Dhaka 1000
   Member *(Ex-officio)* 6/9/94

3. Dr. Md. Mahmudur Rahman
   Assistant Professor
   Department of EEE
   B.U.E.T., Dhaka 1000
   Member m. Rahman 6/9/94

4. Dr. Kazi Khairul Islam
   Associate Professor and
   Head of Department of EEE
   BIT,Rajshahi
   Member *(External)* 6/9/94

ACKNOWLEDGEMENT

I wish to express my sincerest gratitude and indebtedness to Dr. Mohammad Ali Choudhury for his guidance, supervision and moral support throughout the entire period of the thesis work. His initiatives, encouragements, patience and invaluable suggestions are very gratefully acknowledged without which this work would not have been possible.

I wish to express thanks and regards to Dr. Syed Fazl-i Rahman, Professor and Head of the Electrical and Electronic Engineering Department, BUET for his encouragement and cooperation to complete this work successfully.

Sincere thanks are offered to Mr. Mohsin Mollah, Mr. Syed Saiful Islam and Mr. Shah Md. Kabir Sharif for their co-operation. They took great pain for me for which I am truely grateful to them.

Contents

LIST OF FIGURES

List of Tables

Abstract

This thesis investigates the starting performance of inverter fed induction motors. Smooth starting with good control is an important requirement for an induction motor. The major requirement of industries are soft start and variable speed of machine. This thesis shows how sine pulse width modulation (SPWM) can be used to achieve the above requirements. Theoretical as well as practical investigations were carried out to prove that SPWM inverter fed motors successfully fulfill the requirements. For present thesis work pwm inverter is selected. The waveform synthesis of pwm inverter is not simple. A simple technique of pwm inverter waveform synthesis is proposed and used for harmonic analysis in this thesis. The inverter waveforms were analysed using time domain analysis. Since conventional Fourier series method takes more computational time, the time domain method is used. For theoretical prediction d-q axes motor model has been used and Euler's method has been employed to solve the motor equations numerically. Frequency domain analysis takes more computational time because it solves motor equation for many harmonics. The method is inaccurate as frequency domain analysis has to truncate Fourier series to limit computational time. The inaccuracy may increase if pwm waveform is generated by asynchronous method. In asynchronous pwm, the modulated wave may or may not be periodic of fundamental frequency. This phenomenon causes subharmonics to be presented in the pwm wave which cannot be detected by usual Fourier series method. Time domain representation of inverter waveform and subsequent motor equations solution are free from these drawbacks.

CHAPTER 1

INTRODUCTION

Induction motors are the work horse of industries due to their robust and simple construction. These motors can be made completely sealed to operate in hazardous environments because they do not have brushes and commutators. Their only drawback was lack of speed controllability. In this respect dc motors played an important role before the advent of solid state converters. With the introduction of cycloconverters and inverters, ac motors, specially the induction motors became major competitors to dc motors where variable speed is a requirement. Variable speed operation of ac motors can be achieved by changing frequency of the supply, changing the poles and to some extent by varying the applied voltage. Cycloconverters and inverters are static converters which allow simultaneous voltage and frequency change. Cycloconverters are ac to ac converters having different voltage and frequency at the output, whereas, inverters are ac-dc-ac converters having the same criteria. The output voltage and frequency of cycloconverters are limited to a maximum of supply frequency and voltage. As a result they are used in slow speed large ac drives. On the other hand in an inverter, frequency is limited by switching frequency of static devices of the converter only. Hence inverters are used both in slow and high speed drives. The main advantages of variable speed drives are their operation at maximum efficiency with varying load and for resizing of motors. Also starting of ac machines at variable voltage and frequency acts as electrical and mechanical starter for the machine. Low voltage supply at the start ensures low starting current of machines, whereas, low frequency ensures low speed during start up, minimizing breakage of shaft due to excessive torsion which is prevalent during ON line start. This thesis is aimed at time domain analysis

of starting performance of inverter driven induction motors. Reported works used superposition of motor's response to harmonics to obtain start up performance of inverter fed induction motors. The method is computationally involved and time consuming. It is also inaccurate as it truncates terms of Fourier series and also fails to predict subharmonics which are inherent in the waveforms due to simultaneous presence of modulating and carrier frequency. The harmonic analysis of pwm waveforms by Fourier series method is not accurate if the waveforms are not periodic of fundamental frequency. This thesis is directed towards inverter waveform analysis representing waveforms in time domain and incorporation in the inverter-fed motor performance study. Harmonic analysis of inverter waveforms is also carried out by Fast Fourier transform (FFT) using a commercial software. The start up response includes representation of inverter voltage in d-q axis, machine modeling in d-q axis and the solution of inverter-machine equations using numerical technique.

1.1 REVIEW OF STATIC CONVERTER FED INDUCTION MACHINES

The speed of an induction motor is dominantly governed by synchronous speed, slip of the motor and applied voltage. The usual methods of speed control of induction motors are,

- Constant frequency stator voltage control
- Variable voltage variable frequency control
- Variable current variable frequency control
- Slip power regulation.

A.C. voltage controllers are used in application like single phase fractional horse-power drives, in speed control of pump, fan and motors and as solid state starters for medium to large horse power motors. These controllers produce harmonics in the supply line and are characterized by inefficient operation and poor power factor. Because of these disadvantages use of ac voltage controllers for speed regulation of large motors are limited. As the technology developed, static voltage source inverters were introduced for controlling the speed of induction motors. Inverters achieve speed control by changing the frequency of supply. There are two different types of voltage source inverters, square wave and pulse width modulated (pwm) inverters. Square wave inverters were introduced in the 1960s with the innovation of forced commutation technique of silicon controlled rectifiers. Technological advances made possible the use of power transistors and gate turn off (GTO) thyristors as power switches in inverters[1]. Besides voltage source inverters, induction motors can also be supplied from current source inverters.

The most commonly used static converter for a drive system at present is the variable frequency dc link inverter. Variable frequency drives are found in machine tools, textile, paper and steel mill equipments. In most variable frequency ac drives, constant voltage to frequency (v/f) ratio is maintained upto the rated frequency of the motor and stator voltage is maintained at the rated value as the frequency is increased further. Failure to maintain a constant volts/hertz (v/f) ratio affects the output and can cause increase in stator current overheating the motor.

The output of normal square wave inverters have high harmonic contents and they are problematic when operated over a wide range of frequency such as 10 to 200 hz., as filtering is not practical because of the wide range of frequency. The disadvantages of square wave invertes are high harmonic losses and torque pulsation in motors, poor line side power factor, harmonic interference and requirement of dual

power conversion for simultaneous voltage and frequency change [1].

Various techniques have been introduced to improve waveforms of inverters in the past. One such technique is the pulse width modulation (pwm) control. In this method, the switching devices of an inverter are switched ON and OFF many times within a half cycle in order to generate a variable voltage variable frequency supply. The output waveforms of a pulse width modulated inverter has insignificant low order harmonics. PWM control also provides constant v/f ratio of supply and reduces filter size of the applications.

1.2 DRIVE DURING START UP

The starting condition of induction motor is influenced by electrical and mechanical transients. During start, machines draw high currents and speed up quickly. Electrical transient may damage a motor winding, whereas, the mechanical transient may result breakdown of the shaft. The loads experience tremendous torsion on their shaft during starting periods and fail to respond to the fast speed of the motors. A survey of literature shows that the major failures in the form of broken shafts of these units are due to the electromechanical problems during starting periods [2].

The high starting current is reduced by motor connections or by supplying reduced voltage to the system. Mechanical stress during start is limited by controlling speed by reduced frequency of the supply.

Variable voltage variable frequency operation of ac motors by static converters re-

duce starting stresses of motors. Converter fed motors also provide operations at near optimum efficiency at variable loads. Non-compatibility of load is a major problem of motors. Motors are installed to run with certain loads at near optimum efficiency of operation. This operating condition cannot be maintained during the continuous production cycle. Loads may change due to change in economic or operating condition. In such circumstances two scenarios may prevail. The total system is replaced by a new one or the system is run below the recommended operating range. Variable speed drive may, however, adjust to new operating condition at near maximum efficiency without change of motors.

The followings are the requirements of inverter fed drives,

- Reduced harmonics
- Constant voltage to frequency ratio
- Reduced starting current
- Reduced starting speed.

A sine pulse width modulation inverter fed induction motor meets the above requirements of an ac drive.

1.3 REVIEW OF PWM TECHNIQUES

In many industrial application it is often required to control the output voltage of inverters

- to cope with the variations of dc input voltage,
- for voltage regulations and
- for constant volts/frequency ratio of supply.

PWM inverters are used in a wide variety of industrial processes such as uninterruptable power supplies, static frequency changers and variable speed drives. The popularity of pwm inverters is mainly due to their capability to control voltage, frequency and harmonic contents in a single power state. The disadvantages of the normal voltage source and current source inverters have lead to the developments of pulse width modulated converters. In the pulse width modulation technique the switches of the power converters are operated at higher frequencies in a particular pattern so as to produce pulses of varying widths at the output of the inverter. The earliest modulation techniques were single pulse modulation and multiple pulse modulation [3-10,11-15].

In single pulse-modulation there is only one pulse per half cycle and the width of the pulse is varied to control the inverter output voltage. Fig. 1.1(ii) illustrates the generation of gating signals and output voltage of a single phase full bridge inverter. The gating signals are generated by comparing a rectangular reference wave of amplitude A_r with a triangular carrier wave of amplitude A_c. The frequency of the reference signal determines the fundamental frequency of the output voltage. By varying A_r from 0 to A_c, pulse width can be varied from 0 to 180^o . In single pulse modulation dominant harmonic is the third and distortion factor increases significantly at low output voltage. The harmonic contents can be reduced by using several pulses in each half cycle of output voltage. The generation of gating signal for turning ON and OFF the inverter switches in multiple pulse modulation are shown in fig. 1.2. The frequency of the reference signal sets the output frequency

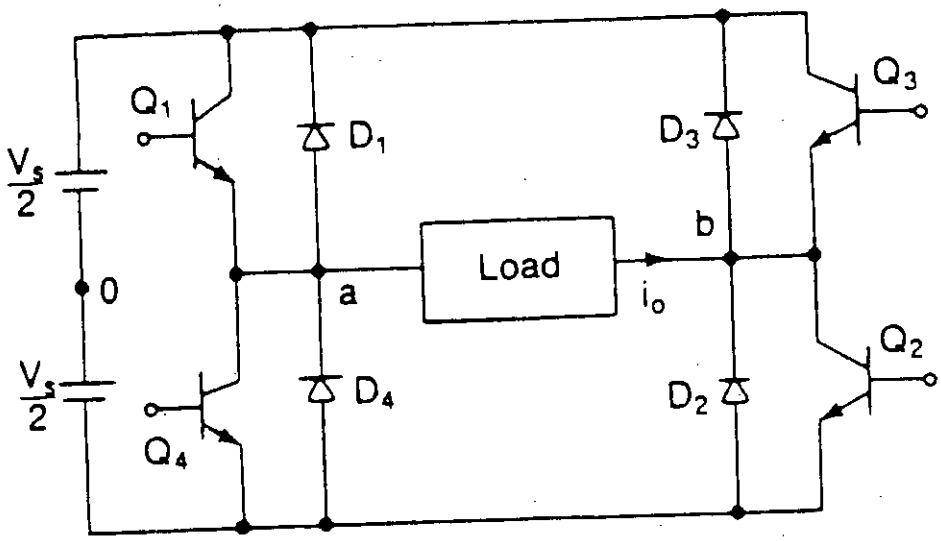

Fig. 1.1 (i) single phase bridge inverter

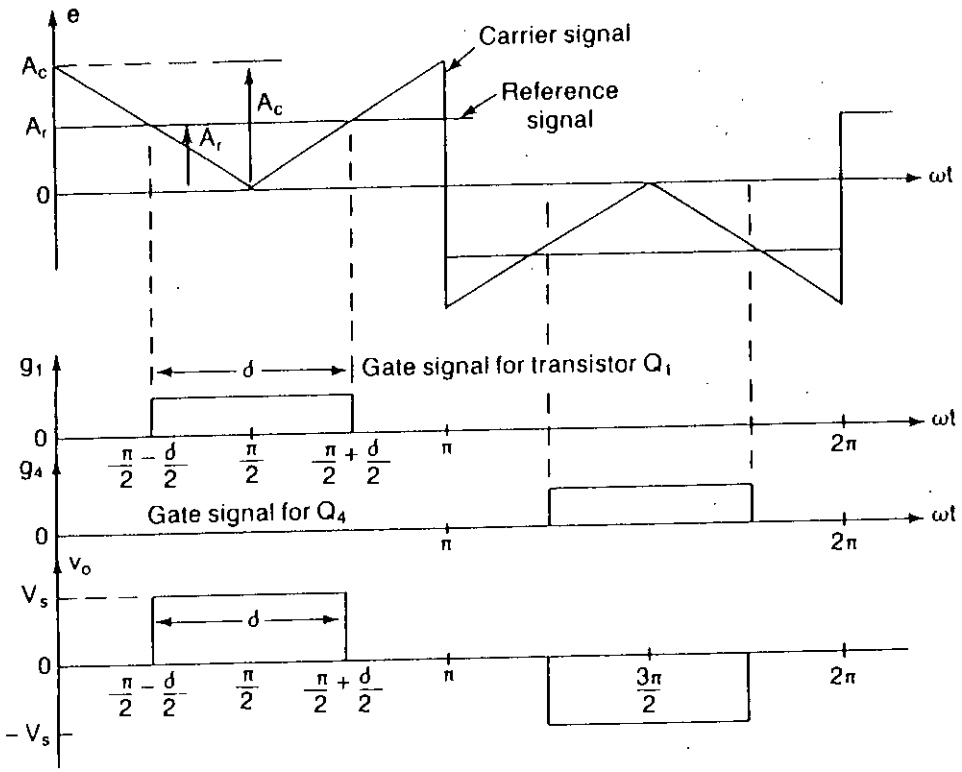

Fig. 1.1 (ii) Illustration of single-pulse width modulation for inverter switching.

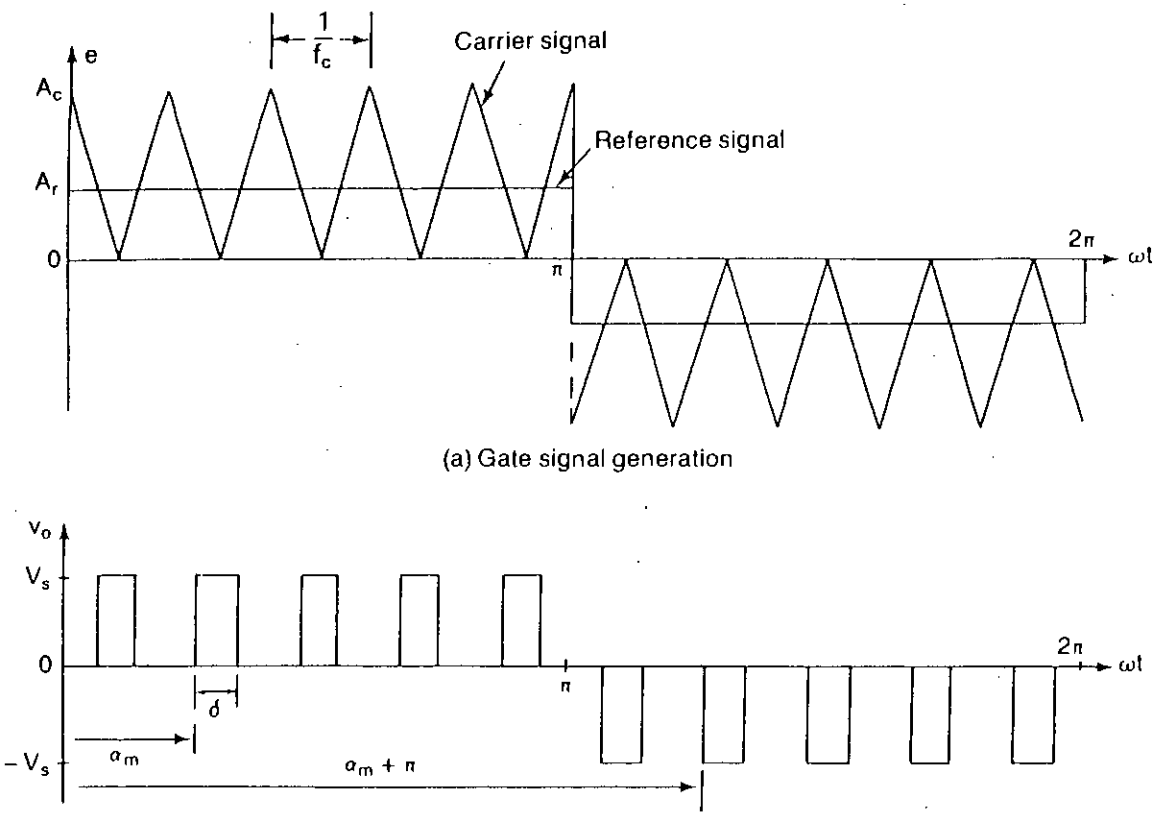

Fig. 1.2 Illustration of multiple-pulse width modulation for inverter switching.

and the carrier frequency f_c determines the number of pulses per half cycle, N_p. The order of harmonics is the same as that of single pulse modulation. The distortion factor is reduced significantly compared to that of single pulse modulation. However, due to large number of switching per half cycle, the switching loss would increase. With larger value of N_p the amplitudes of the lower harmonics would be lower but the amplitudes of the higher order harmonics would increase. This technique is capable of providing inverter output voltage with low harmonic content.

Among several pwm techniques sinusoidal pulse width modulation (SPWM) is very common. At the beginning, two different types, namely the synchronous and asynchronous sine pulse width modulation schemes were used for switching power converters [7,6,16-28]. In sine pulse width modulation the width of each pulse is varied in proportion to the amplitude of a sine wave evaluated at the center of the same pulse. The distortion factor and low order harmonics are reduced significantly. The gating signals as shown in fig. 1.3 are generated by comparing a triangular carrier wave with sine wave. The crossover points determine the points of commutation. Except at low frequency range the carrier is synchronized with the modulating signal and an odd integer (multiple of three, five etc.) ratio is maintained to improve the harmonic content. The fundamental output voltage can be varied by changing modulation index [8-10,13,29-30]. If the modulation index is less than unity only carrier frequency harmonic with the fundamental frequency related side bands appear at the output [31]. The voltage of inverter can be increased by changing modulation index until maximum voltage is obtained in square wave mode of operation. The distortion factor is significantly less compared to that of multiple-pulse modulation. The output voltage of an inverter contains harmonics. The pwm pushes the harmonics into a high frequency range around carrier frequency f_c and its multiples. For drive applications the fixed carrier frequency modulation was found

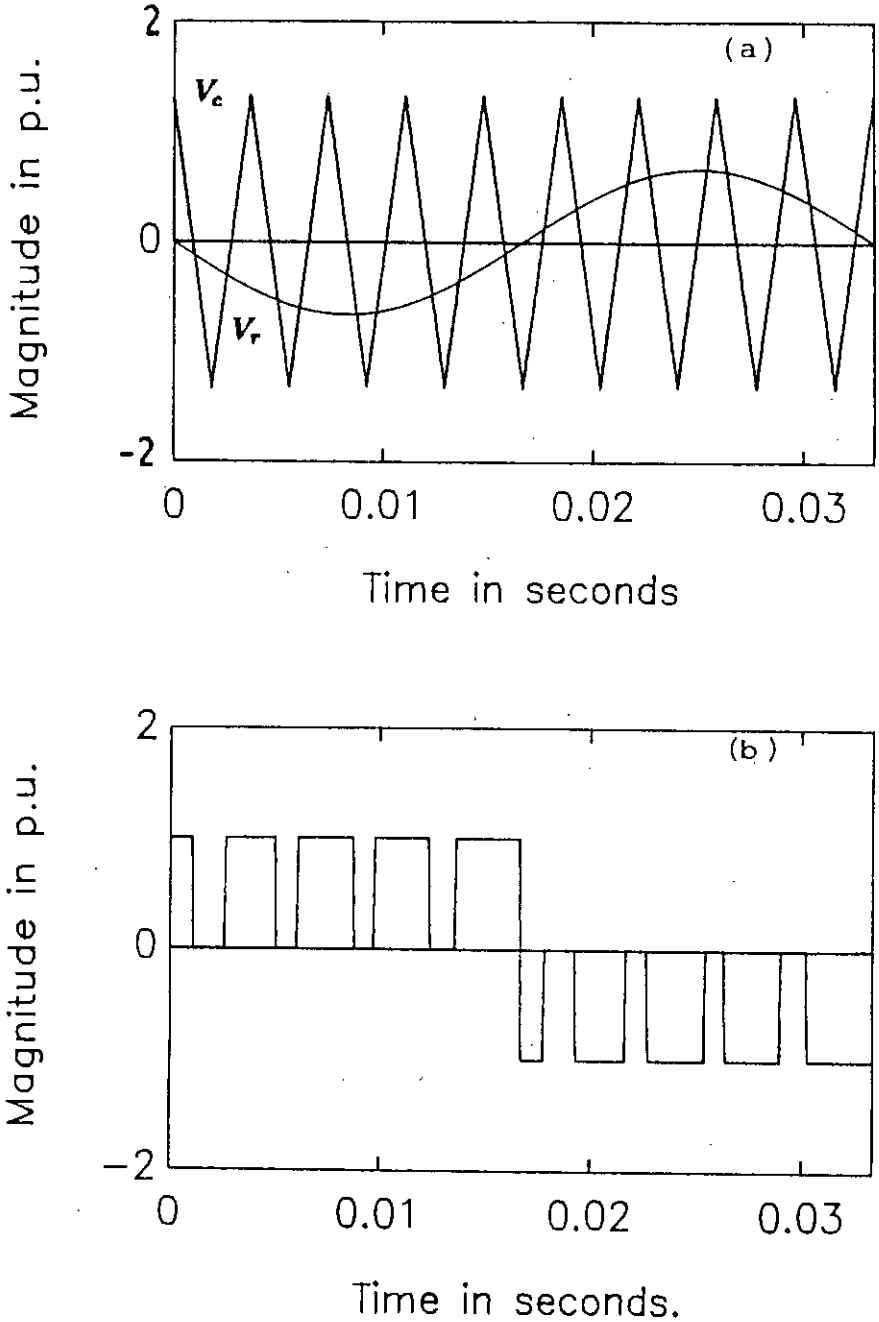

Fig. 1.3 Illustration of sinusoidal-pulse width modulation (SPWM).

a) Sine reference and carrier wave.

b) Modulated wave.

to be problematic at different frequencies. Over modulation is normally avoided in applications requiring low distortion [like uninterruptable power supplies (UPSs)]. In order to overcome the drawbacks of ordinary sine pulse width modulation variable ratio pwm schemes were introduced. At present three distinct sinusoidal pulse width modulation schemes are in use for inverters [6,7,29,32]. These are,

- Natural sampled
- Symmetric regular sampled and
- optimum sine pwm

In regular sampling method sine wave is replaced by sampled or stepped sine wave as shown in fig. 1.4. The stepped sine wave is not a sampled approximation of sine wave. It is divided in specified intervals say 20^o each and are controlled individually to control the magnitude of the fundamental component and to eliminate specific harmonics. Regular sampled pwm method is very popular in microcomputer implementation [7,10,29,33]. Optimized pwm waveform do not follow well defined modulation process [29-30,33-45]. This pwm approach is based on certain performance criteria [8,35,43,46]. As a result of the developments of microprocessor technology the implementation of optimized pulse width modulation for switching inverters has become feasible [30,40]. The technique of selected harmonic elimination pwm has received considerable attention in the past [47]. In this method the notches are created at predetermined angles of the square wave which permits voltage control as well as elimination of selected harmonics. The notch angles can be programmed so that the rms ripple current for specified load condition is minimum. Microcomputers are specially adaptable to this type of pwm technique where switching angles are stored in lookup table in the ROM. In current controlled

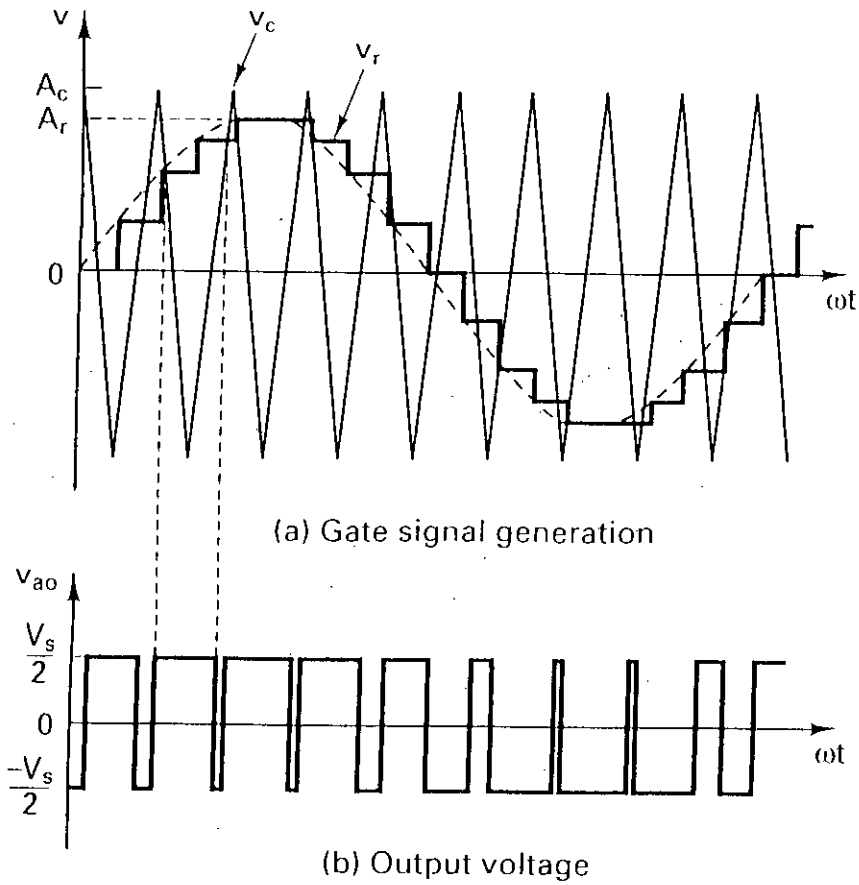

Fig. 1.4 Illustration of regular sampled sine-pulse width modulation for inverter switching.

pwm scheme the feedback current tracks the reference current within a hysteresis band. Two more types of pwm strategy have been reported recently for inverter operation. They are bang-bang sampled pwm technique and the delta modulation (dm) technique. The principle of bang-bang sampling is based on the motor current hysteresis comparison with a reference waveform to produce the modulated waveform [6,8,33,40-43]. In recent years delta modulation has been finding its way for generating switching waveforms for inverters [10,18,29,48]. In delta modulation a triangular wave is allowed to oscillate within a defined window above and below the reference sine wave V_R . The inverter switching function which is identical to the output voltage V_o is generated from the vertices of the triangular wave V_C as shown in fig. 1.5 . If the frequency of the modulating wave is changed keeping the slope of the triangular wave constant the number of pulses and the pulse width of the modulated wave would change. The fundamental output voltage can be upto 1.27 V_{DC} and is dependent on the peak amplitude A_r and frequency f_r of the reference voltage. Delta modulation can control the voltage to frequency ratio automatically. Voltage to frequency ratio control is a desirable feature in ac motor control. Analyses and the applications of the pwm inverters in drives are also important areas of research [9,17,30,33,41-43]. Due to the complexity of modulation process, a general approach for such study has not been developed so far.

1.4 THESIS OBJECTIVES

Starting performance study of induction motors are important for designer to predict initial current, speed and torque responses of motors. In designing starters to limit electrical transient, the initial current prediction is necessary, whereas, limiting mechanical transients require the knowledge of speed and torque responses of

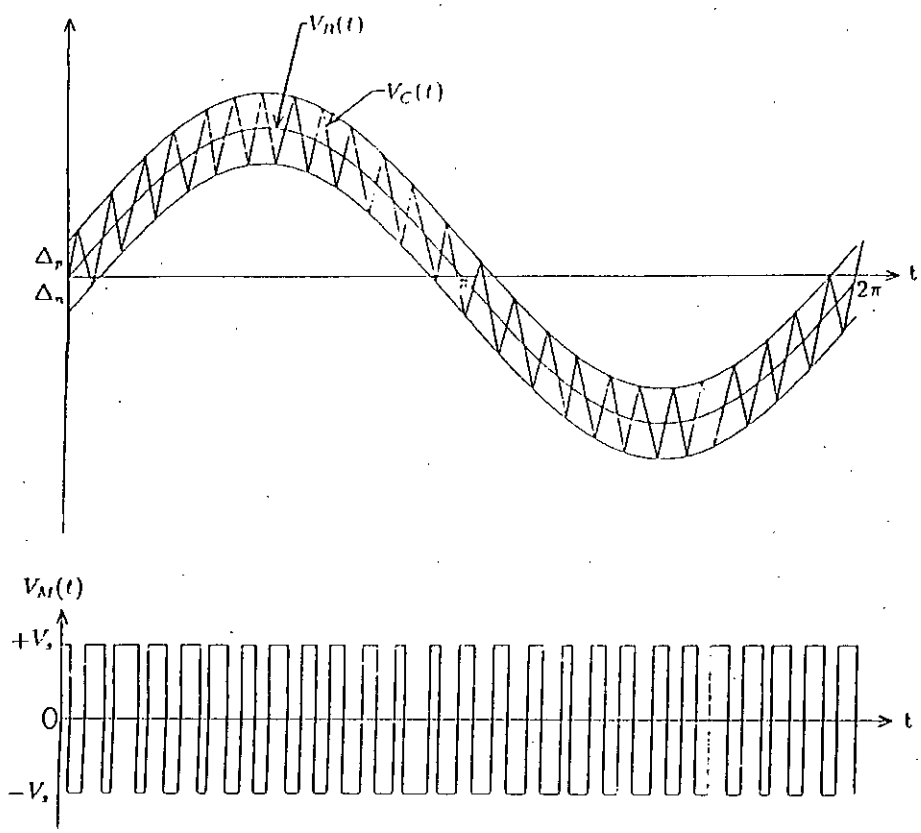

Fig. 1.5 Illustration of the DM technique for inverter switching.

motors. For sinusoidal inputs, such study has been done by d-q axes formulation of motor equations and solving the equations by numerical method. With the advent of solid state converters for ac motors' speed control, such analysis became standard using frequency domain study by Fourier series or transforms. However, predictions made by reported methods are computationally time consuming and inaccurate. To overcome these drawbacks of frequency domain analysis an investigation is carried out in this thesis to represent static inverter waveforms in time domain and solve d-q axes motor equations in time domain by numerical methods. For study purpose the most popular and versatile converter, namely the pwm inverter is taken for investigation. The waveform synthesis of pwm inverter (as such any converters) are not simple. In this thesis a simple technique of pwm inverter waveform synthesis is proposed and subsequently used for harmonics analysis. Harmonic analysis gives insight to the pwm inverter waveform properties. It would give way for transient and steady state analysis of motors in frequency domain if necessary. However, in this thesis waveform synthesis results are used for time domain analysis of starting performance of induction machines.

1.5 THESIS ORGANIZATION

Variable speed induction motors play important roles in modern Industries. With the introduction of solid state devices it has became easier to control speed of induction motors. Inverters using sine pulse width modulation (SPWM) achieve better control of speed is achieved. The SPWM waveforms analysis is shown in chapter 2. Single phase and three phase pwm waveforms are analysed in frequency domain and in time domain. Chapter 2 includes spectral analysis for different operating frequencies, modulation indices and number of pulses. An easy method for

determination of switching points of SPWM waveforms is proposed and successfully used in this thesis. The proposed method is described in chapter 2. The objective of this thesis is to study starting performance of induction motors. To study this performance a machine model is included in chapter 3. Machine performances for different inputs such as sinusoidal, pwm and square wave inverter voltages are presented in chapter 3. The inverter fed induction motor performance is studied using time domain solution of the motor and inverter voltage equations which are developed in chapter 2. Claims and conclusions of this research are summarized in chapter 4 with recommendation for future work.

CHAPTER 2

SINE PWM WAVEFORM ANALYSIS

2.1 INTRODUCTION

This chapter describes the analysis of SPWM waveform and harmonics generated by pwm inverter waveforms. A simplified method has been used for determining the switching points of spwm inverter waveforms. Time domain analysis has been used for investigating the response of induction motor instead of frequency domain or Fourier series analysis. Frequency domain analysis requires determination of individual response to each harmonics which is very tedious and time consuming. The method is also inaccurate due to truncation of harmonics. The proposed method is simpler for analysing the waveform and formulating inverter waveform equations.

The features of the sine pwm techniques as applied to the operation of inverters are investigated and summarised in this chapter. Spectrum analysis has been carried out for both single phase and three phase inverter waveforms. This chapter

also includes the synthesis of d-q axis waveforms of inverter. These waveforms are subsequently used in the analysis of starting performance of SPWM inverter-fed induction motor. Proper choice of modulation parameters such as modulation index, carrier frequency etc. during start up can be selected from the harmonics study presented in this chapter.

Modulation of static converter waveform is a common method of harmonic minimization and for simultaneous voltage and frequency control of inverter. High frequency carrier modulation reduces filter size of converter applications. Sine pulse width modulation in various forms are the most common technique of obtaining required switching waveforms of different converters. Triangular and delta modulation are two widely used modulation process in converters. In triangular modulation reference sine wave is modulated by a high frequency carrier triangular wave. A number of methods have been used for solution of switching points in studies like harmonic determination and performance predictions of applications. However, most of these methods are mathematically involved and time consuming. In this thesis a new technique for solution of switching points of spwm waveforms is presented. This technique involves solutions of simple algebraic equations requiring insignificant time for solution.

2.2 SINGLE PHASE PWM WAVEFORM SYNTHESIS

inverter-fed machine performance study starts with the waveform and machine representation in mathematical form and their computer solution by numerical techniques. The first step is to determine the switching points of inverter waveforms. A new technique easier than the previously reported techniques is used for switching

point determination of pwm waveforms generated by sine triangular modulation. The switching points thus determined are used for subsequent harmonic analysis of pwm inverter waveforms and also for representing the waveforms in time domain. The formulation of this method, simulation and results in waveforms of 1-phase inverter and their spectrum are presented in this thesis. It is expected that this analytical method will ease the microcomputer implementation of pwm switching of static power converters and provide the facility for on-line modulation parameter variation.

2.3 SWITCHING POINT DETERMINATION

Various techniques are in use for determination of switching points of spwm waveforms. All the techniques are computationally involved or approximate methods. For the purpose of this thesis an easy method for finding switching points of spwm inverter operation is proposed. The proposed solution technique assumes pulse width modulation to be generated by comparing a sine modulating wave (which determines the frequency of the inverter wave) with a high frequency sine carrier wave. In conventional method the switching frequency is generated by comparing sine modulating wave with high frequency carrier triangular wave. Basically high frequency triangular and sine wave performs the same function of carrier modulation and if carrier wave is assumed to be sinusoidal the proposed solution technique requires no approximation and is more accurate. The proposed method is illustrated in fig. 2.1 and described below.

Assume that the modulating sine wave is,

$$V_r = A_m sin\omega_m t \tag{2.1}$$

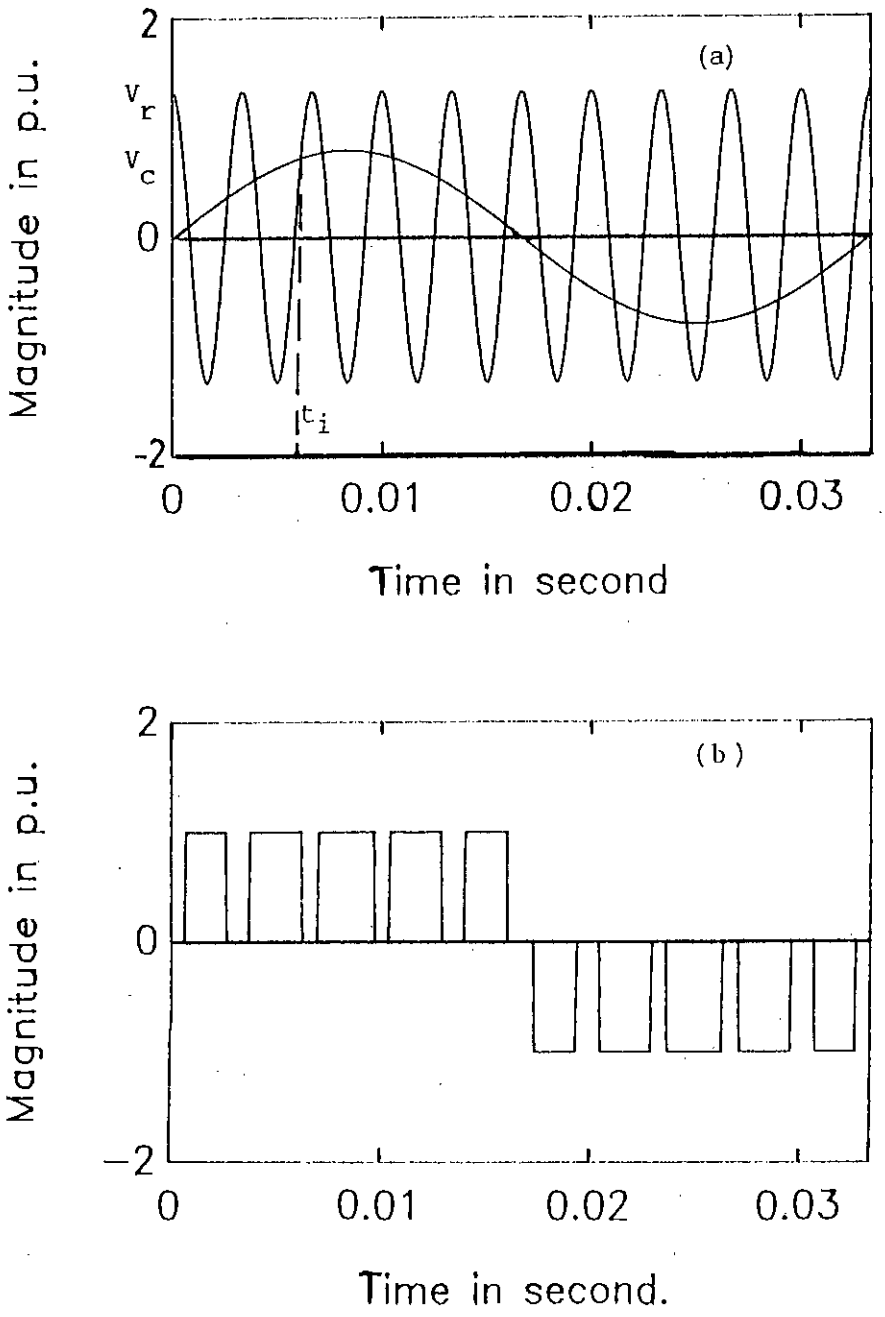

Fig. 2.1 Illustration of sinusoidal-pulse width modulation.

a) Sine-reference and carrier waves.

b) Modulated wave.

and the carrier modulating wave is,

$$V_c = A_c sin\omega_c t \tag{2.2}$$

The intersections of these two waves give the switchover points of pulse width modulated wave. Hence at intersections, their magnitudes are equal and following relationship holds,

$$V_r = V_c \tag{2.3}$$

Where t_i's are the switching points. Equation 2.3 can be rearranged as

$$A_m sin\omega_m t_i = A_c sin\omega_c t_i \tag{2.4}$$

or,

$$\frac{A_m}{A_c} sin\omega_m t_i = sin N\omega_m t_i \tag{2.5}$$

or,

$$m sin\omega_m t_i = sin N\omega_m t_i \tag{2.6}$$

where m is the modulation index ($m = \frac{A_m}{A_c}$)

and

$$\omega_c = N\omega_m \tag{2.7}$$

where, N is the multiple of ω_m by which ω_c is related to ω_m or number of pulse/cycle of modulated wave.

Equation 2.6 is a transcendental equation and can be solved numerically to evaluate the switching points t_is of the resulting modulated wave m(t). Once the switching instances of modulated wave are determined for certain modulation index m and number of pulse/cycle N, the modulated wave and inverter waves can be represented analytically as described in the following section and may be used for inverter waveform study and subsequent application performance analysis.

2.4 INVERTER WAVEFORM EQUATION

Switching of single phase inverters can be done in such a way that the output wave form appears like a modulated wave as shown in fig.2.1(b). For this type of switching the inverter output voltage have components of low frequency harmonics. The switching waveform is the processed modulator output waveform and appears like the waveform shown in fig.2.1(b). This switching waveform of fig. 2.1(b) can be represented by the following expressions,

For one cycle:

$$s_T(t) = \sum_{i=1,2..}^{N_{\frac{p}{2}}} \left[g(t, t_i, t_{i+1}) - g(t, t_i + \frac{T}{2}, t_{i+1} + \frac{T}{2}) \right] \tag{2.8}$$

For multiple cycle:

$$s(t) = \sum_{A=0,T,2T..}^{2T} \sum_{i=1,2..}^{N_{\frac{1}{2}}} \left[g(t, t_i + A, t_{i+1} + A) - g(t, t_i + \frac{T}{2} + A, t_{i+1} + \frac{T}{2} + A) \right] \quad (2.9)$$

Switching points of single phase SPWM inverter can be obtained from equation 2.6 and converted to one cycle and multiple cycle of a single phase inverter waveform using equations 2.8 and 2.9.

In triangular modulated pwm inverter waveforms investigation is usually made on parameter variations of modulation index m and number of pulse N per cycle of modulating wave. Simulated single phase inverter waveforms for 30 and 70 Hz operations are shown in figs. 2.2 and 2.3 for constant modulating index and constant number of pulse per cycle. Corresponding spectrum of the waveforms are shown in figs. 2.4 and 2.5. These waveforms and spectra are obtained using a commercial software named Mathlab [49]. Typical spectral variation of triangular modulated inverter waves for variation of modulating index and carrier frequency for constant operating frequency are shown in figs. 2.6 and 2.7 respectively. Figs. 2.8 - 2.11 illustrates the experimental generation of sine pwm waveforms by comparison of sine and triangular waves.

Features of modulation of converter waveforms are evident from these illustration. Following observations are made on the basis of results of the illustrations.

- Increase in Carrier frequency causes dominant harmonics to occur at higher frequency. This is advantageous because higher frequency dominant harmonics would require small filters for smoothing converter waveforms. However, the increase in carrier frequency is limited by switching frequency of static de-

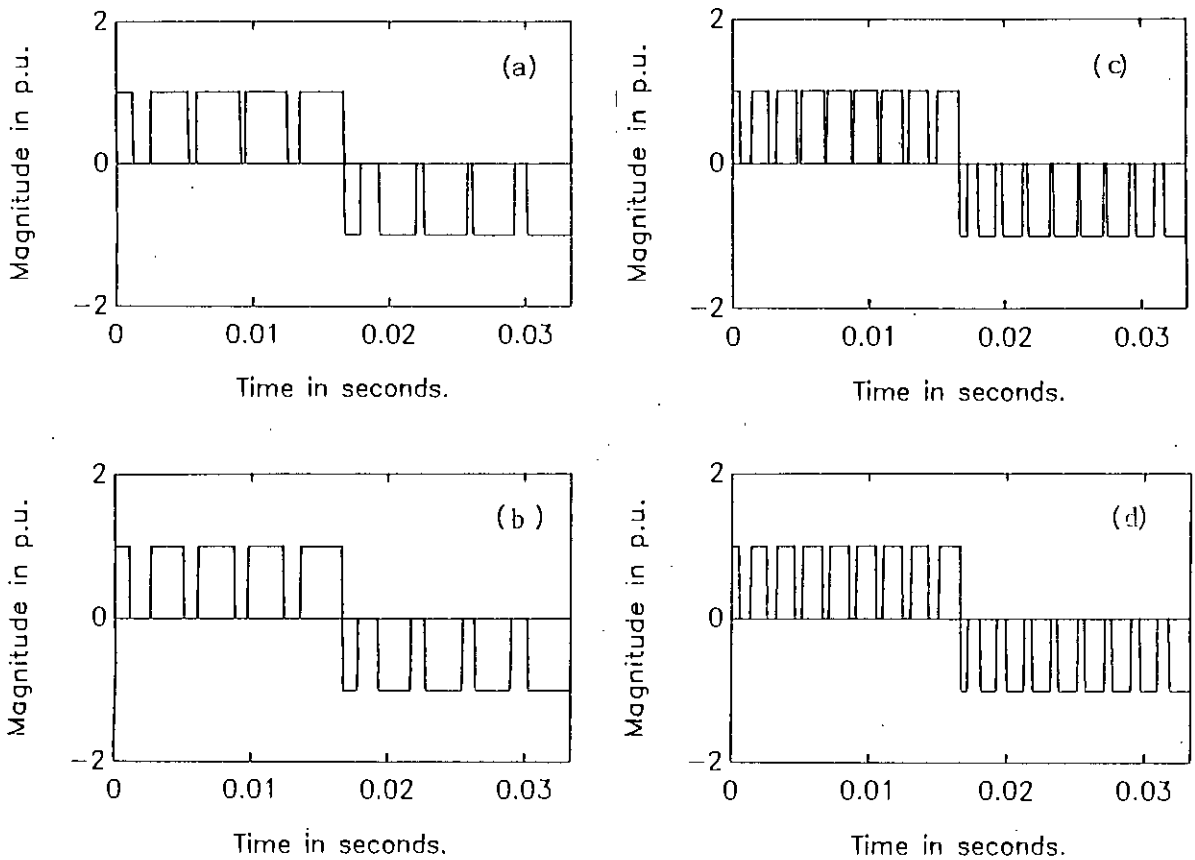

Fig. 2.2 Simulated single-phase SPWM inverter waveforms for f=30 Hz.

a) m=0.8 and N=9 **b) m=0.5 and N=9**

c) m=0.8 and N=17 **d) m=0.5 and N=17**

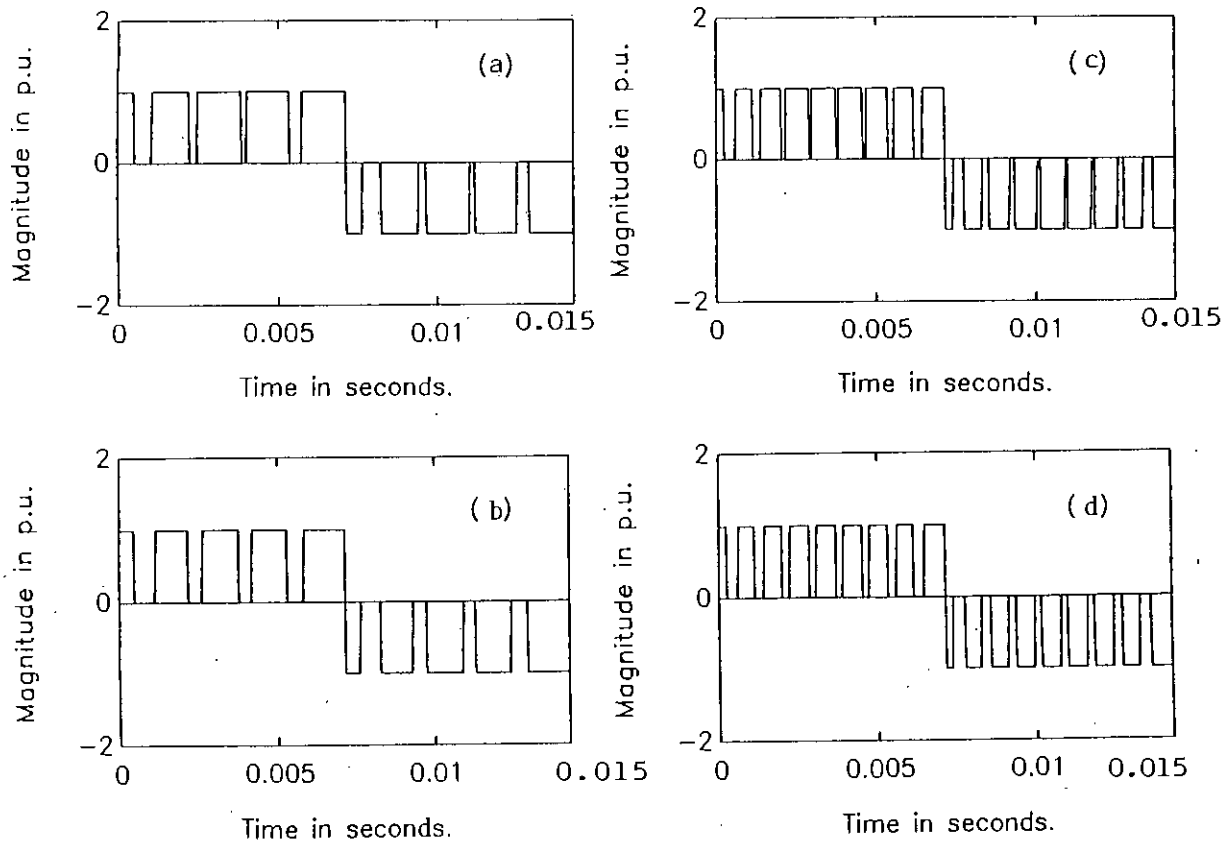

Fig. 2.3 Simulated single-phase SPWM inverter waveforms for f=70 Hz.

a) m=0.8 and N=9 **b) m=0.5 and N=9**

c) m=0.8 and N=17 **d) m=0.5 and N=17**

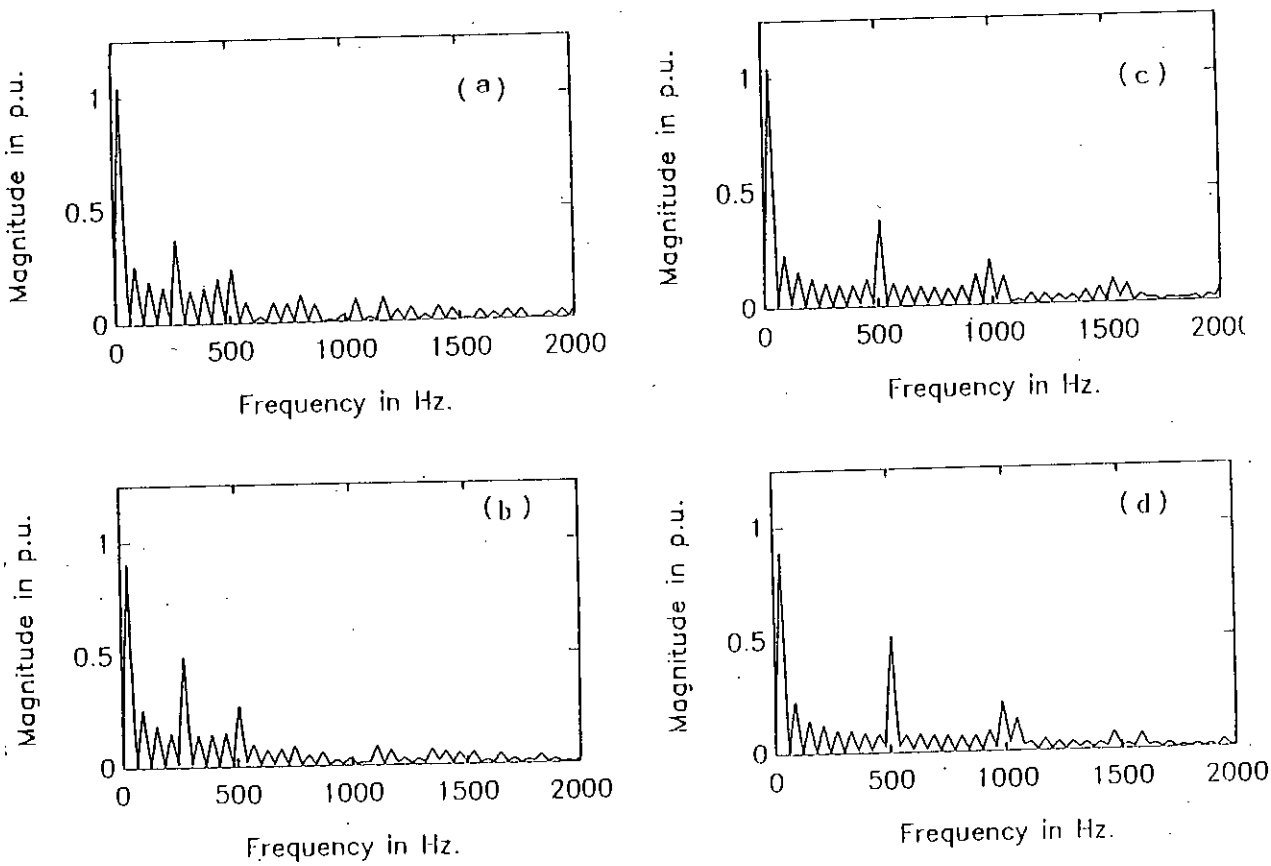

Fig. 2.4 Simulated spectrum of waveforms of Fig. 2.2

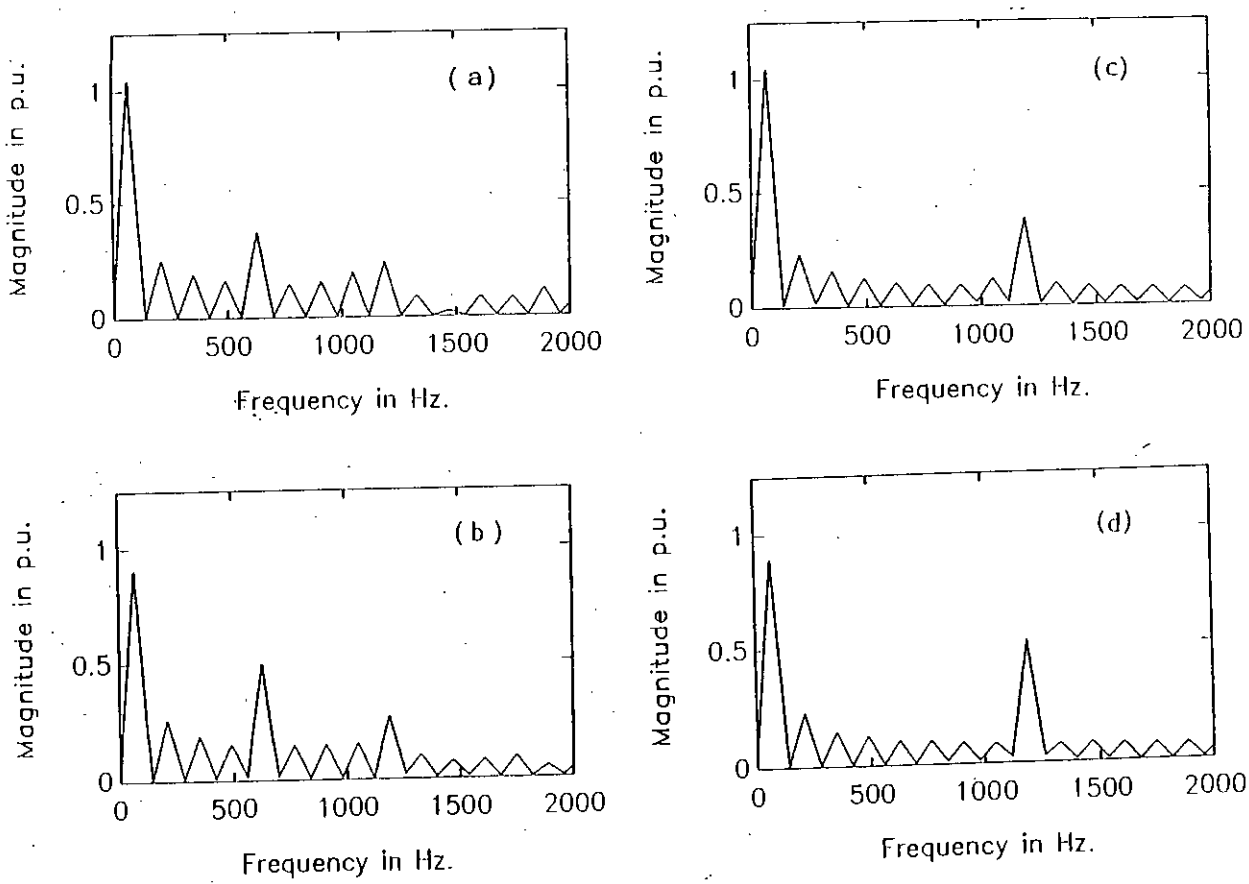

Fig. 2.5 Simulated spectrum of waveforms of Fig. 2.3.

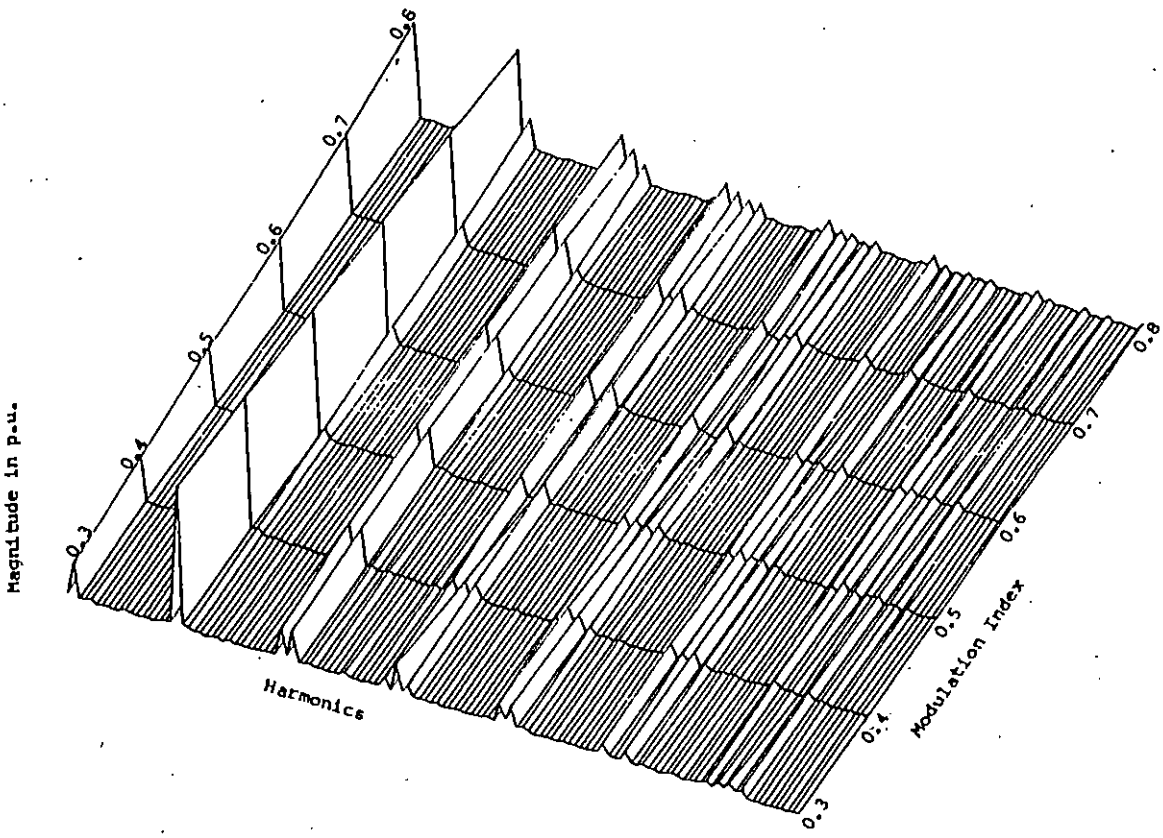

Fig. 3.6 Result of spectral analysis of SPWM waveforms (f=30 Hz., N=19 and m=0.3 to 0.8).

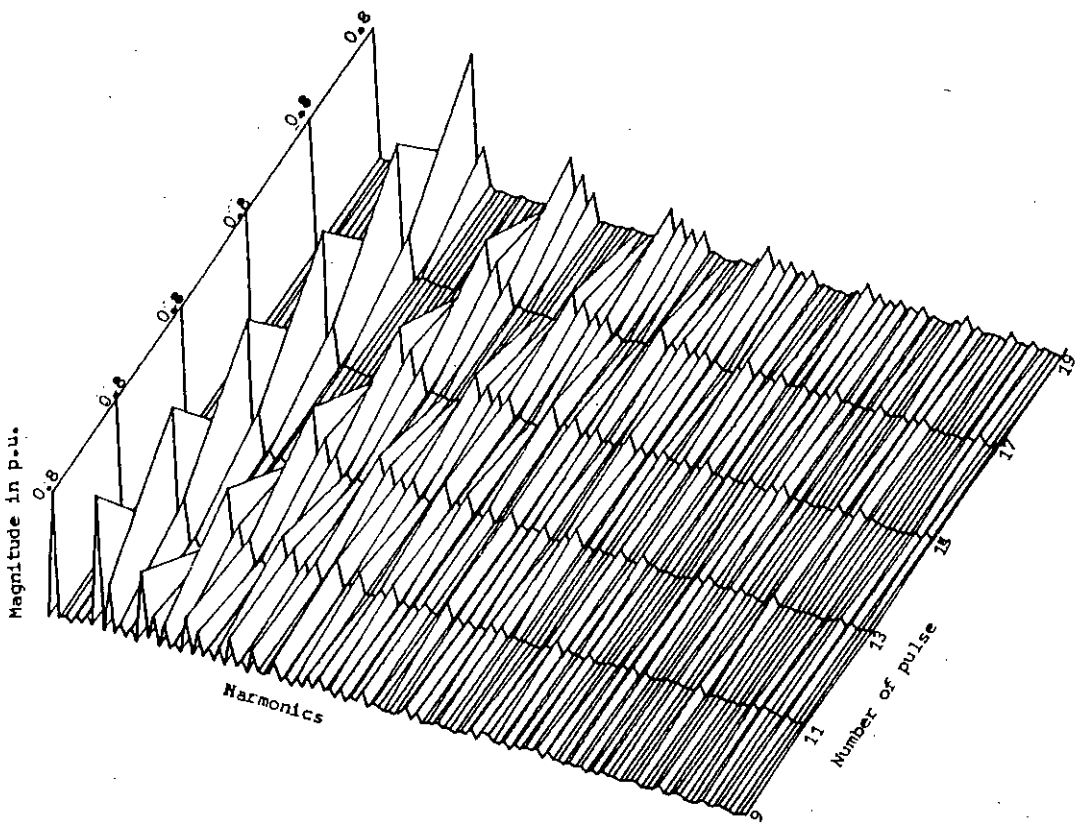

Fig. 2.7 Result of spectral analysis of SPWM waveforms (f=30 Hz., N=9 to 19 and m=0.8).

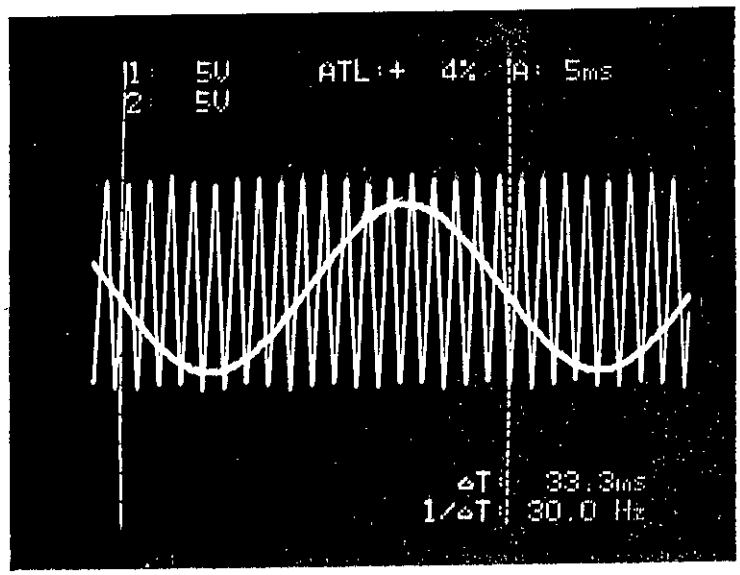

(a)

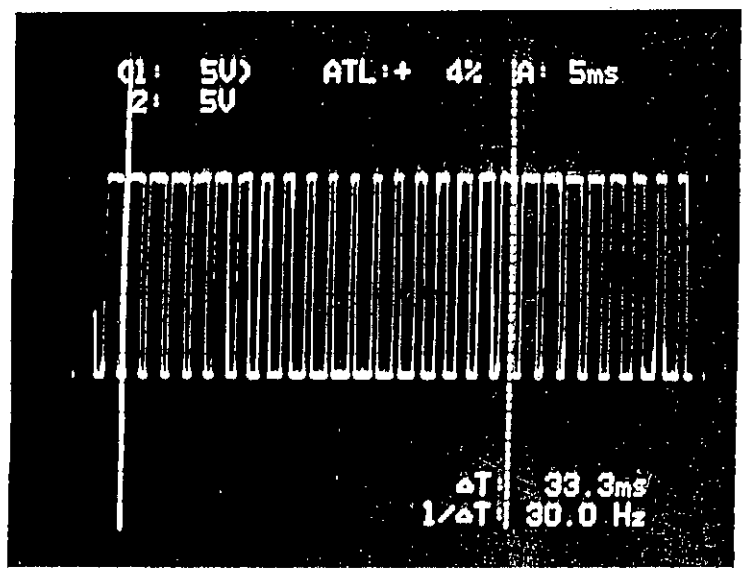

(b)

Fig. 2.8 Experimental photograph of sine-pulse width modulation.

a) Sine-reference and carrier waves.

b) Modulated wave.

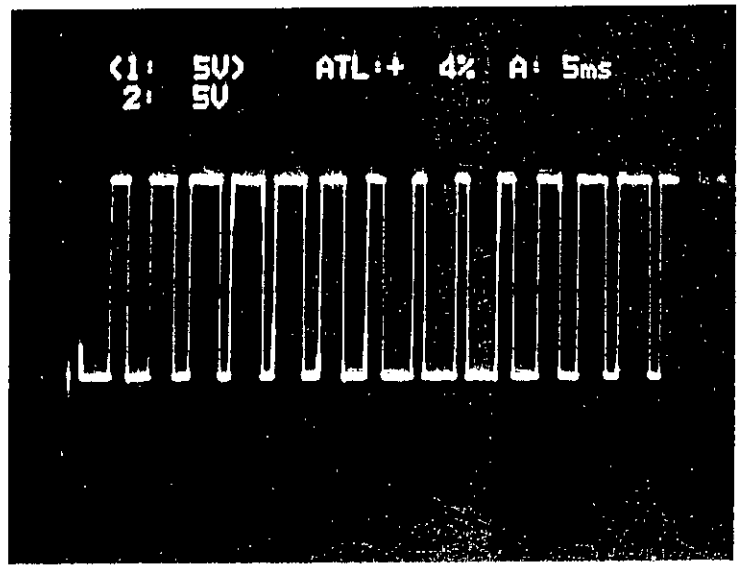

(a)

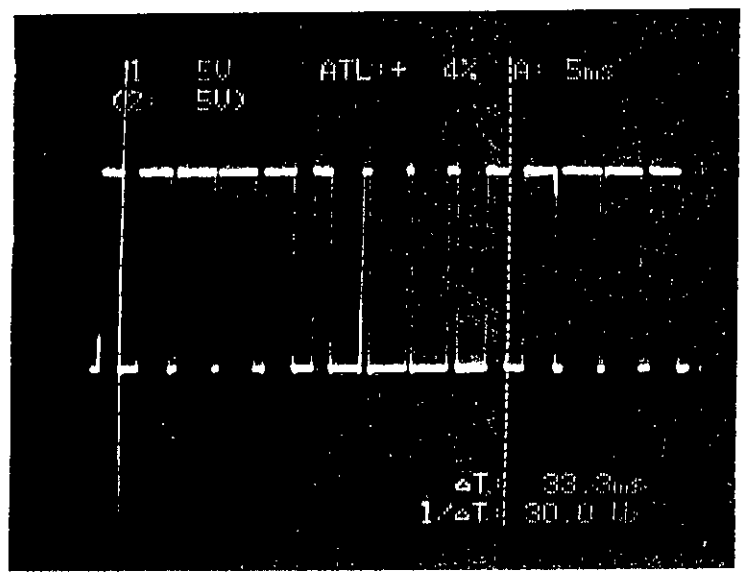

(b)

Fig. 2.9 Practical waveforms of single-phase SPWM inverter for f=30 Hz.
a) N=9 and m=0.5 b) N=9 and m=0.8

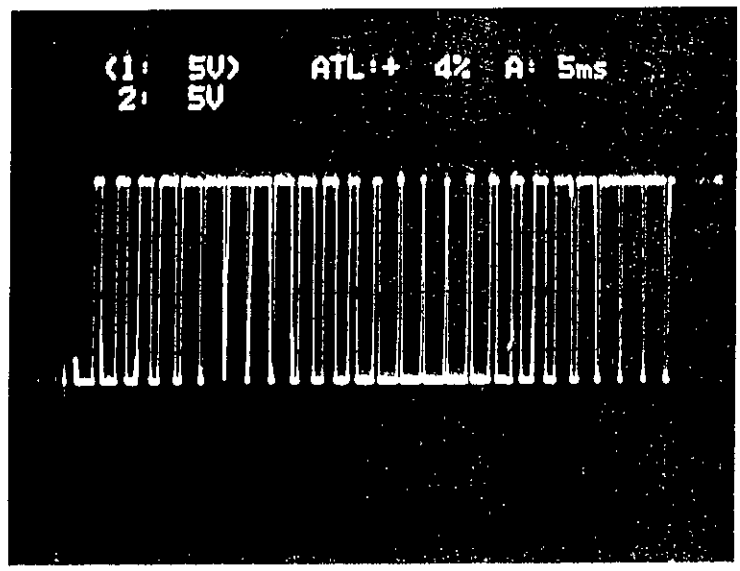

(c)

Fig. 2.9 Practical waveforms of single-phase SPWM inverter.
c) N=17 and m=0.8

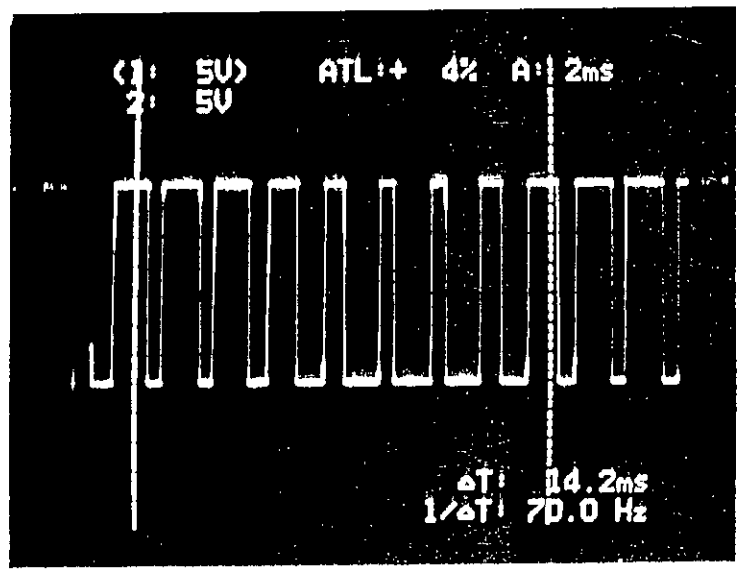

(a)

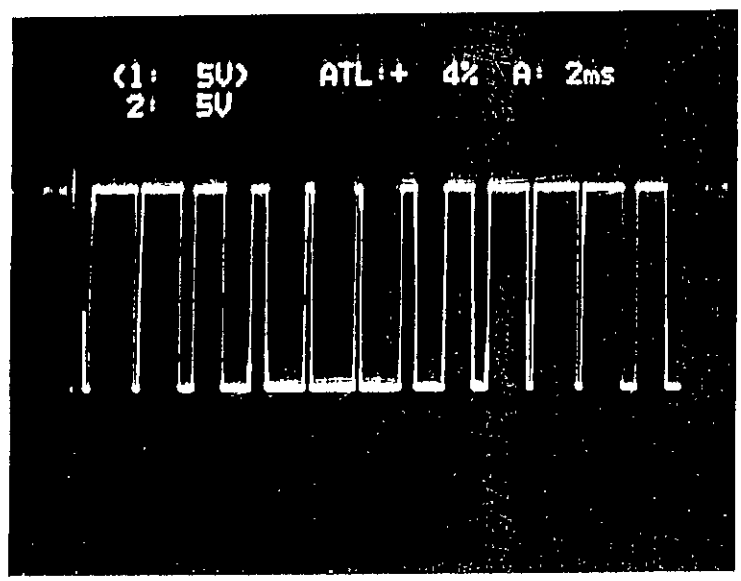

(b)

Fig. 2.10 Practical waveforms of single-phase SPWM inverter for f=70 Hz.
a) N=9 and m=0.5 b) N=9 and m=0.8

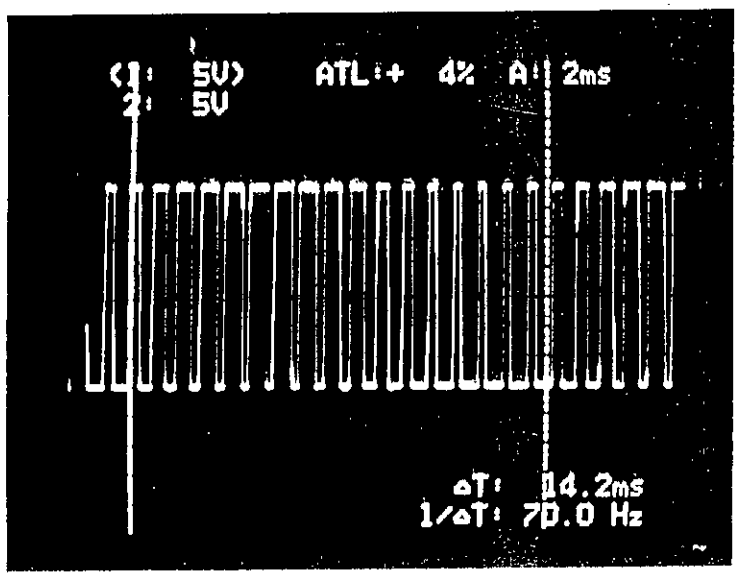

(a)

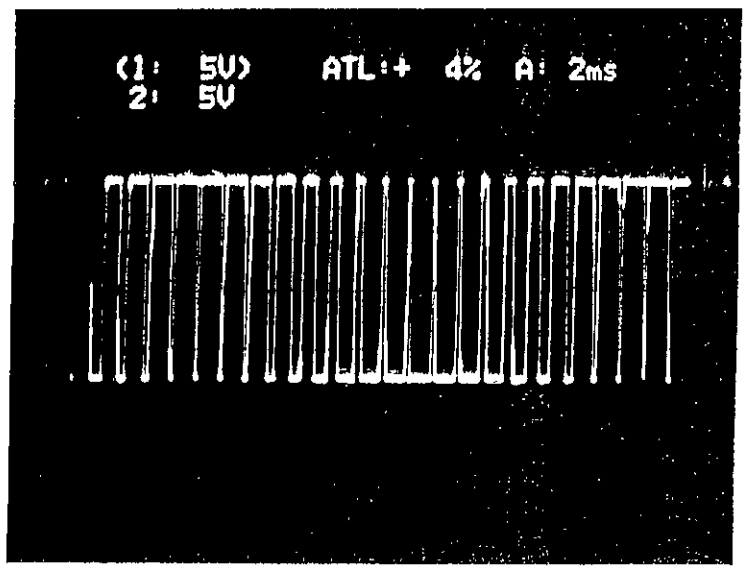

(b)

Fig. 2.11 Practical waveforms of single-phase SPWM inverter for f=70 Hz.
a) N=17 and m=0.5 b) N=17 and m=0.8

vices in converters. Number of switching per second of these devices increase as carrier frequency increases. As a result carrier frequency increase is limited by the highest switching frequency of static device in the converter. The highest switching frequency static devices vary from device to device resulting variation of cost of the converter.

- Increase of modulation index $\frac{A_m}{A_c}$ [other parameters remaining constant] causes fundamental output voltage to increase. The voltage increase with modulation index is linear. Variation of modulation index hence provides a means for voltage variation in application where controllable voltage is desired.

- Variation of frequency requires simultaneous voltage and carrier frequency control in drives. Carrier frequency adjustment is necessary to retain switching frequency of devices constant. Voltage control is necessary to maintain constant torque operation ($\frac{v}{f}$ =const). Under these conditions the waveforms of inverter gradually goes into square wave mode of operation and the spectrum of waveform contains dominant harmonics which are low order multiples of fundamental.

The results of these analysis are presented in table 2.1 - 2.4 for waveforms of single phase inverter.

2.5 3-PHASE WAVEFORM ANALYSIS

Knowing the representation of switching waveforms, by proper phase staggering($120^o - 120^o$) and addition of scaled waves, the output voltages of three phase pwm inverter can be obtained. The method for obtaining inverter output voltages is

No. of carrier pulse per half cycle.	Harmonics occurs at frequency	Magnitude			
	in Hz				
10	1000	.05	.36	.36	.05
10	2000	.08	.17	.18	.07
10	3000	0.0	.905	.1	0.0
20	1000	0.0	.05	.07	0.0
20	2000	0.0	.375	.35	0.0
20	3000	0.0	.05	.05	0.0
30	1000	0.0	.05	.07	0.0
30	2000	0.0	.07	.06	0.0
30	3000	0.0	.35	.36	0.0

Table 2.1 Result of spectral analysis of SPWM for f=50 Hz., m=0.4 and N=10, 20 and 30 respectively.

No. of carrier pulse per half cycle.	Harmonics occurs at frequency	Magnitude			
	in Hz				
10	1000	.05	.375	.35	.07
10	2000	.00	.10	.10	.00
10	3000	0.0	.07	.05	0.0
20	1000	0.0	0.0	0.0	0.0
20	2000	0.5	.375	.35	0.0
20	3000	0.0	.05	.05	0.0
30	1000	0.0	.05	.07	0.0
30	2000	0.0	.07	.06	0.0
30	3000	0.0	.35	.35	0.0

Table 2.2 Result of spectral analysis of SPWM for f=50 Hz., m=0.6 and N=10, 20 and 30 respectively.

No. of carrier pulse per half cycle.	Harmonics occurs at frequency	Magnitude			
	in Hz				
10	1000	.105	.375	.35	.12
10	2000	.08	.10	.10	.08
10	3000	0.5	.07	.07	0.5
20	1000	0.0	0.0	0.0	0.0
20	2000	0.1	.375	.35	0.12
20	3000	0.0	.05	.05	0.0
30	1000	0.0	.05	.07	0.0
30	2000	0.0	.07	.06	0.0
30	3000	0.0	.375	.35	0.0

Table 2.3 Result of spectral analysis of SPWM for f=50 Hz., m=0.8 and N=10, 20 and 30 respectively.

Modulation Index	Harmonics occurs at frequency	Magnitude			
	in Hz				
.4	1000	.105	.375	.35	.12
.4	2000	.08	.10	.10	.08
.4	3000	0.5	.07	.07	0.5
.6	1000	0.0	0.0	0.0	0.0
.6	2000	0.1	.375	.35	0.12
.6	3000	0.0	.05	.05	0.0
.8	1000	0.0	.05	.07	0.0
.8	2000	0.0	.07	.06	0.0
.8	3000	0.0	.375	.35	0.0

Table 2.4 Result of spectral analysis of SPWM for f=50 Hz., N=15 and m=0.4, 0.6 and 0.8 respectively.

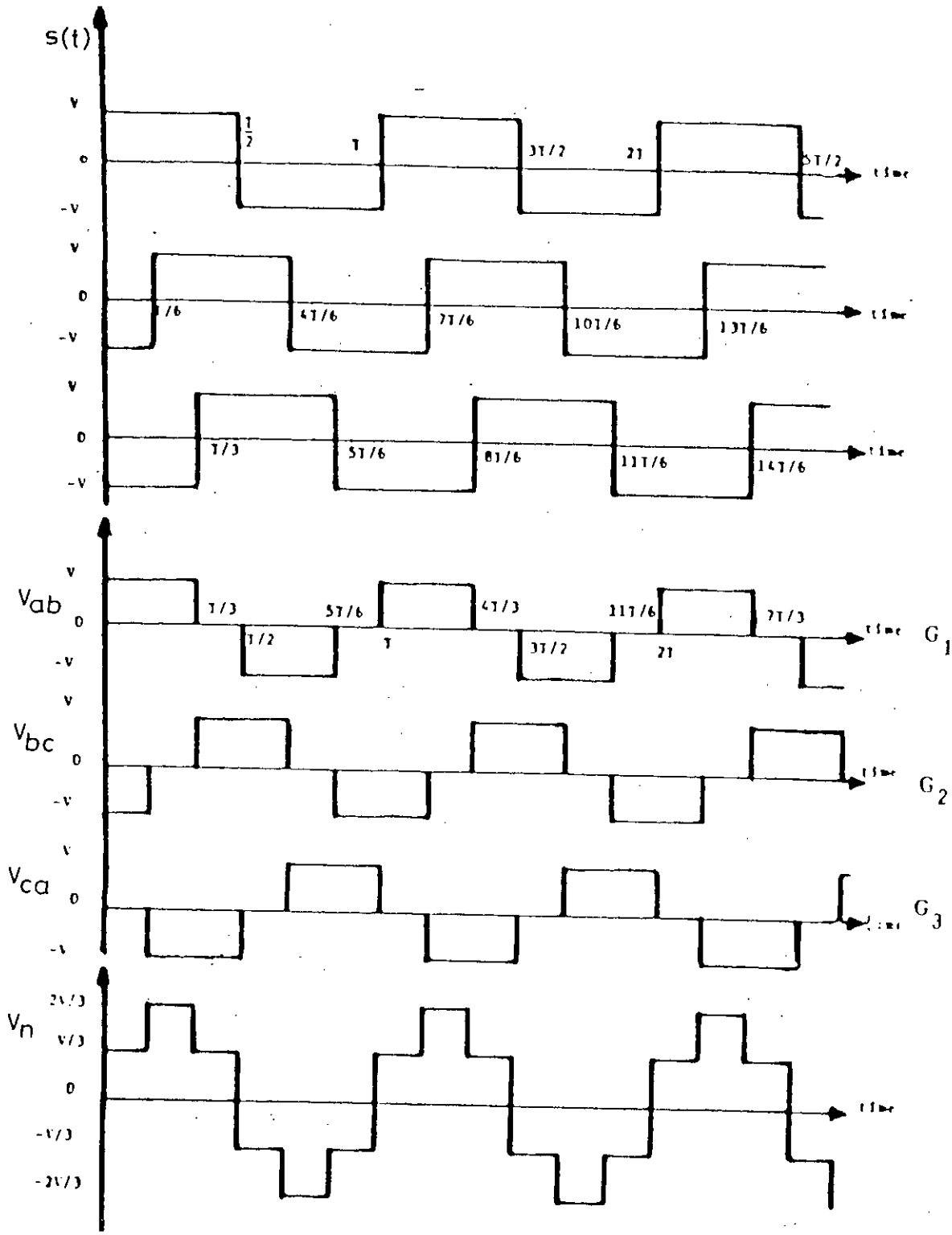

Fig. 2.12 The illustration of defining the three phase inverter output from the switching waveforms.

illustrated in fig. 2.12 for the square wave mode of operation gap. Line to line voltages of three phase inverter are obtained by the addition of scaled modulated wave with the phase shifted scaled modulated wave.

One of the goal of this thesis is to analyse the start up performance of inverter-fed induction motor. Spectrum analysis and time domain analysis of the voltage waveforms are required to the fulfill this objective. Mathematical expressions for different voltages i.e. line voltages, neutral voltage, d-q axes voltage are required for this analysis. A switching function s(t) can be obtained from a modulated waveform as illustrated in fig. 2.1(b) and equations 2.8, 2.4

For one cycle:

$$s_T(t) = \sum_{i=1,2..}^{N_{\frac{T}{2}}} \left[g(t, t_i, t_{i+1}) - g(t, t_i + \frac{T}{2}, t_{i+1} + \frac{T}{2}) \right] \tag{2.10}$$

For multiple cycle:

$$s(t) = \sum_{A=0,T,2T..}^{ZT} \sum_{i=1,2..}^{N_{\frac{T}{2}}} \left[g(t, t_i + A, t_{i+1} + A) - g(t, t_i + \frac{T}{2} + A, t_{i+1} + \frac{T}{2} + A) \right] \tag{2.11}$$

Three phase pwm inverter waveforms is obtained by multiplying time addition of phase staggered switching waves and gating the resultant waves by the line to line voltage waveform of unity magnitude in square wave mode of operation. Gating by line to line voltage of square mode of operation is necessary because inverter

line voltages cannot be more than V in either direction. The analytical expressions for line to line voltages in terms of switching waveforms (shown in fig. 2.12) are obtained as,

$$V_{ab} = \frac{1}{2}V_{dc}\left[s(t) + s(t+\frac{T}{6})\right]u(t)G_1 \tag{2.12}$$

$$V_{bc} = \frac{1}{2}V_{dc}\left[s(t-\frac{T}{6}) + s(t-\frac{T}{3})\right]u(t)G_2 \tag{2.13}$$

$$V_{ca} = \frac{1}{2}V_{dc}\left[s(t-\frac{T}{2}) + s(t+\frac{T}{3})\right]u(t)G_3 \tag{2.14}$$

where, V_{ab}, V_{bc}, V_{ca} are line to line voltages of the inverter.

Since,

$$s\left(t-\frac{T}{2}\right) = -s\left(t\right) \tag{2.15}$$

$$s\left(t-\frac{T}{3}\right) = -s\left(t+\frac{T}{6}\right) \tag{2.16}$$

and

$$s\left(t+\frac{T}{3}\right) = -s\left(t-\frac{T}{6}\right) \tag{2.17}$$

Equations 2.12, 2.13 and 2.14 can be written as,

$$V_{ab} = \frac{1}{2}V_{dc}\left[s(t) + s(t+\frac{T}{6})\right]u(t)G_1 \tag{2.18}$$

$$V_{bc} = \frac{1}{2}V_{dc}\left[s(t-\frac{T}{6}) - s(t+\frac{T}{6})\right]u(t)G_2 \tag{2.19}$$

$$V_{ca} = \frac{1}{2}V_{dc}\left[-s(t) - s(t-\frac{T}{6})\right]u(t)G_3 \tag{2.20}$$

In equations 2.18, 2.19 and 2.20 G_1, G_2 and G_3 are line to line waveforms of unity magnitude in the square mode of operation. Line to neutral voltage of the inverter are given by following expressions,

$$V_{an} = \frac{1}{3}(V_{ab} - V_{ca}) \tag{2.21}$$

$$V_{bn} = \frac{1}{3}(V_{bc} - V_{ab}) \tag{2.22}$$

$$V_{cn} = \frac{1}{3}(V_{ca} - V_{bc}) \tag{2.23}$$

where V_{an}, V_{bn} and V_{cn} are line to neutral voltages of the inverter.

The expressions for line to neutral voltages of the inverter can be written in terms of switching waveforms as,

$$V_{an} = \frac{V_{dc}}{6}\left[\left(s(t) + s(t+\frac{T}{6})\right)G_1 - \left(-s(t) - s(t-\frac{T}{6})\right)G_3\right]u(t) \tag{2.24}$$

$$V_{bn} = \frac{V_{dc}}{6}\left[\left(s(t-\frac{T}{6}) - s(t+\frac{T}{6})\right)G_2 - \left(s(t) + s(t+\frac{T}{6})\right)G_1\right]u(t) \tag{2.25}$$

$$V_{cn} = \frac{V_{dc}}{6}\left[\left(-s(t) - s(t-\frac{T}{6})\right)G_3 - \left(s(t-\frac{T}{6}) - s(t+\frac{T}{6})\right)G_2\right]u(t) \tag{2.26}$$

For machine performance analysis using d-q axes transformation, direct and quadrature axes voltages V_d and V_q are required. These voltages are obtained as [50],

$$\begin{bmatrix} V_d \\ V_q \end{bmatrix} = \frac{2}{3} \begin{bmatrix} 0 & \frac{\sqrt{3}}{2} & -\frac{\sqrt{3}}{2} \\ 1 & -\frac{1}{2} & -\frac{1}{2} \end{bmatrix} \begin{bmatrix} V_{ab} \\ V_{bc} \\ V_{ca} \end{bmatrix} \tag{2.27}$$

Hence,

$$V_d = \frac{1}{\sqrt{3}} [V_{bc} - V_{ca}] \tag{2.28}$$

$$V_q = \frac{1}{3} [2V_{ab} - V_{bc} - V_{ca}] \tag{2.29}$$

By substitution of equations 2.18, 2.19 and 2.20 in equations 2.28 and 2.29,

$$V_d = \frac{V_{dc}}{2\sqrt{3}} \left[\left(s(t - \frac{T}{6}) - s(t + \frac{T}{6}) \right) G_1 - \left(s(t) - s(t - \frac{T}{6}) \right) G_3 \right] \tag{2.30}$$

$$V_q = \frac{V_{dc}}{6} \left[2 \left(s(t) + s(t + \frac{T}{6}) \right) G_1 - \left(s(t - \frac{T}{6}) - s(t + \frac{T}{6}) \right) G_2 - \left(-s(t) - s(t - \frac{T}{6}) \right) G_3 \right] \tag{2.31}$$

Typical voltage waveforms for $V_{ab} V_{an}, V_d$ and V_q are shown in fig.2.13 to 2.15 to illustrate the validity of equations 2.18, 2.24, 2.30 and 2.34 in graphical form for modulation index of m=0.4 and m=0.8. These waveforms are obtained using Mathlab [49].

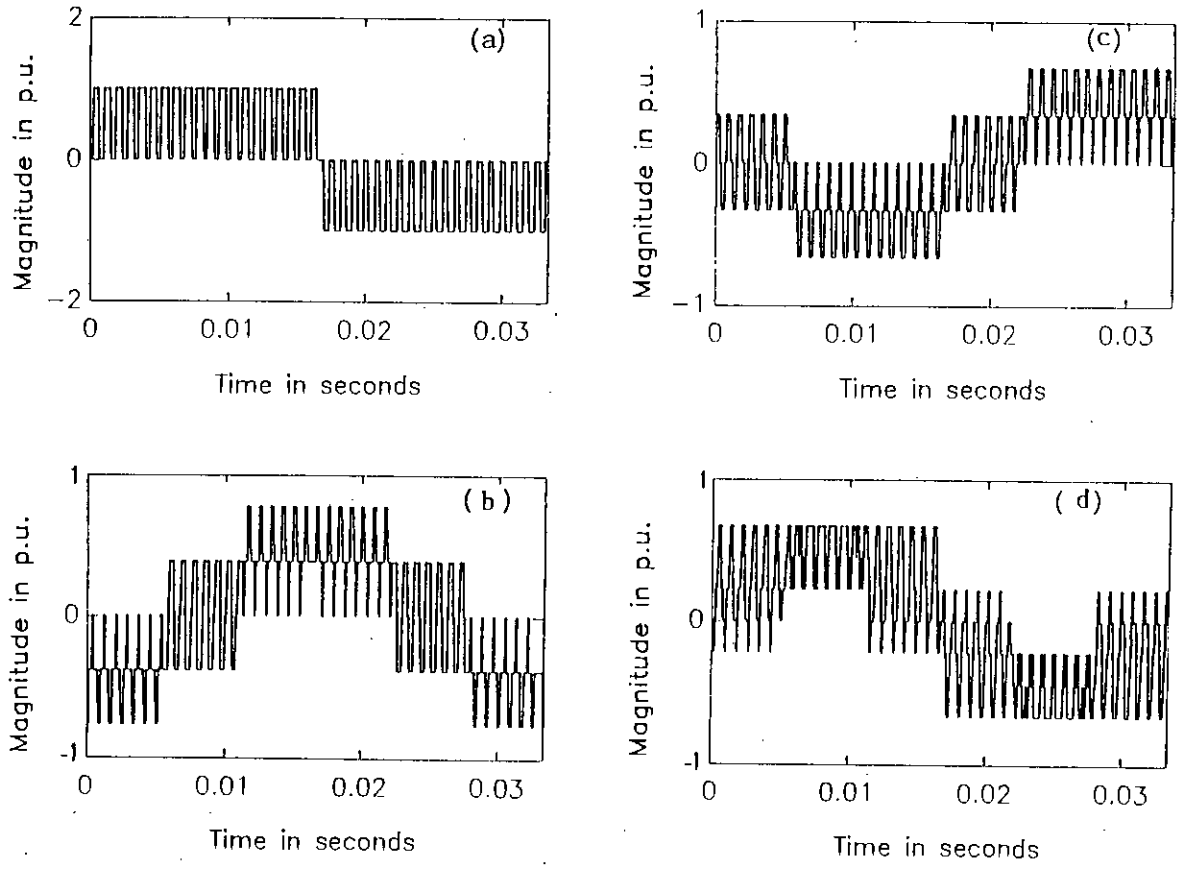

Fig. 2.13(i) Simulated waveforms of three-phase SPWM inverter (f=30 Hz., N=40 and m=0.4).

a) Line voltage. **b) Neutral voltage.**

c) d-axis voltage. **d) q-axis voltage.**

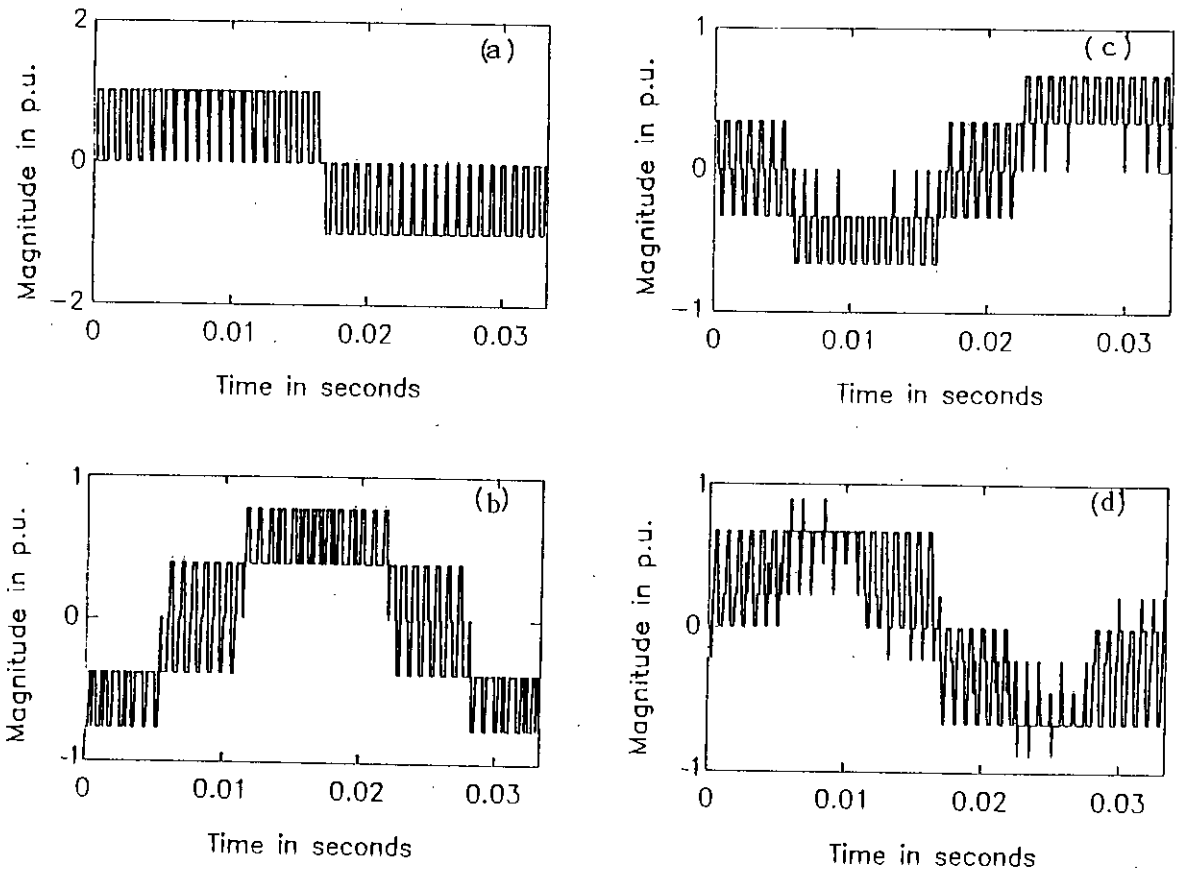

Fig. 2.13(ii) Simulated waveforms of three-phase SPWM inverter (f=30 Hz., N=40 and m=0.8).

a) Line voltage. **b) Neutral voltage.**

c) d-axis voltage. **d) q-axis voltage.**

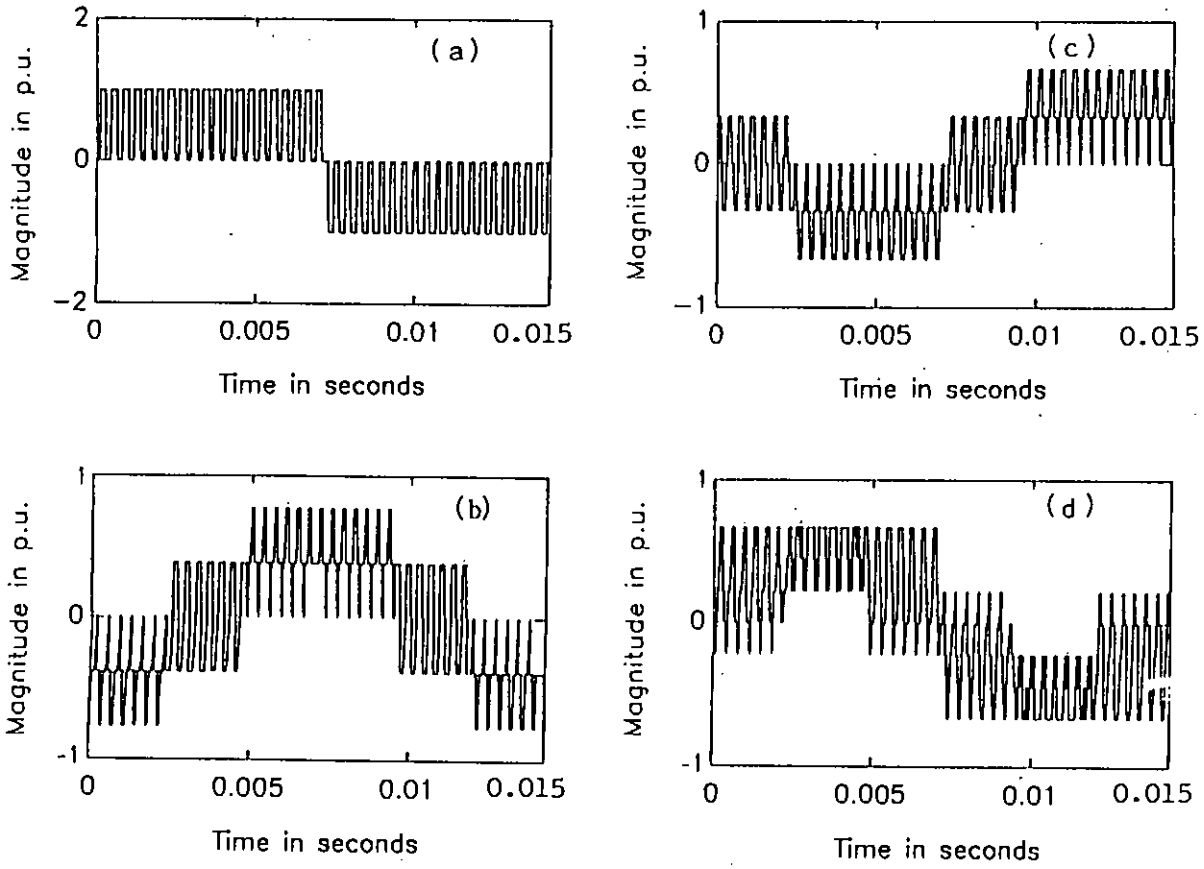

Fig. 2.14: Simulated waveforms of three-phase SPWM inverter (f=70 Hz., N=40 and m=0.4).

a) Line voltage. **b) Neutral voltage.**

c) d-axis voltage. **d) q-axis voltage.**

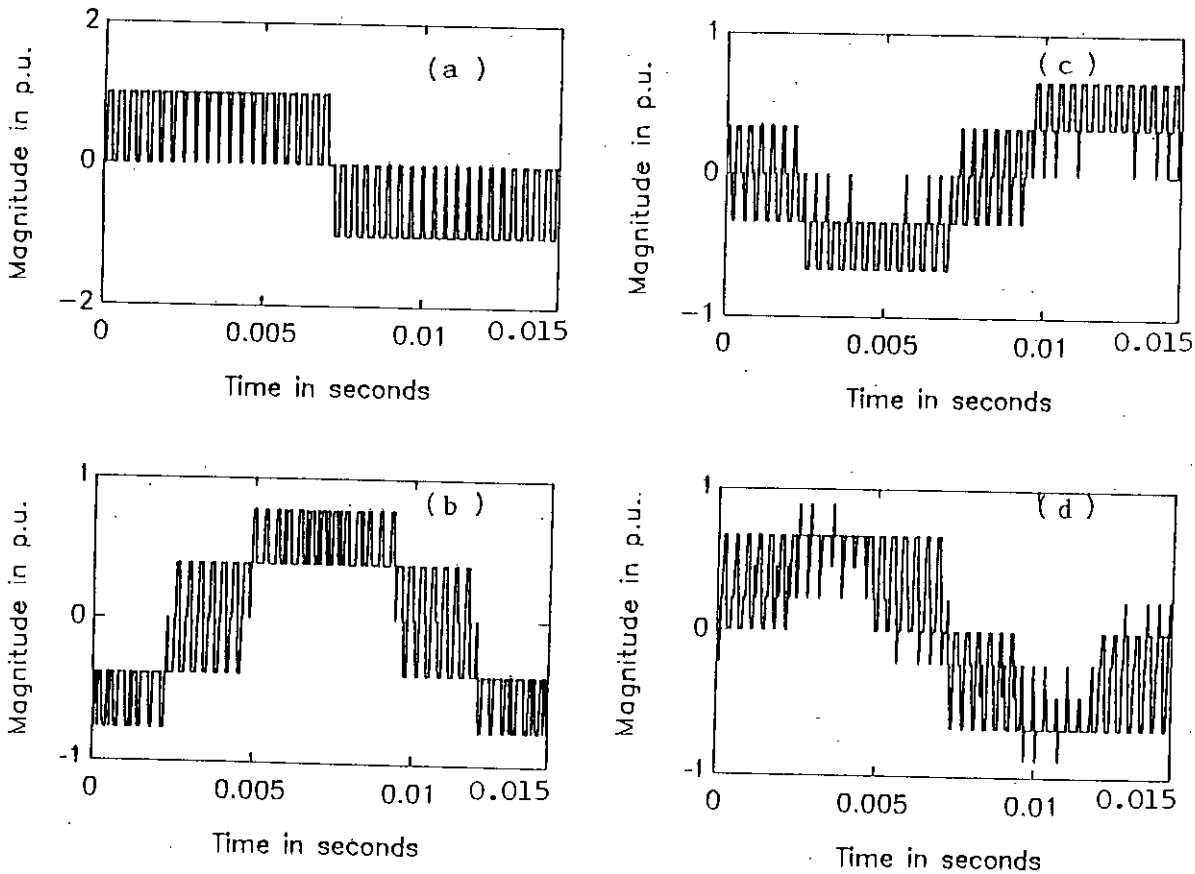

Fig. 2.15(i) Simulated waveforms of three-phase SPWM inverter (f=70 Hz., N=40 and m=0.8).

a) Line voltage. b) Neutral voltage.

c) d-axis voltage. d) q-axis voltage.

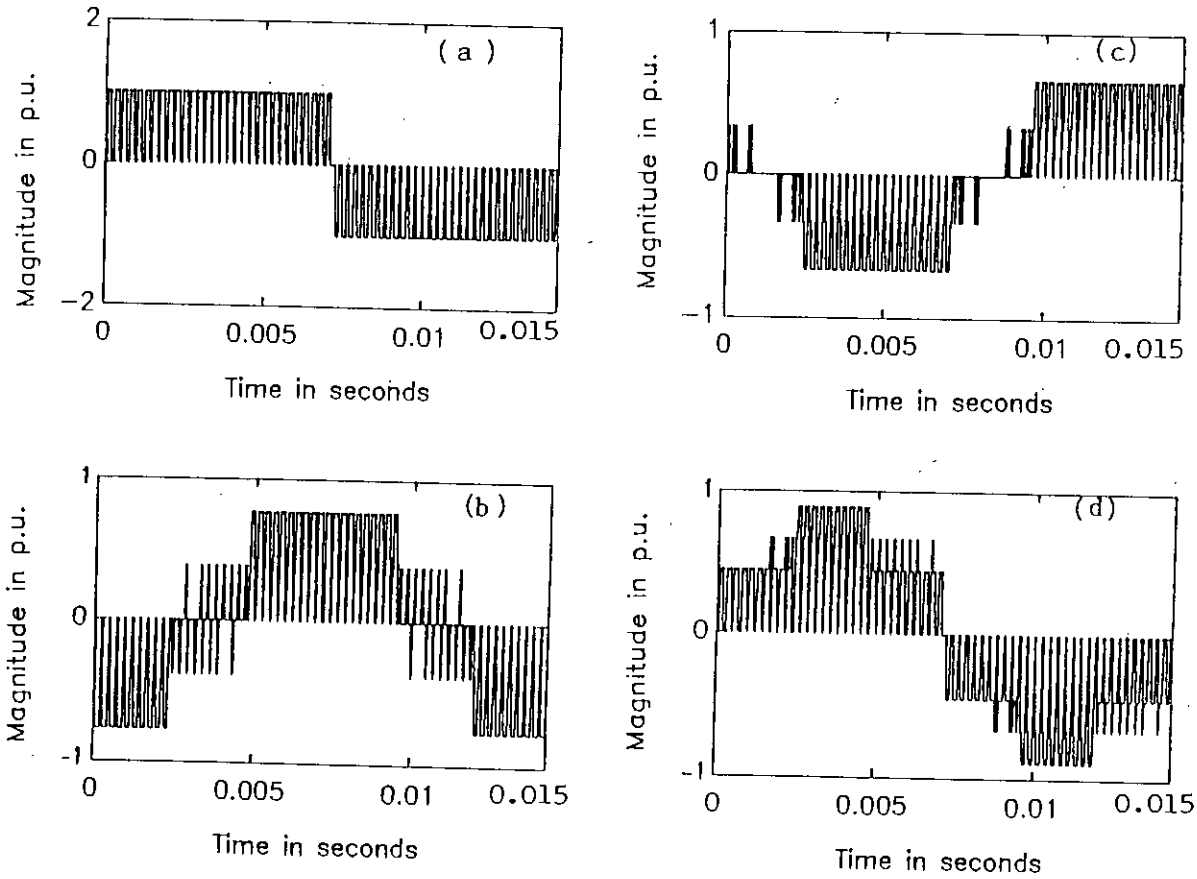

Fig. 2.15(ii) Simulated waveforms of three-phase SPWM inverter (f=70 Hz., N=60 and m=0.8).

a) Line voltage. **b) Neutral voltage.**

c) d-axis voltage. **d) q-axis voltage.**

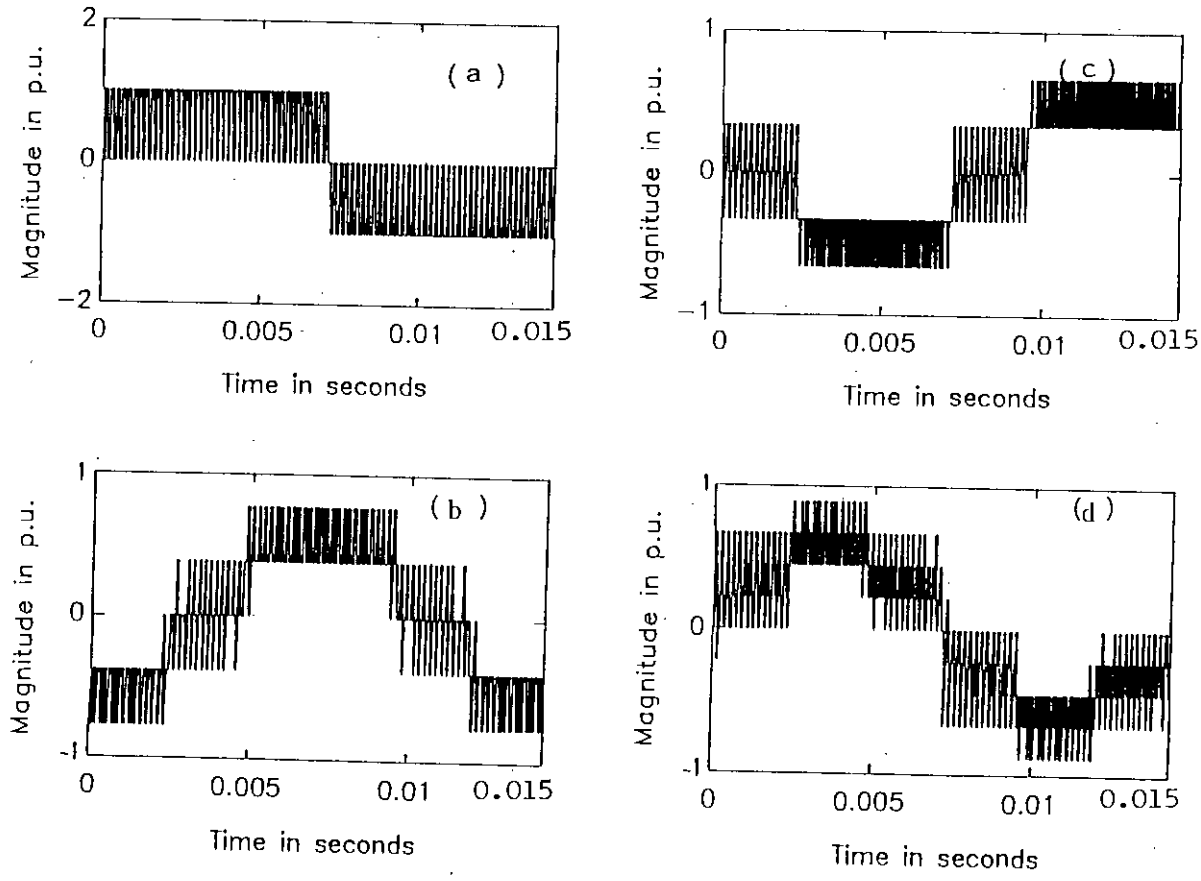

Fig. 2.15(iii) Simulated waveforms of three-phase SPWM inverter (f=70 Hz., N=80 and m=0.8).

a) Line voltage. b) Neutral voltage.

c) d-axis voltage. d) q-axis voltage.

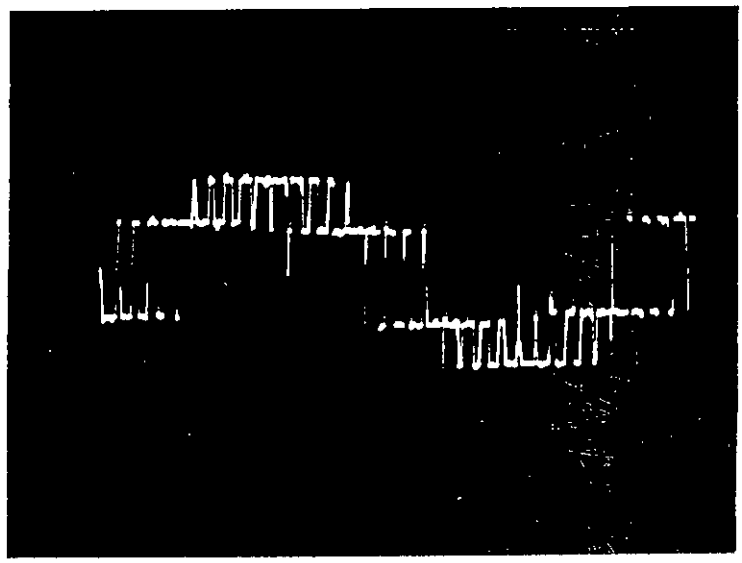

(a)

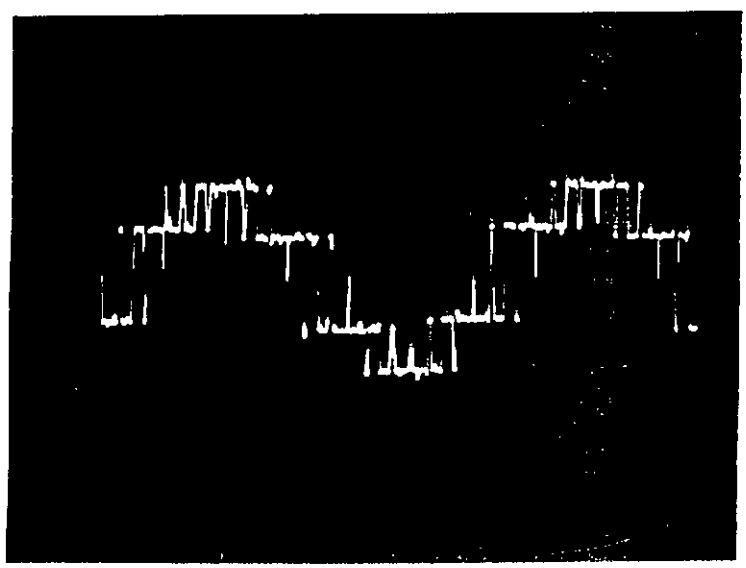

(b)

Fig. 2.16 Experimental neutral voltage waveforms of three-phase SPWM inverter.

a) 20 Hz. b) 30 Hz.

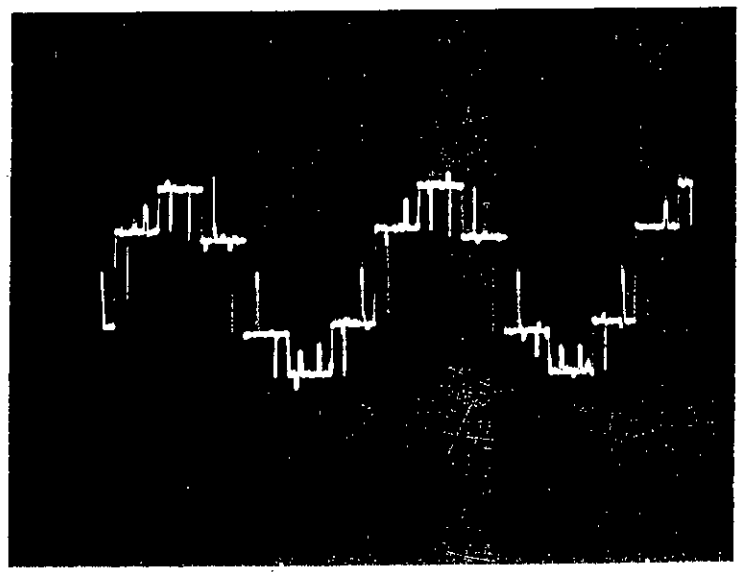

(c)

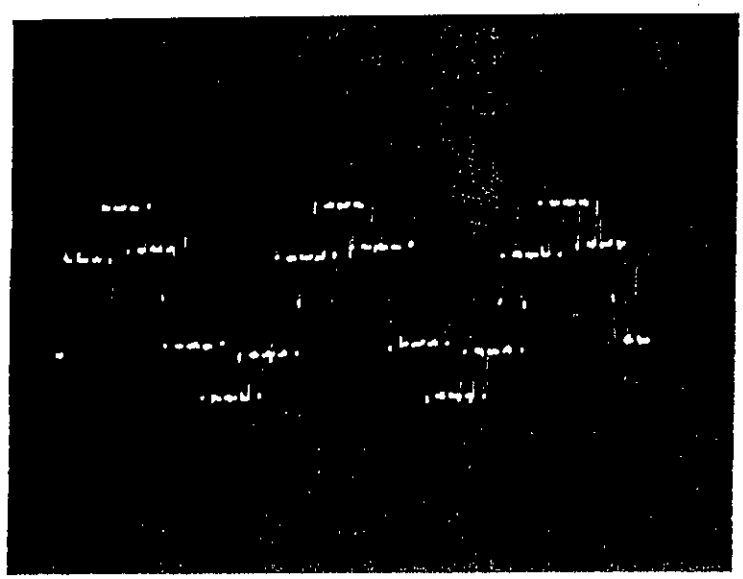

(d)

Fig. 2.16 Experimental neutral voltage waveforms of three-phase SPWM inverter.

c) 40 Hz. d) 50 Hz.

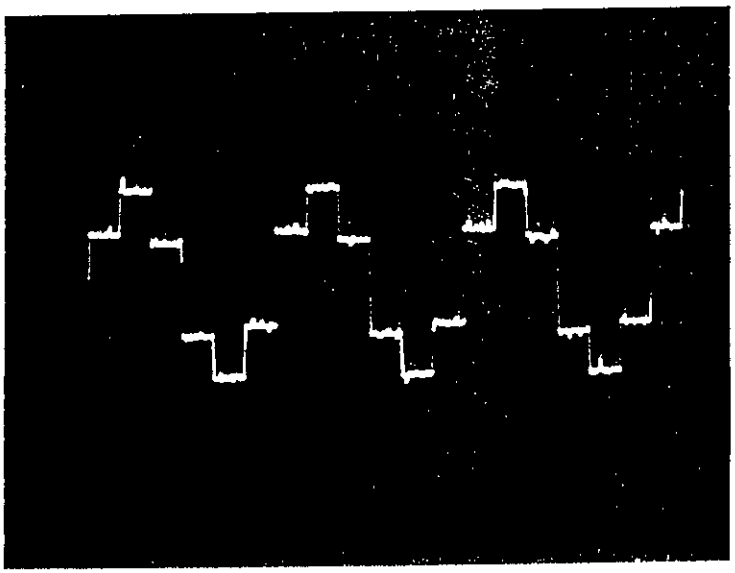

(e)

Fig. 2.16 Experimental neutral voltage waveforms of three-phase SPWM inverter.
e) 60 Hz.

Fig 2.16 illustrates experimental line to neutral voltage waveforms of a spwm inverter for 20 to 60 Hz operation with pulse dropping characteristics as inverter goes into higher operating frequency.

Fig 2.17 shows experimental line to neural voltage waveforms at constant 50 Hz operation of spwm inverter illustrating the trend of change in carrier frequency.

The spectrums of the theoretically obtained voltage waveforms mentioned above are shown in fig 2.18.

An attempt has been made to simulate the above mentioned situation and to produce same voltage waveforms practically maintaining same operating conditions. The practical waveforms were taken close to theoretical condition but due to lack of proper facilities, recording of exact conditions were not possible. The trend of the practical waveforms, however, shows that theoretical predictions give similar results and it can be said that under perfect practical condition the theoretically predicted waveforms and practical waveforms will exactly be same.

2.6 DISCUSSIONS OF SPECTRAL VARIATIONS OF 3-PHASE INVERTER WAVES

Fig. 2.19 is the three dimensional spectral variation of SPWM wave for constant modulating carrier frequency with modulation index as variable parameter. The spectra show fundamental of SPWM wave increase with modulation index linearly and dominant harmonics occur at carrier frequency and multiples of carrier frequency. Fig. 2.19 is the spectra of line to line voltage, whereas, figs. 2.20, 2.21 and

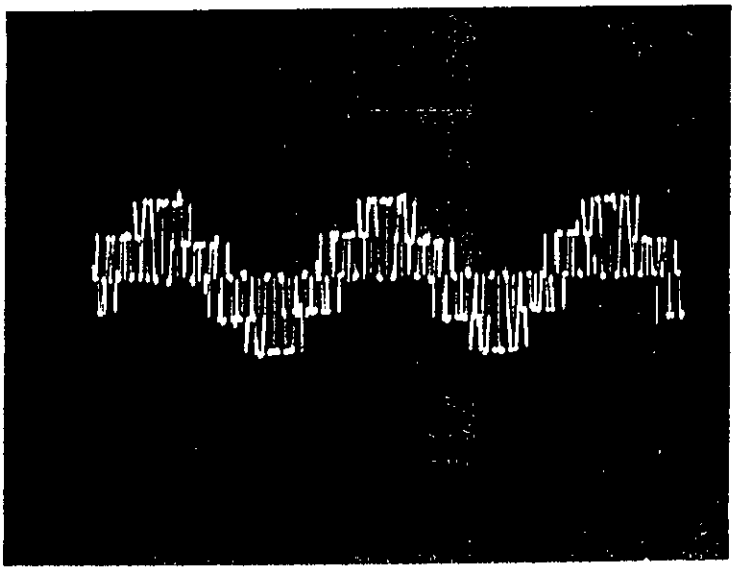

(a)

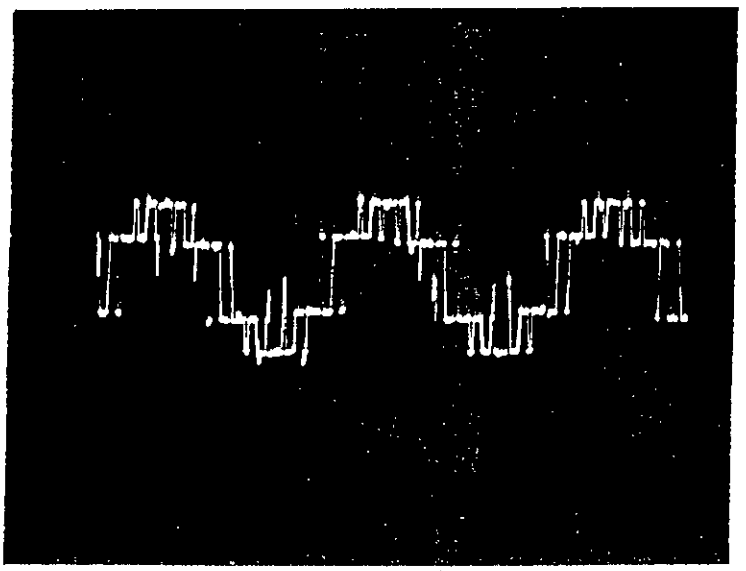

(b)

Fig. 2.17 Experimental neutral voltage waveforms of three-phase SPWM inverter for different N ($N_1 < N_2 < N_3$).

a) N_1 pulses b) N_2 pulses

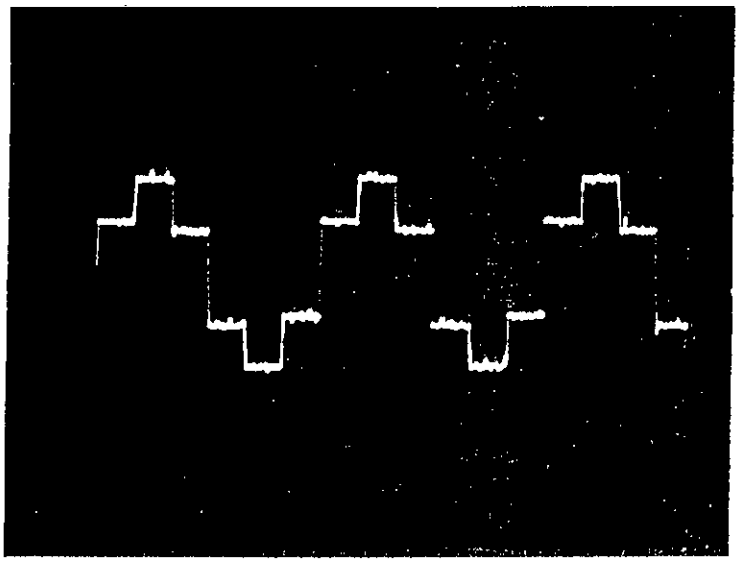

(c)

Fig. 2.17 Experimental neutral voltage waveforms of three-phase SPWM inverter for different N ($N_1 < N_2 < N_3$).

a) N_3 pulses

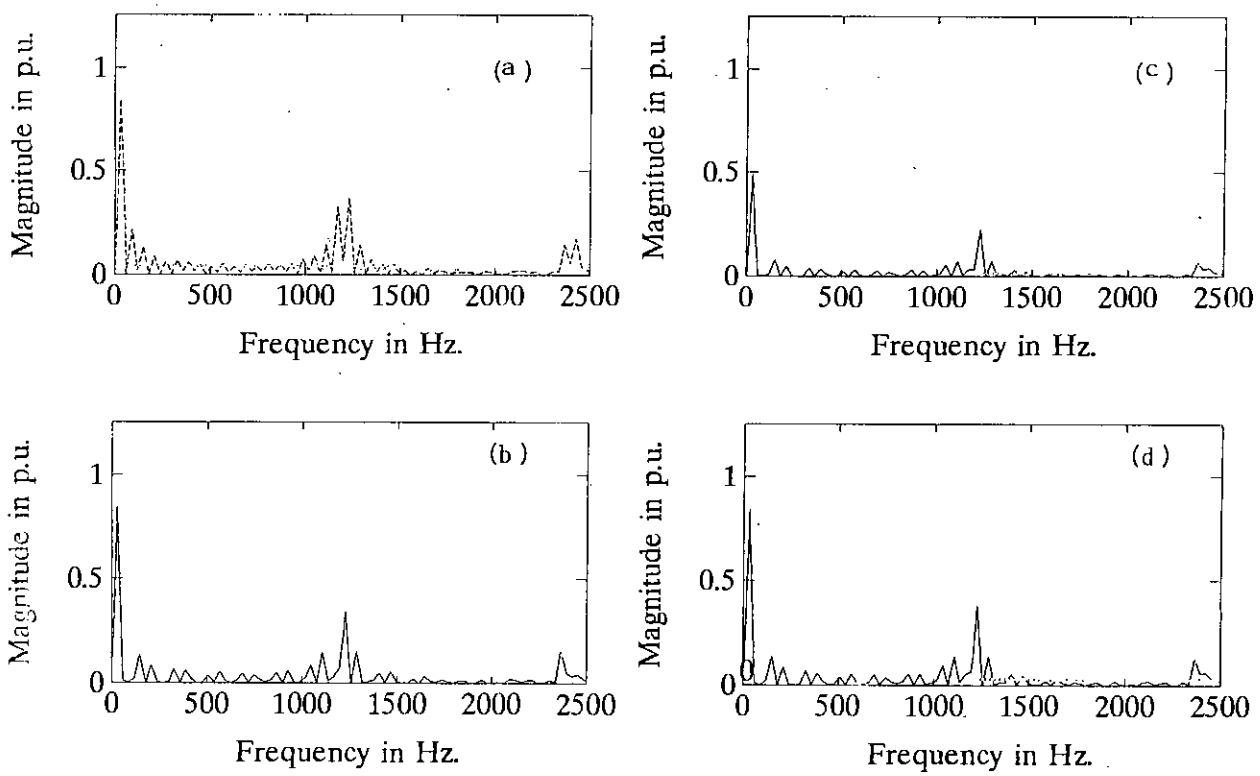

Fig. 2.18 Simulated spectrum of line, neutral, d-axis and q-axis voltages f= 30 Hz., N=80 and m=0.8).

a) Spectrum of line voltage. b)Spectrum of neutral voltage.

c) Spectrum of d-axis voltage. d) Spectrum of q-axis voltage.

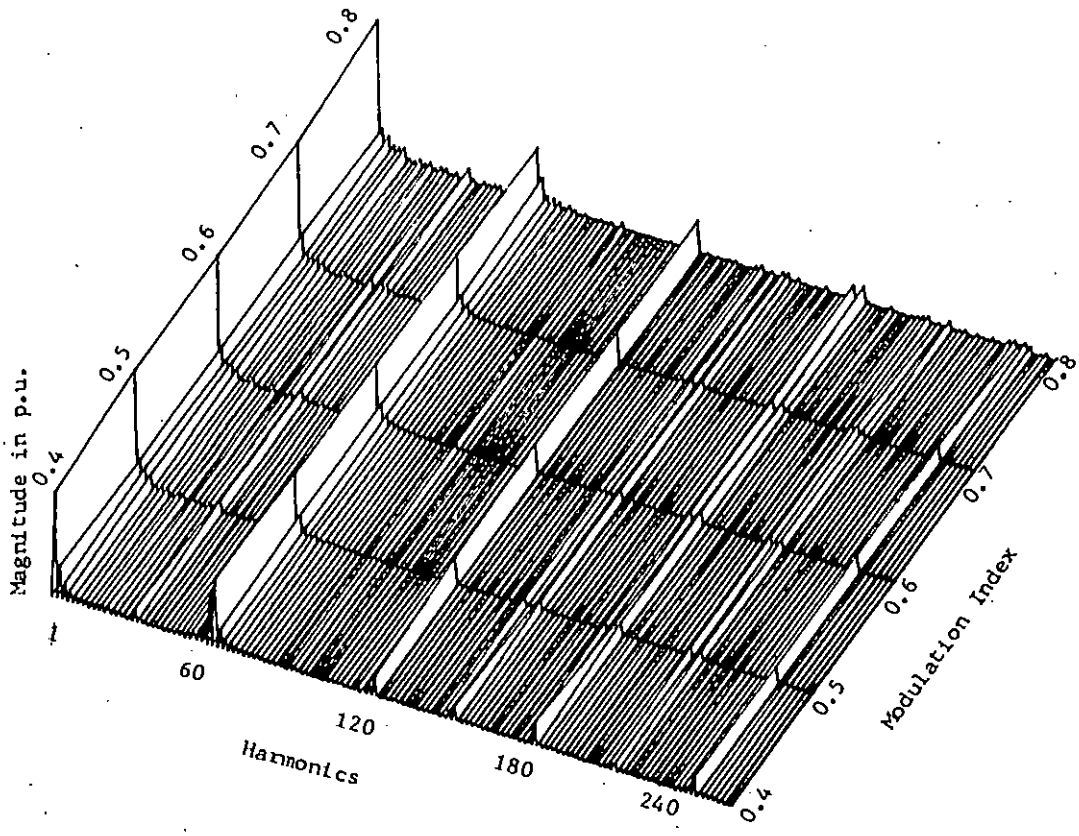

Fig. 2.19 Three dimensional spectrum of line voltage of SPWM inverter for f=30 Hz., N=60 and variable modulation index.

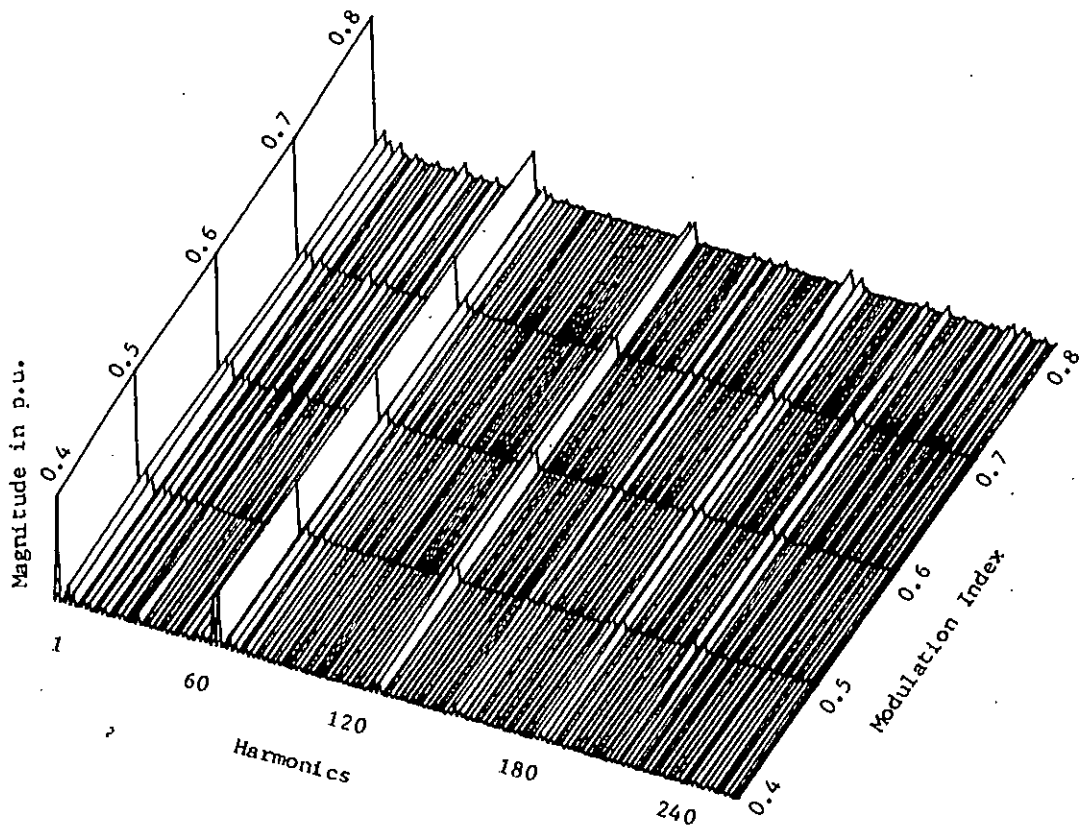

Fig. 2.20 Three dimensional spectrum of neutral voltage of SPWM inverter for f=30 Hz., N=60 and variable modulation index.

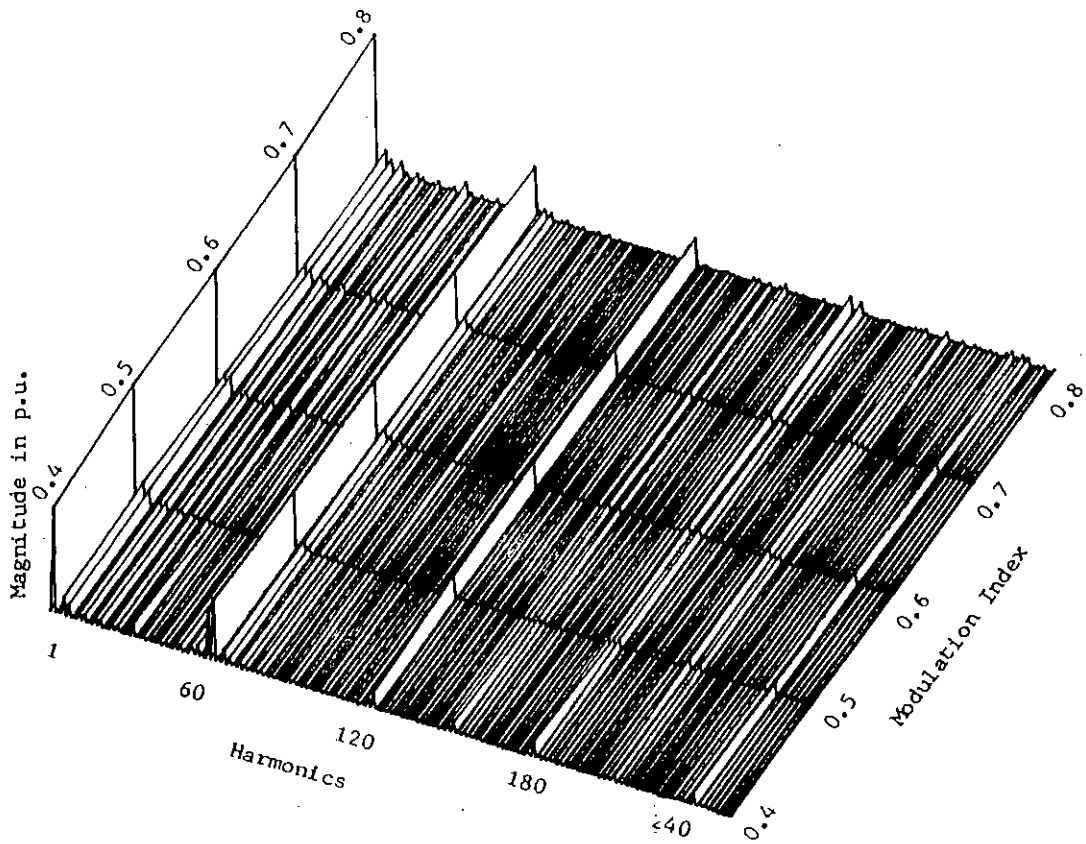

Fig. 2.21 Three dimensional spectrum of direct-axis voltage of SPWM inverter for f=30 Hz., N=60 and variable modulation index.

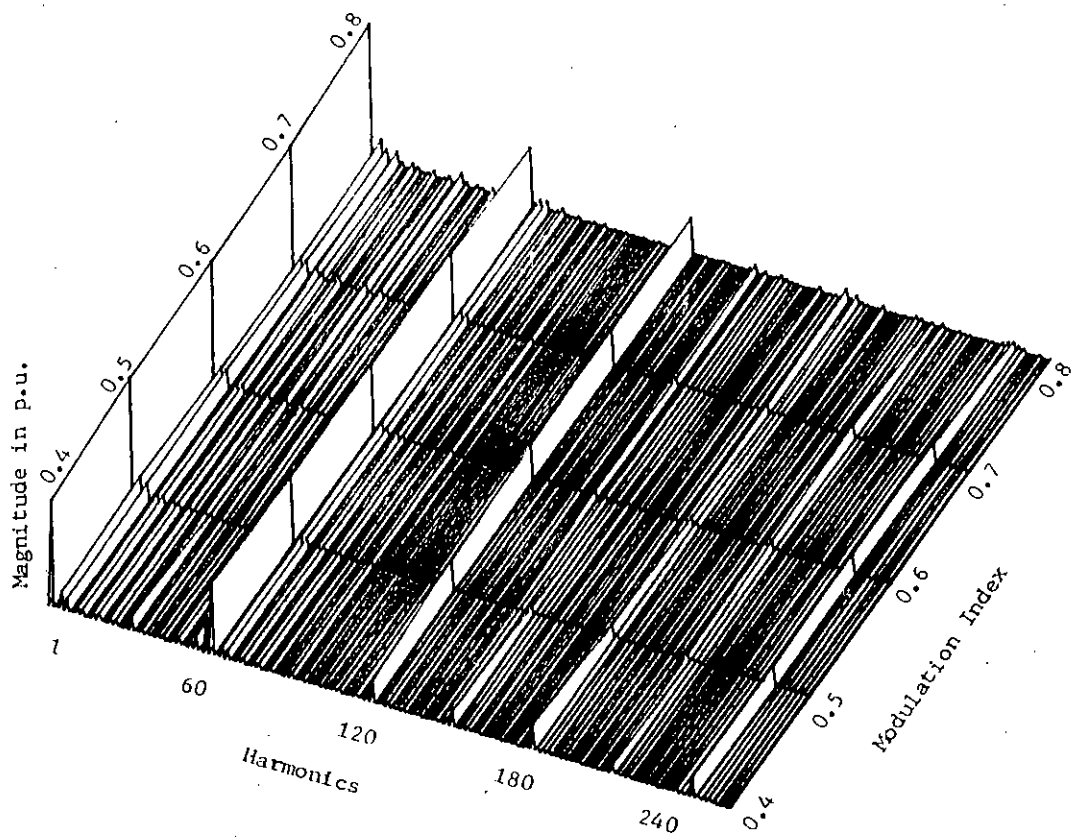

Fig. 2.22 Three dimensional spectrum of quadrature-axis voltage of SPWM inverter for f=30 Hz., N=60 and variable modulation index.

2.22 are spectra of line to neutral, d and q axes inverter voltages. The difference between 2.19 and 2.20, 2.21, 2.22 is in the magnitude of low frequency harmonics. Fig. 2.19 shows that line to line voltages at low frequency harmonics are quite significant. Low frequency components in spectra of fig. 2.20, 2.21, 2.22 are low compared to that of fig. 2.19. Figs. 2.23, 2.24, 2.25 and 2.26 are spectra of same waves but for different operating frequency (i.e. at 50 Hz.) and different carrier frequency (N=60). The properties of these spectra are same as those of figs. 2.19, 2.20, 2.21 and 2.22. Figs. 2.27, 2.28, 2.29, 2.30, fig. 2.31, 2.32, 2.33, 2.34 and figs. 2.35, 2.36, 2.37, 2.38 are spectra of SPWM inverter at different operating frequency for variable modulation index. As apparent from the study the trend of spectra are all same, however, actual occurrence of harmonics are at different frequencies. This is because the spectral plots are in harmonic orders (multiples of fundamental). Hence occurrence of first dominant harmonic in 30 Hz., 50 Hz. and 70 Hz. operations with N=40 are at 30x40, 50x40 and 70x40 Hz. (1.2 kHz., 2 kHz. and 2.8 kHz.) respectively. The shift in frequencies due to change in operating frequency change has many implications. One of them is that with constant carrier frequency, the switching of inverter switches become faster and may reach beyond operating range of device switching. Hence in SPWM technique as inverter goes to high frequency operation, the switching frequency (number of pulse per cycle) may have to be reduced as dictated by device rating. In summary it can be said that spectral variation of three phase line to line voltage are retained as in single phase voltage spectra. But the low frequency harmonics in line to neutral, d and q axes voltages are reduced. All other observations made for single phase inverter waves (section 2.4) apply equally for three phase inverter waveforms.

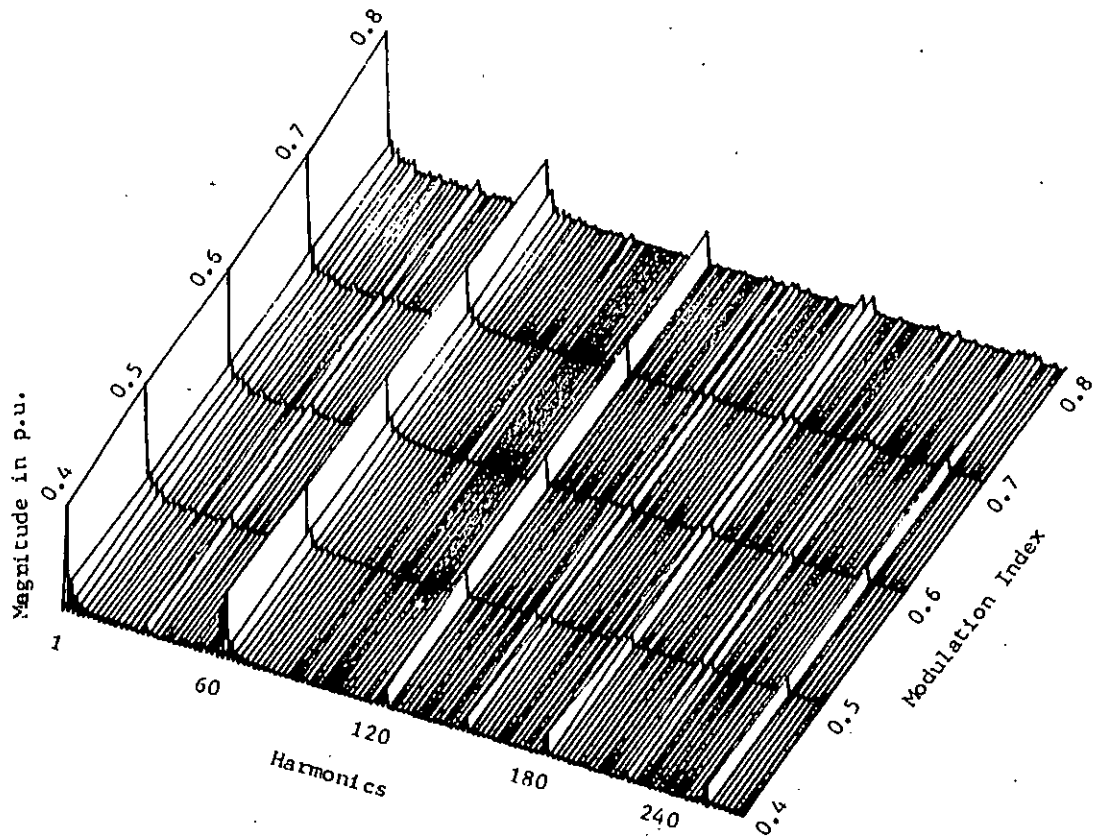

Fig. 2.23 Three dimensional spectrum of line voltage of SPWM inverter for for f=50 Hz., N=60 and variable modulation index.

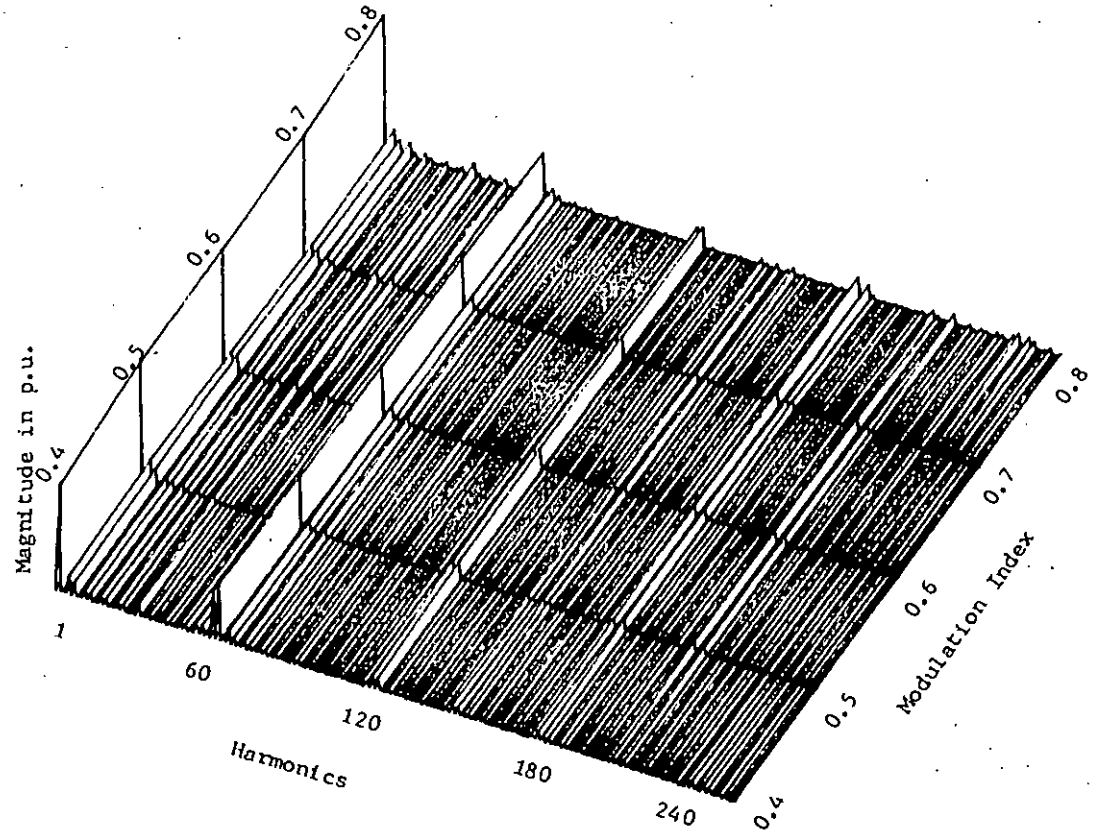

Fig. 2.24 Three dimensional spectrum of neutral voltage of SPWM inverter for f=50 Hz., N=60 and variable modulation index.

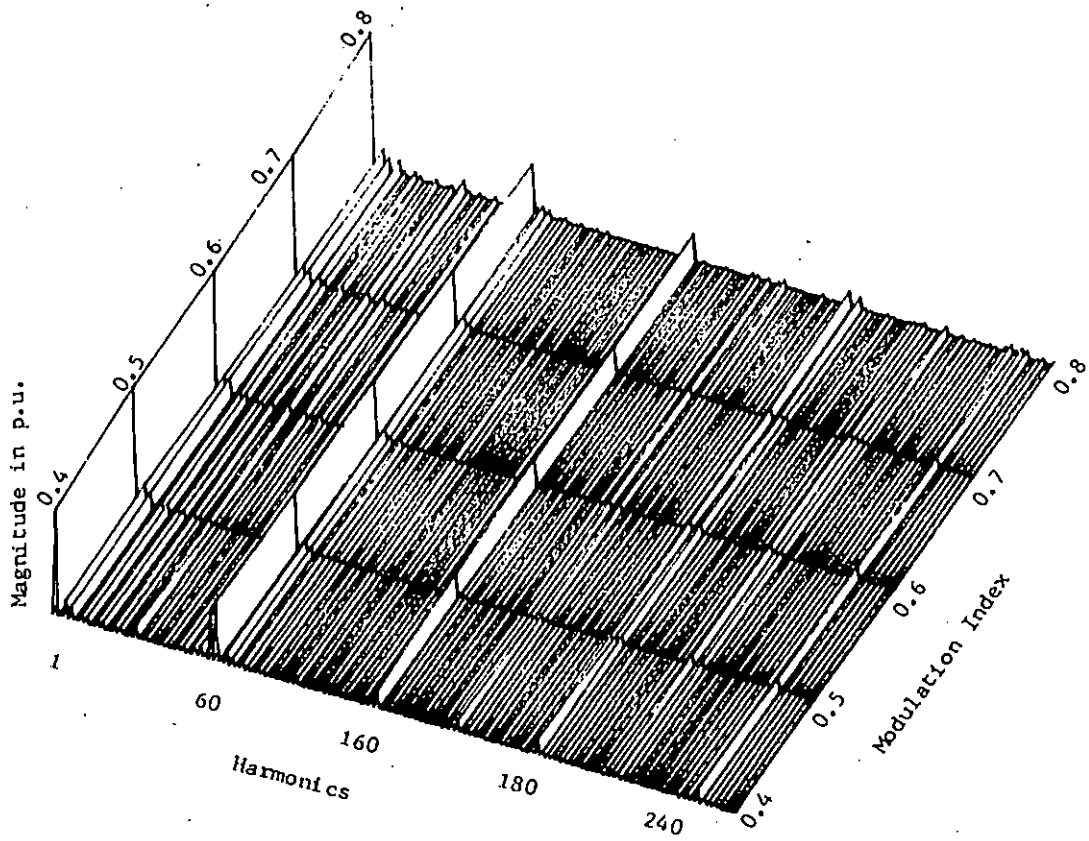

Fig. 2.25 Three dimensional spectrum of direct-axis voltage of SPWM inverter for f=50 Hz., N=60 and variable modulation index.

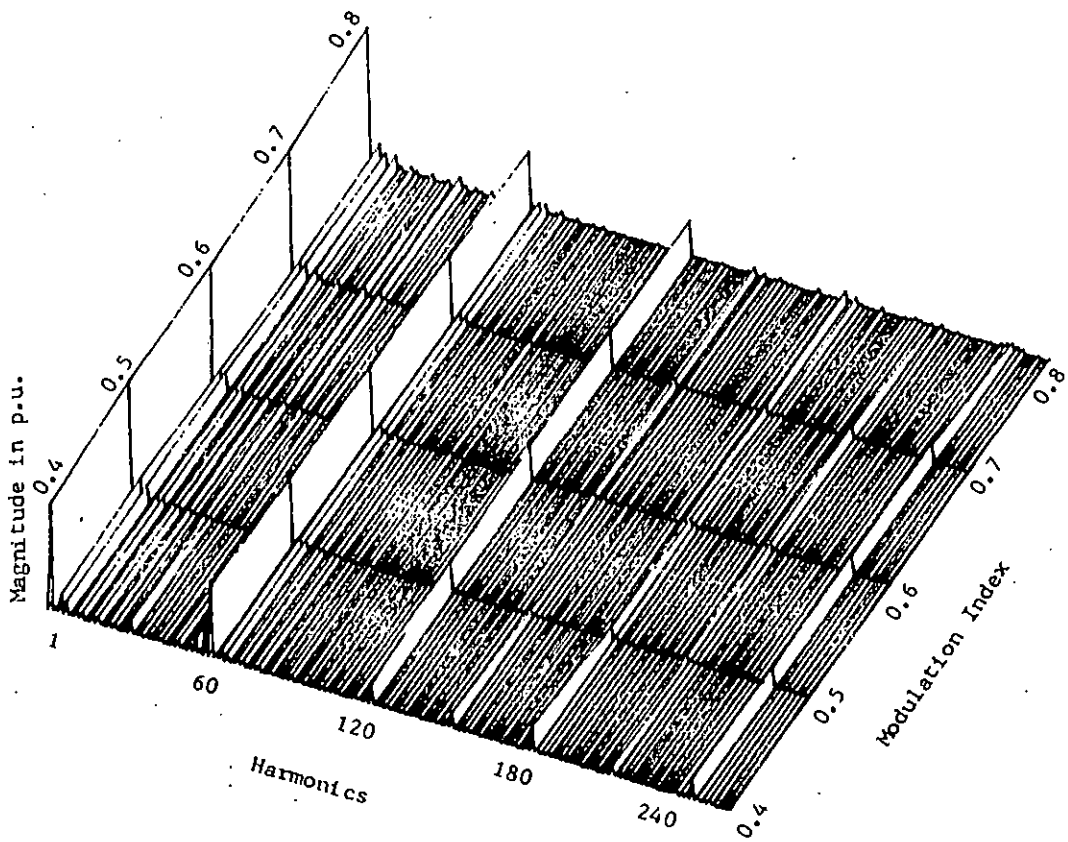

Fig. 2.26 Three dimensional spectrum of quadrature-axis voltage of SPWM inverter for f=50 Hz., N=60 and variable modulation index.

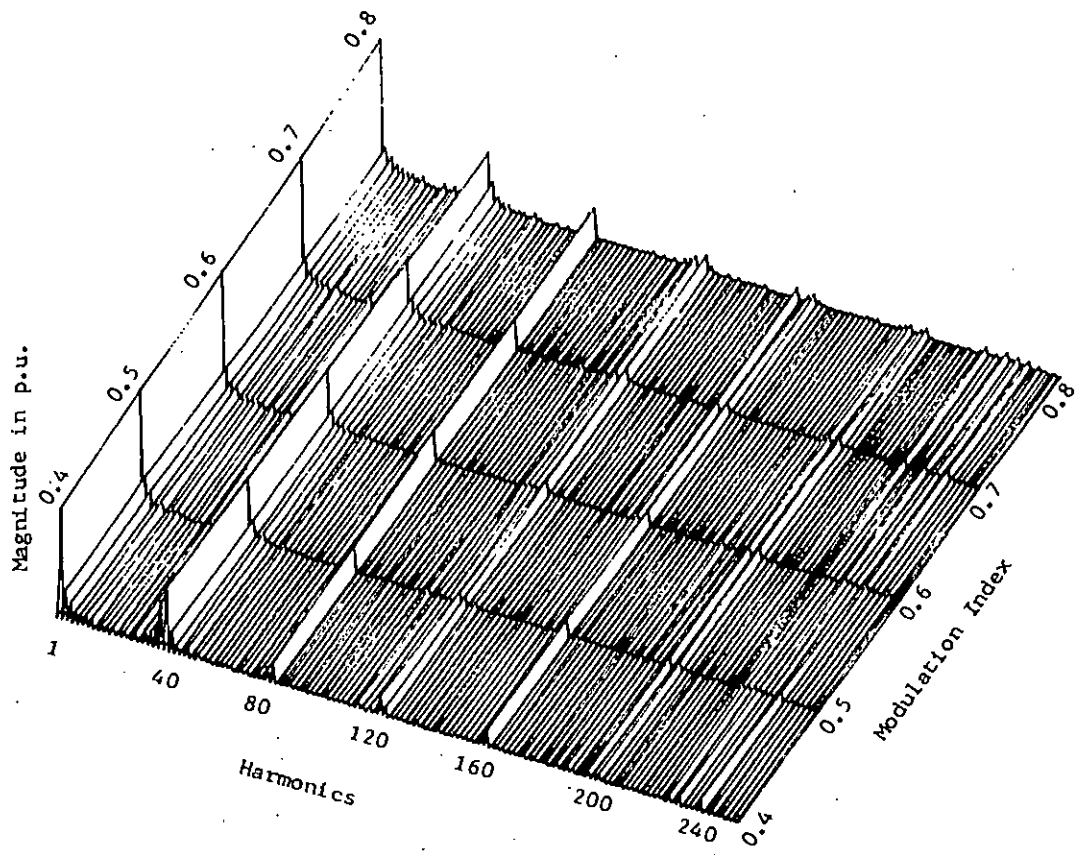

Fig. 2.27 Three dimensional spectrum of line voltage of SPWM inverter for f=30 Hz., N=40 and variable modulation index.

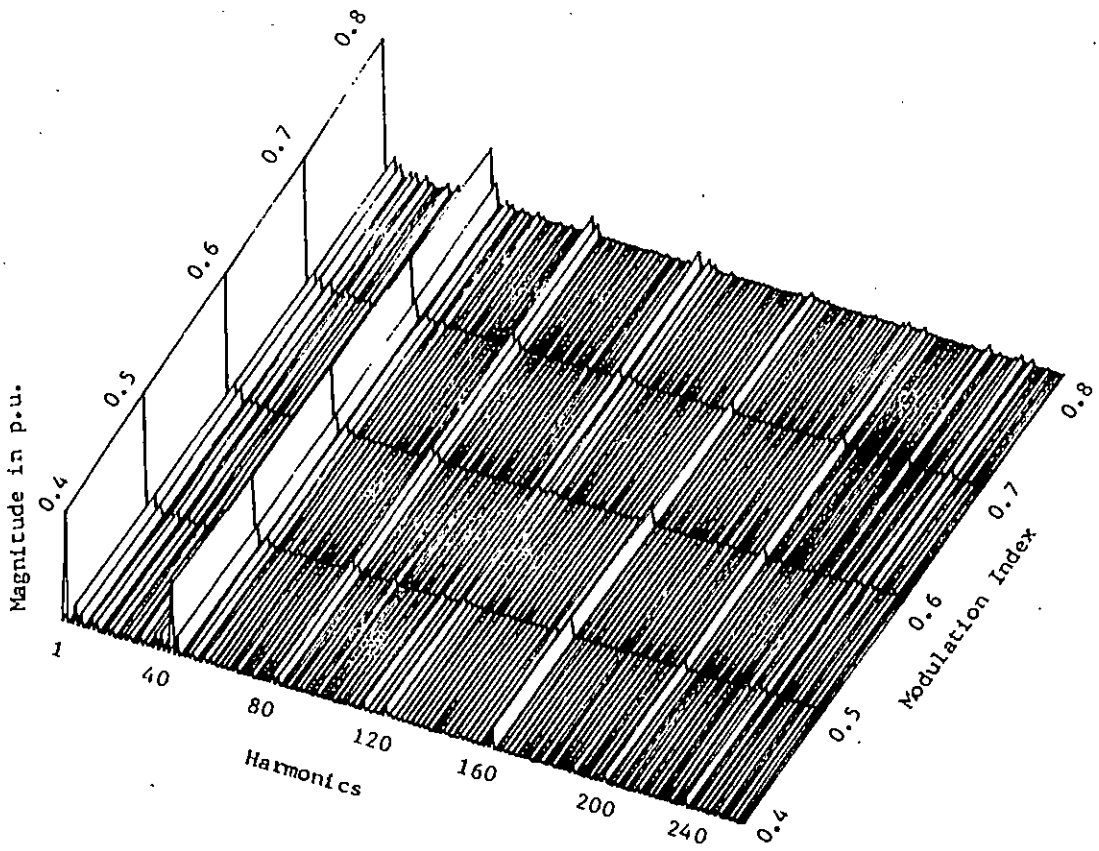

Fig. 2.28 Three dimensional spectrum of neutral voltage of SPWM inverter for f=30 Hz., N=40 and variable modulation index.

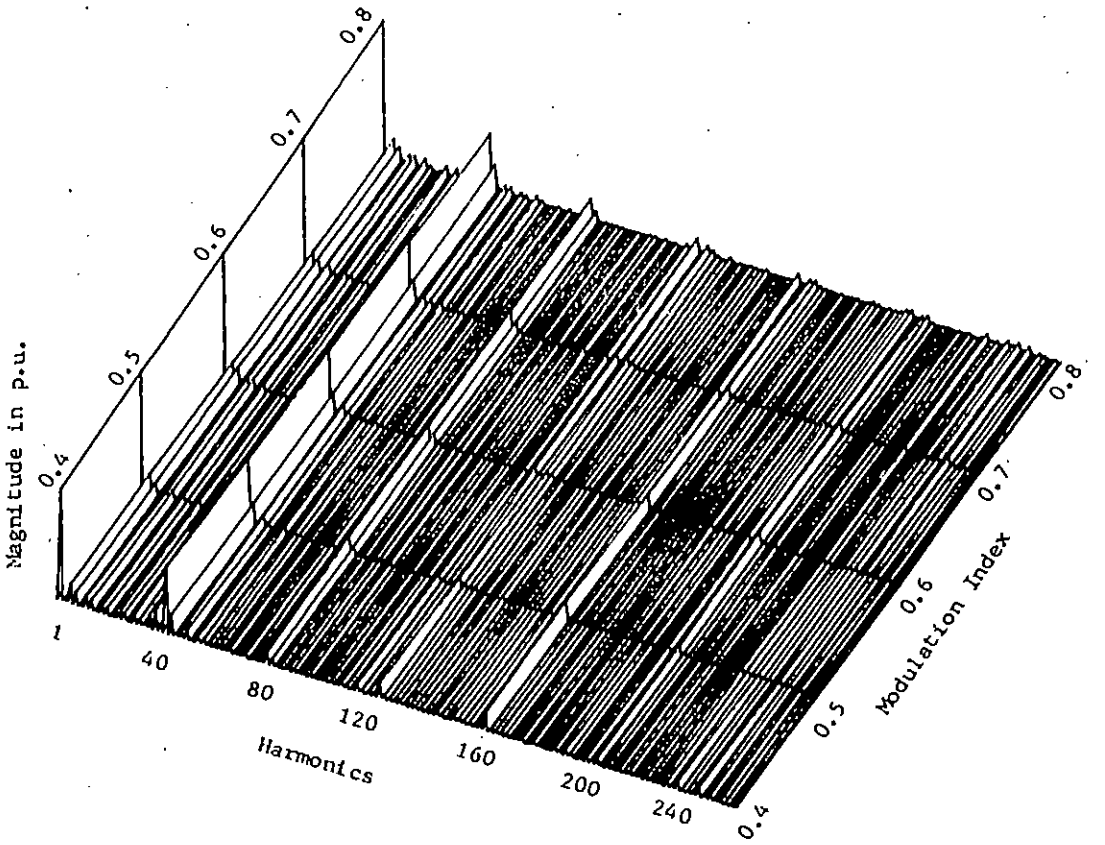

Fig. 2.20 Three dimensional spectrum of direct-axis voltage of SPWM inverter for f=30 Hz., N=40 and variable modulation index.

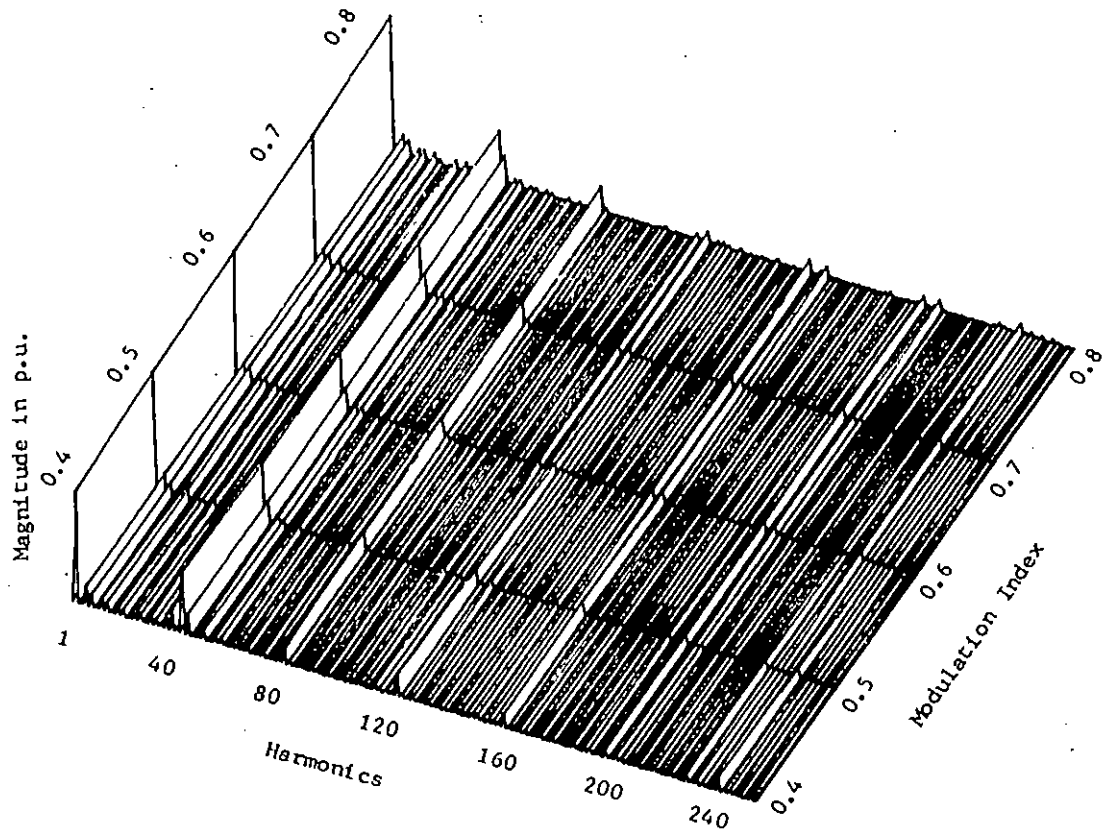

Fig. 2.30 Three dimensional spectrum of quadrature-axis voltage of SPWM inverter for f=30 Hz., N=40 and variable modulation index.

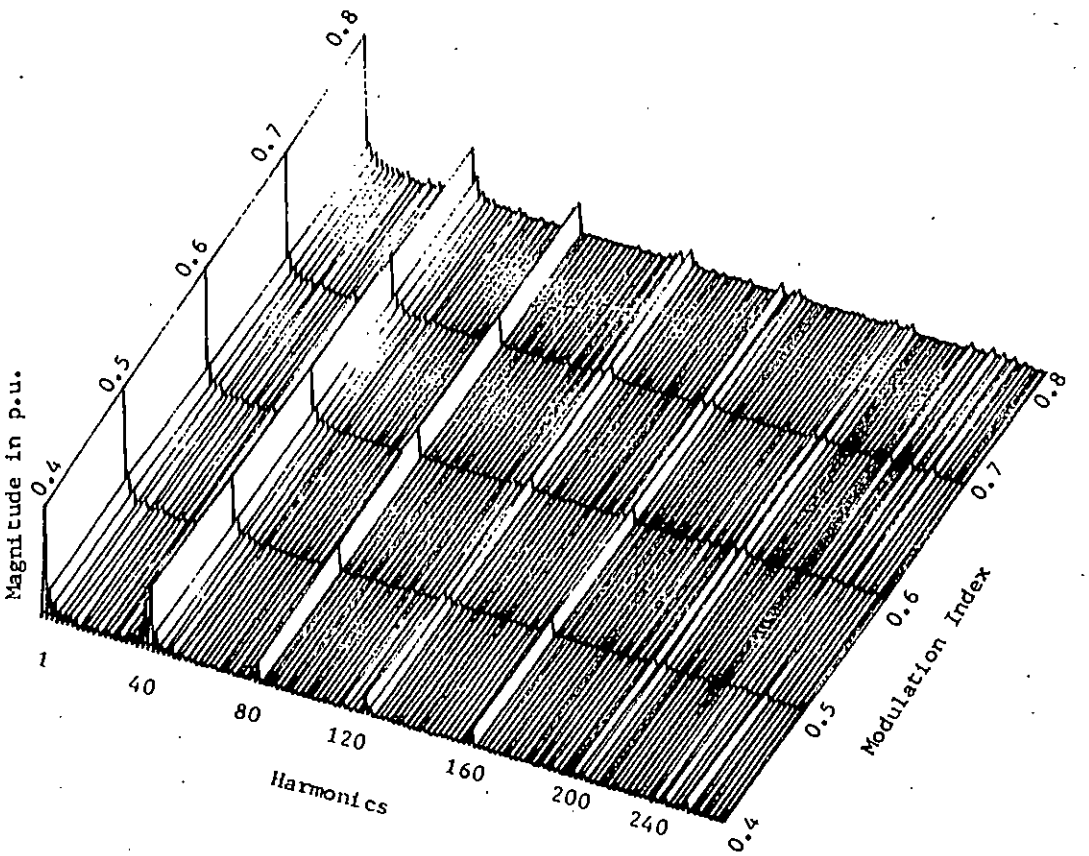

Fig. 2.31 Three dimensional spectrum of line voltage of SPWM inverter for, f=50 Hz., N=40 and variable modulation index.

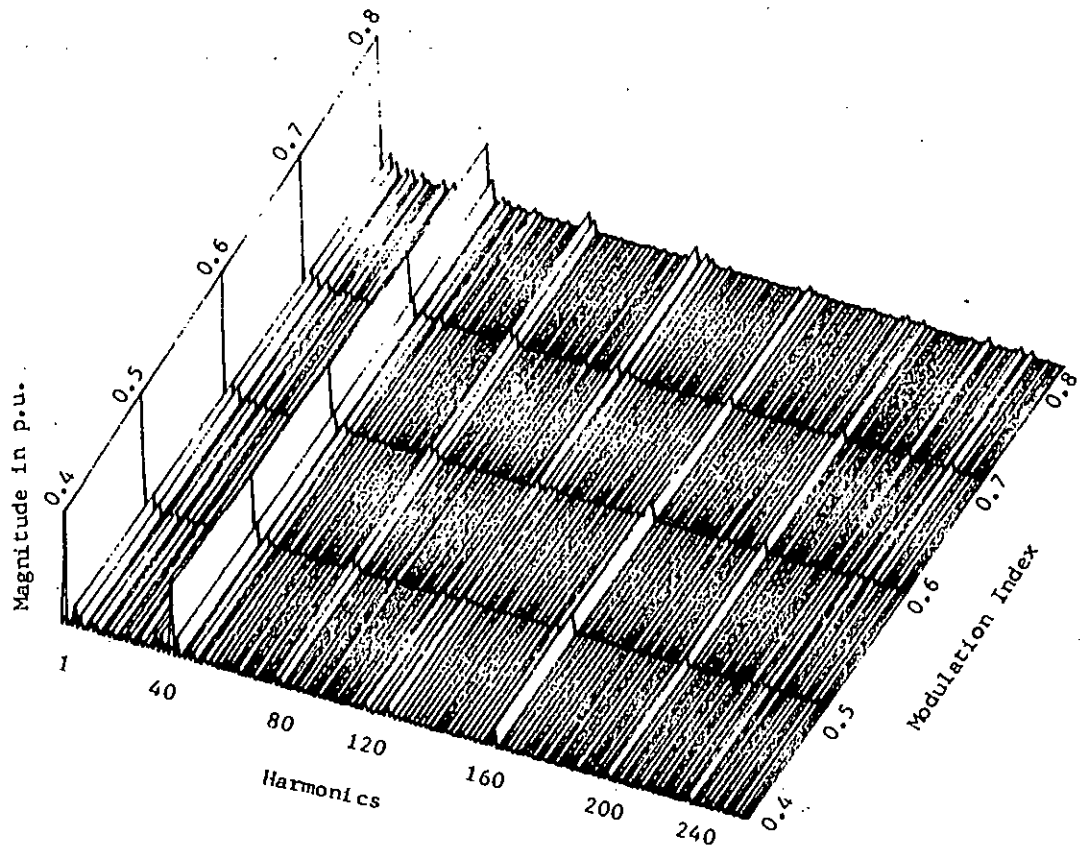

Fig. 2.32 Three dimensional spectrum of neutral voltage of SPWM inverter for f=50 Hz., N=40 and variable modulation index.

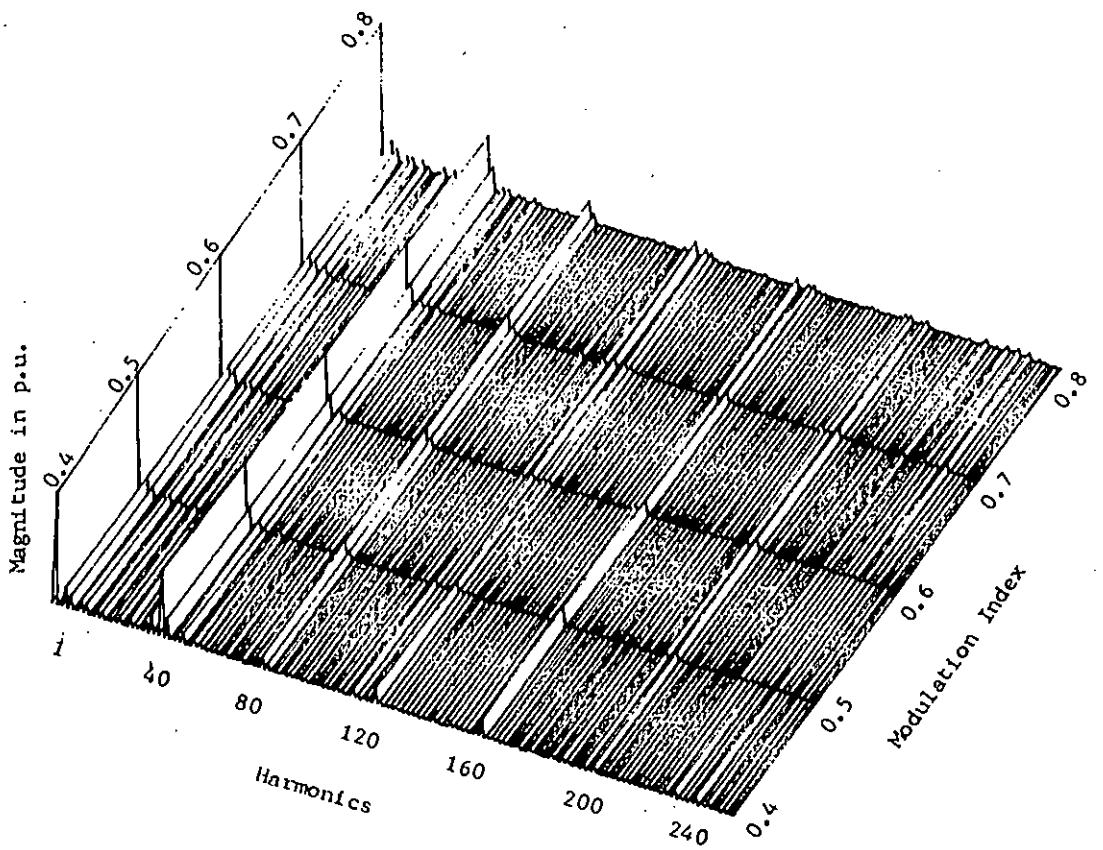

Fig. 2.33 Three dimensional spectrum of direct-axis voltage of SPWM inverter for f=50 Hz., N=40 and variable modulation index.

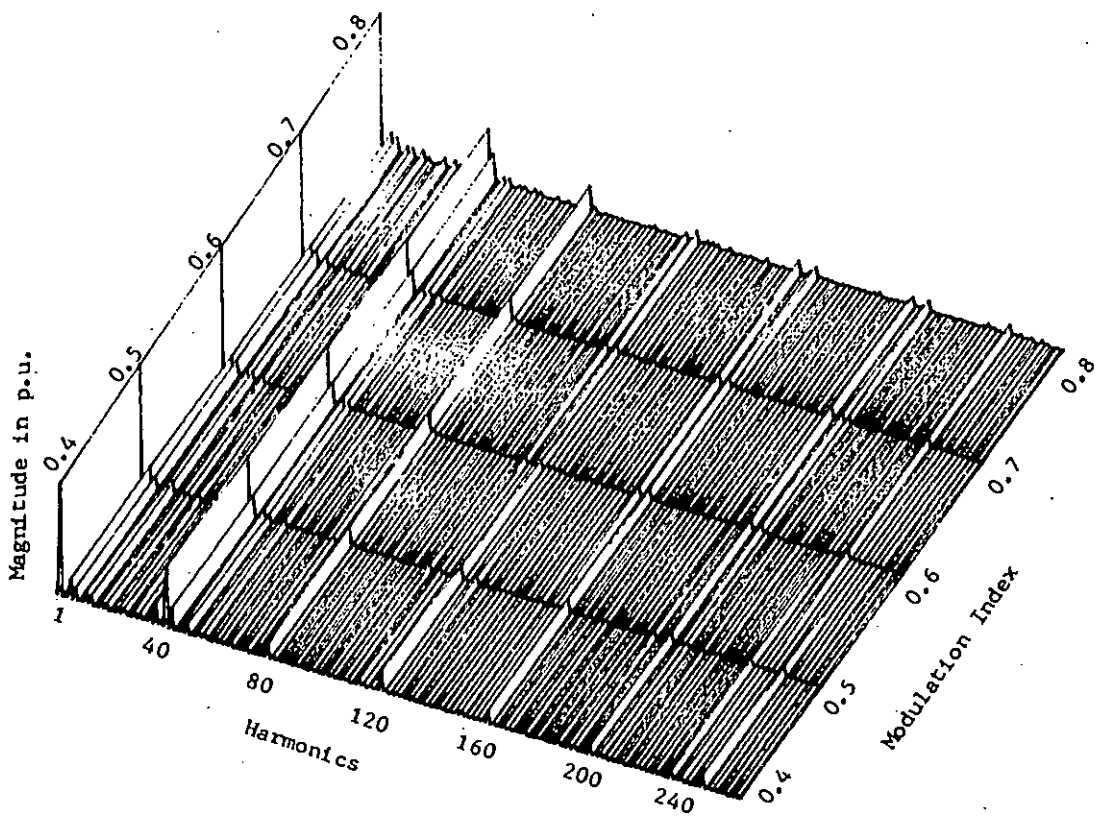

Fig. 2.34 Three dimensional spectrum of quadrature-axis voltage of SPWM inverter for f=50 Hz., N=40 and variable modulation index.

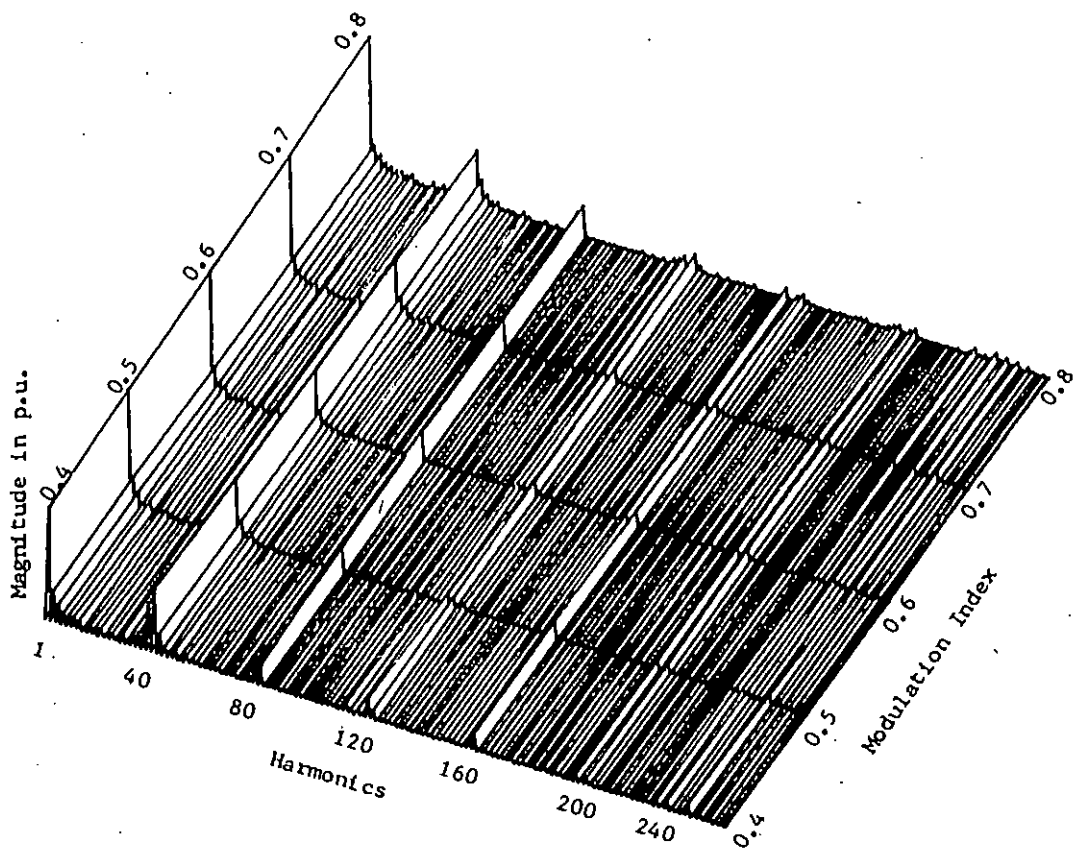

Fig. 2.35 Three dimensional spectrum of line voltage of SPWM inverter for f=70 Hz., N=40 and variable modulation index.

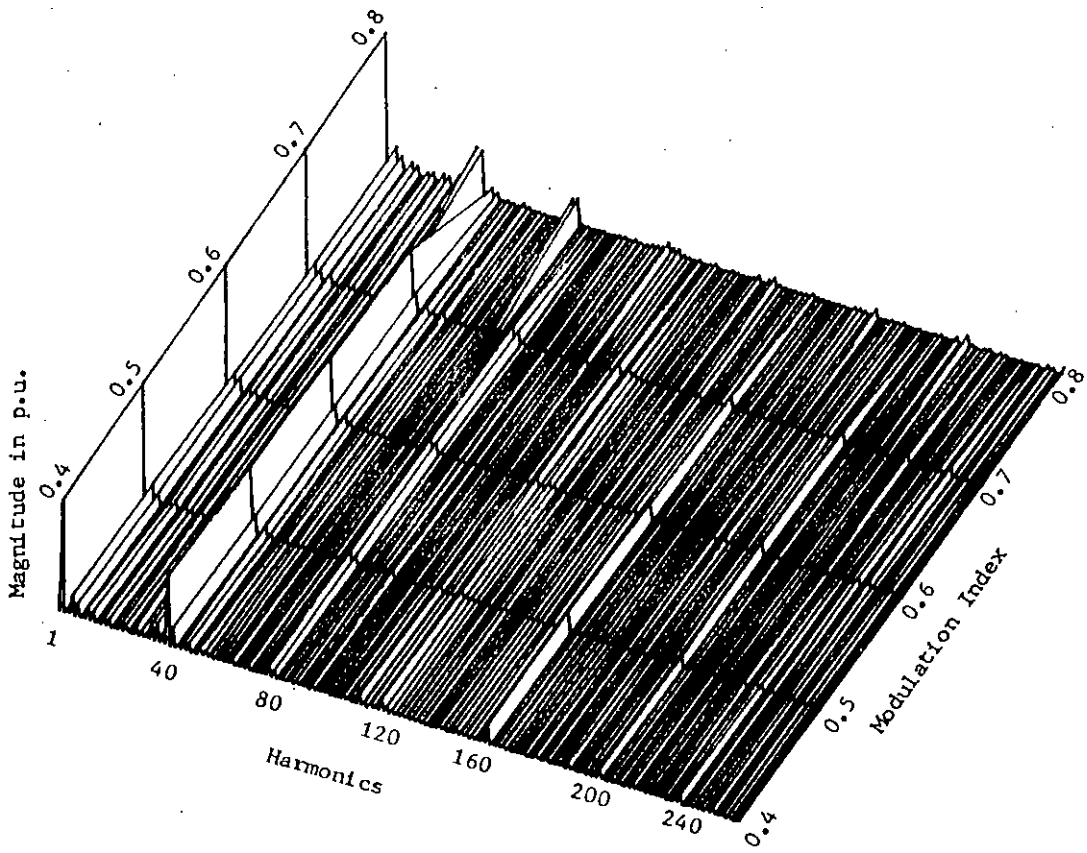

Fig. 2.36 Three dimensional spectrum of neutral voltage of SPWM inverter for f=70 Hz., N=40 and variable modulation index.

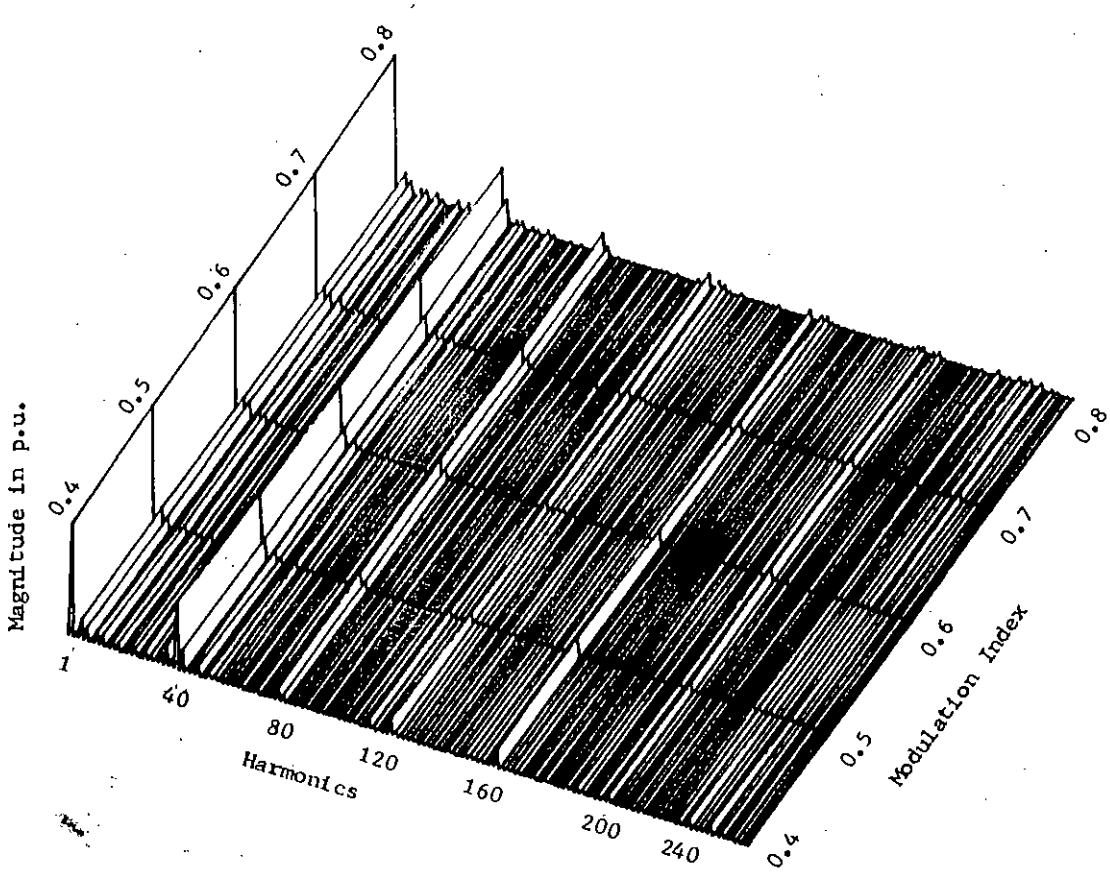

Fig. 2.37 Three dimensional spectrum of direct-axis voltage of SPWM inverter for f=70 Hz., N=40 and variable modulation index.

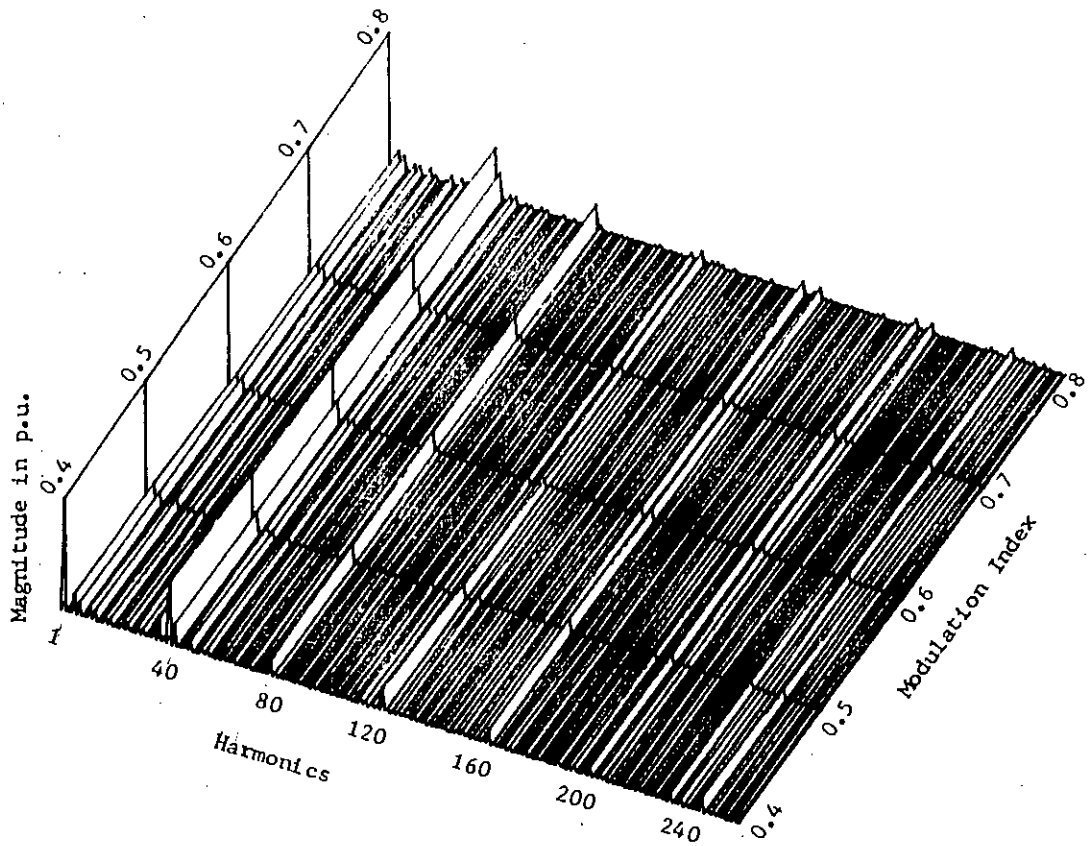

Fig. 2.38 Three dimensional spectrum of quadrature-axis voltage of SPWM inverter for f= 70 Hz., N=40 and variable modulation index.

CHAPTER 3

STARTING PERFORMANCE OF INDUCTION MACHINE

3.1 INTRODUCTION

Starting performances of a.c. machines with sinusoidal input are evaluated theoretically by numerical solution of machine-voltage equations in d-q axes. Induction machine in d-q axes can be represented by five simultaneous differential equations, from which both transient and steady state performances of the machine can be predicted. Such predictions are necessary for estimating machines' time response, peak starting current, torque and speed etc. As static converters are being introduced in adjustable speed a.c. drives, study of transient performances of the machines are being subject of investigation just like their predecessors (i.e. utility fed machines). Since static converter voltages are non sinusoidal, the solution of converter-fed induction machines are not straight forward. Conventional method of performance evaluation of an inverter-fed induction machine requires representing

the input voltages in their harmonic components and the machine in its harmonic model . Solution of these models are carried out for individual harmonics and overall performance is evaluated by superposition of individual responses. The computational involvement in such analysis is complex and time consuming, and the accuracy of the predicted results are dependent on the number of harmonics considered.

For square wave inverters, truncation of Fourier series in inverter-fed machine performance analysis may be practical due to the occurrence of low order harmonics and as high frequency harmonics diminishes gradually. But advanced PWM inverters have dominant harmonics near carrier and multiples of carrier frequencies. Hence truncation of Fourier series at a frequency lower than carrier frequency would cause significant series truncation error in the results. If a large number of harmonics are to be considered in the performance analysis, time required for computation of performance would be prohibitively high.

In this thesis, time domain analysis is proposed for evaluating starting performance of pulse width modulated inverter-fed induction machines. In this method inverter voltages are defined in time domain and machine responses to nonsinusoidal pwm voltage waves are evaluated at each interval of time and the process is continued for desired time span. Such evaluation is free from errors encountered in frequency domain analysis (due to Fourier series truncation) and requires less computational time.

3.2 STARTING PERFORMANCE OF IM DUE TO SINE INPUT

3.2.1 VOLTAGE EQUATIONS

Utility supply voltages can be represented in d-q axes. The d-q axes voltages V_d and V_q are obtained by the following transformation [50].

$$\begin{bmatrix} V_q \\ V_d \end{bmatrix} = \frac{2}{3}\begin{bmatrix} 0 & \frac{\sqrt{3}}{2} & -\frac{\sqrt{3}}{2} \\ 1 & -\frac{1}{2} & -\frac{1}{2} \end{bmatrix}\begin{bmatrix} V_{ab} \\ V_{bc} \\ V_{ca} \end{bmatrix} \tag{3.1}$$

where,

$$V_{ab} = V_m sin(\omega t) \tag{3.2}$$

$$V_{bc} = V_m sin(\omega t - 120^o) \tag{3.3}$$

$$V_{ca} = V_m sin(\omega t - 240^o) \tag{3.4}$$

3.2.2 MACHINE MODEL

Motor performance analysis requires suitable motor model. In this thesis d-q axis motor equivalent circuits has been used as machine model . Fig. 3.1 shows d-q axes motor equivalent circuit for an inverter-fed induction motor [50]. The motor equations based on this model can be derived as follows

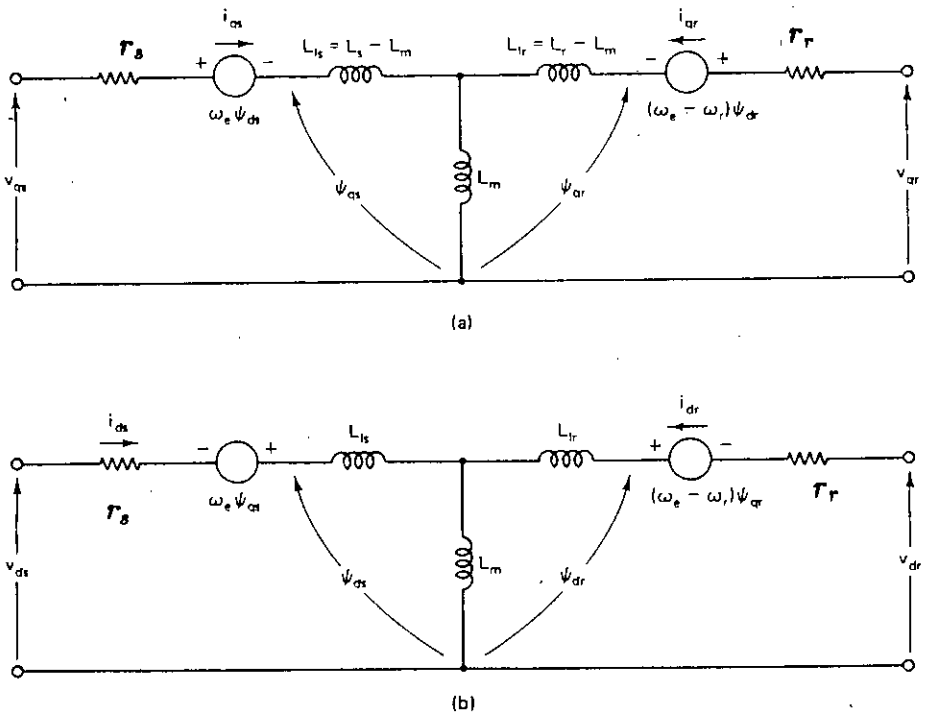

Fig. 3.1 D-Q equivalent circuits of induction machine.

a) q-axis circuit.

b) d-axis circuit.

In synchronously rotating axis

Stator side equations are

$$V_{qs} = r_s i_{qs} + \frac{d\psi_{qs}}{dt} + \omega_e \psi_{ds} \tag{3.5}$$

$$V_{ds} = r_s i_{ds} + \frac{d\psi_{ds}}{dt} - \omega_e \psi_{qs} \tag{3.6}$$

Rotor side equations are

$$V_{qr} = r_r i_{qr} + \frac{d\psi_{qr}}{dt} + (\omega_e - \omega_r)\,\psi_{dr} \tag{3.7}$$

$$V_{dr} = r_r i_{dr} + \frac{d\psi_{dr}}{dt} - (\omega_e - \omega_r)\,\psi_{qr} \tag{3.8}$$

where,

$$\psi_{qs} = L_{ls} i_{qs} + L_m\,(i_{qs} + i_{qr}) \tag{3.9}$$

$$\psi_{qr} = L_{lr} i_{qr} + L_m\,(i_{qs} + i_{qr}) \tag{3.10}$$

$$\psi_{ds} = L_{ls} i_{ds} + L_m\,(i_{ds} + i_{dr}) \tag{3.11}$$

$$\psi_{dr} = L_{lr} i_{dr} + L_m\,(i_{ds} + i_{dr}) \tag{3.12}$$

Substituting equation 3.9 to 3.12 in 3.5 to 3.8 and taking into consideration that

$$L_s = L_{ls} + L_m \tag{3.13}$$

$$L_r = L_{lr} + L_m \tag{3.14}$$

and

$$p = \frac{d}{dt} \tag{3.15}$$

The following matrix relationship can be obtained,

$$\begin{bmatrix} V_{qs} \\ V_{ds} \\ V_{qr} \\ V_{dr} \end{bmatrix} = \begin{bmatrix} r_s + L_s p & \omega_e L_m & L_m p & \omega_e L_m \\ -\omega_e L_s & r_s + L_s p & -\omega_e L_m & L_m p \\ L_m p & (\omega_e - \omega_r) L_m & r_r + L_r p & (\omega_e - \omega_r) L_r \\ -(\omega_e - \omega_r) L_m & L_m p & -(\omega_e - \omega_r) L_r & r_r + L_r p \end{bmatrix} \begin{bmatrix} i_{qs} \\ i_{ds} \\ i_{qr} \\ i_{dr} \end{bmatrix} \tag{3.16}$$

In the stationary axis $\omega_e = 0$, $V_{qr} = 0$ and $V_{dr} = 0$, hence model stands as

$$\begin{bmatrix} V_{qs} \\ V_{ds} \\ 0 \\ 0 \end{bmatrix} = \begin{bmatrix} r_s + L_s p & 0 & L_m p & 0 \\ 0 & r_s + L_s p & 0 & L_m p \\ L_m p & -\omega_r L_m & r_r + L_r p & -\omega_r L_r \\ \omega_r L_m & L_m p & \omega_r L_r & r_r + L_r p \end{bmatrix} \begin{bmatrix} i_{qs} \\ i_{ds} \\ i_{qr} \\ i_{dr} \end{bmatrix} \tag{3.17}$$

Further simplification can be made by setting derivatives of V_{qs} and V_{ds} voltage equations to zero as,

$$\begin{bmatrix} V_{qs} \\ V_{ds} \\ 0 \\ 0 \end{bmatrix} = \begin{bmatrix} r_s & 0 & 0 & 0 \\ 0 & r_s & 0 & 0 \\ L_m p & -\omega_r L_m & r_r + L_r p & -\omega_r L_r \\ \omega_r L_m & L_m p & \omega_r L_r & r_r + L_r p \end{bmatrix} \begin{bmatrix} i_{qs} \\ i_{ds} \\ i_{qr} \\ i_{dr} \end{bmatrix} \tag{3.18}$$

To make computation easier it is desired to change the d-q axes voltage dependency from two variables to a single variable. Flux can be expressed in terms of currents

and thus computer solution of equation 3.18 can be made easier. For making this simplification let,

$$\psi = \begin{bmatrix} \psi_{qs} & \psi_{ds} & \psi_{qr} & \psi_{dr} \end{bmatrix} \tag{3.19}$$

and

$$L = \begin{bmatrix} L_s & 0 & L_m & 0 \\ 0 & L_s & 0 & L_m \\ L_m & 0 & L_r & 0 \\ 0 & L_m & 0 & L_r \end{bmatrix} \tag{3.20}$$

then

$$L^{-1} = \frac{1}{L_s L_r - {L_m}^2} \begin{bmatrix} L_r & 0 & -L_m & 0 \\ 0 & L_r & 0 & -L_m \\ -L_m & 0 & L_s & 0 \\ 0 & -L_m & 0 & L_s \end{bmatrix} \tag{3.21}$$

As

$$i = L^{-1}\psi \tag{3.22}$$

Substitution of $L_s L_r - {L_m}^2 = A$ and equations 3.22, 3.19 and 3.21 in 3.18 gives the required single variable dependent equation as,

$$\begin{bmatrix} V_{qs} \\ V_{ds} \\ 0 \\ 0 \end{bmatrix} = \begin{bmatrix} \frac{r_s L_r}{A} & 0 & -\frac{r_s L_m}{A} & 0 \\ 0 & \frac{r_s L_r}{A} & 0 & -\frac{r_s L_m}{A} \\ -\frac{r_r L_m}{A} & 0 & \frac{r_r L_s}{A} + p & -\omega_r \\ 0 & -\frac{r_r L_m}{A} & \omega_r & \frac{r_r L_s}{A} + p \end{bmatrix} \begin{bmatrix} \psi_{qs} \\ \psi_{ds} \\ \psi_{qr} \\ \psi_{dr} \end{bmatrix} \tag{3.23}$$

The above simplified form of machine model equations require simultaneous differential equation solution . The voltage equations can be obtained from inverter voltage waveform of section 2.5. The single variable flux used in equation 3.19 can

be found by using these voltage equations of inverter waveforms. Flux information can be obtained from the following equation,

$$\begin{bmatrix} \psi_{qs} \\ \psi_{ds} \\ \psi_{qr} \\ \psi_{dr} \end{bmatrix} = \begin{bmatrix} \frac{r_s L_r}{A} & 0 & -\frac{r_s L_m}{A} & 0 \\ 0 & \frac{r_s L_r}{A} & 0 & -\frac{r_s L_m}{A} \\ -\frac{r_r L_m}{A} & 0 & \frac{r_r L_s}{A} + p & -\omega_r \\ 0 & -\frac{r_r L_m}{A} & \omega_r & \frac{r_r L_s}{A} + p \end{bmatrix}^{-1} \begin{bmatrix} V_{qs} \\ V_{ds} \\ 0 \\ 0 \end{bmatrix} \tag{3.24}$$

Knowing flux information equation 3.22 can be used to obtain the currents as,

$$\begin{bmatrix} i_{qs} \\ i_{ds} \\ i_{qr} \\ i_{dr} \end{bmatrix} = \begin{bmatrix} \frac{L_r}{A} & 0 & -\frac{L_m}{A} & 0 \\ 0 & \frac{L_r}{A} & 0 & -\frac{L_m}{A} \\ -\frac{L_m}{A} & 0 & \frac{L_s}{A} & 0 \\ 0 & -\frac{L_m}{A} & 0 & \frac{L_s}{A} \end{bmatrix} \begin{bmatrix} \psi_{qs} \\ \psi_{ds} \\ \psi_{qr} \\ \psi_{dr} \end{bmatrix} \tag{3.25}$$

The information about torque can be found from the following equation,

$$T_e = \frac{3}{2}\left(\frac{P}{2}\right) L_m \left(i_{qs} i_{dr} - i_{ds} i_{qr}\right) \tag{3.26}$$

where,

P = number of poles

T_e = developed torque

Finally speed can be obtained from the following expression,

$$(T_e - T_l) = \frac{2}{P} J \frac{d\omega_r}{dt} \tag{3.27}$$

$$\frac{P}{2J}(T_e - T_l) = \frac{d\omega_r}{dt} \tag{3.28}$$

where,

J = moment of inertia

T_l = load torque

3.3 COMPUTER PROGRAM

A wound rotor induction motor has been used for computer simulation and experimental purpose. Machine parameters were obtained experimentally and the values are given in appendix-A. A program has been developed to simulate the transient response of machine and the output of this program is used to study the following,

- Machine speed vs. time
- Line current vs. time
- Torque vs. time
- Torque vs. speed

A flow chart of the computer program is shown in appendix-B. The program was executed for different input voltages such as sinusoidal, SPWM and square wave voltages.

3.4 RESULTS

Fig. 3.2 show theoretically evaluated starting response of an induction motor. Starting speed, line current torque vs. time and torque vs. speed are shown in figs. 3.2 (a)-(d). All these characteristics were obtained for utility sine input by time domain analysis. Since the motor is a small one ($\frac{1}{4}$ hp, 400v l-l), the responses are fast and current during start is low. Low current during start for a small machine

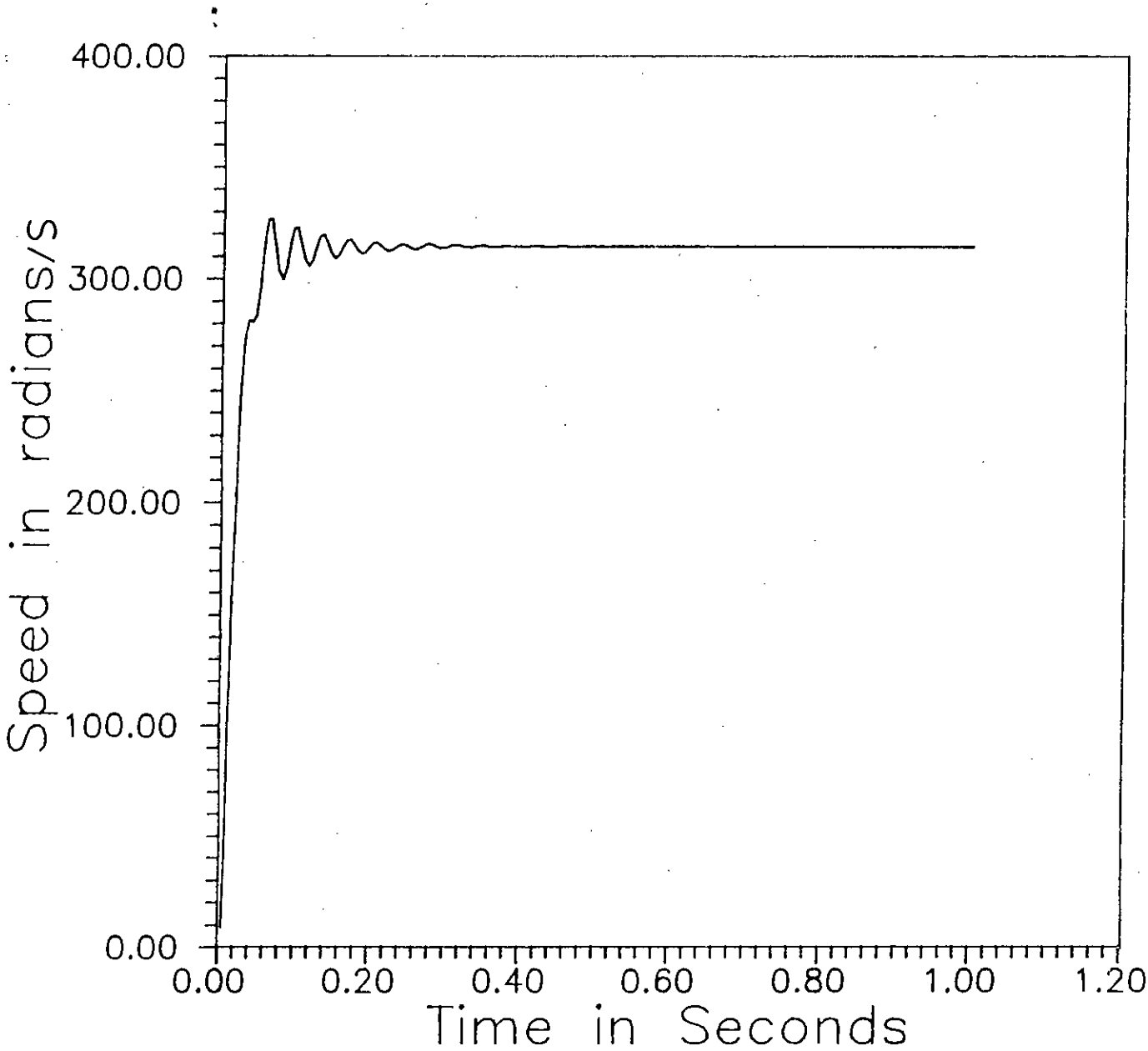

Fig. 3.2 a) Speed vs. time characteristic of induction machine for sinusoidal input (time domain analysis).

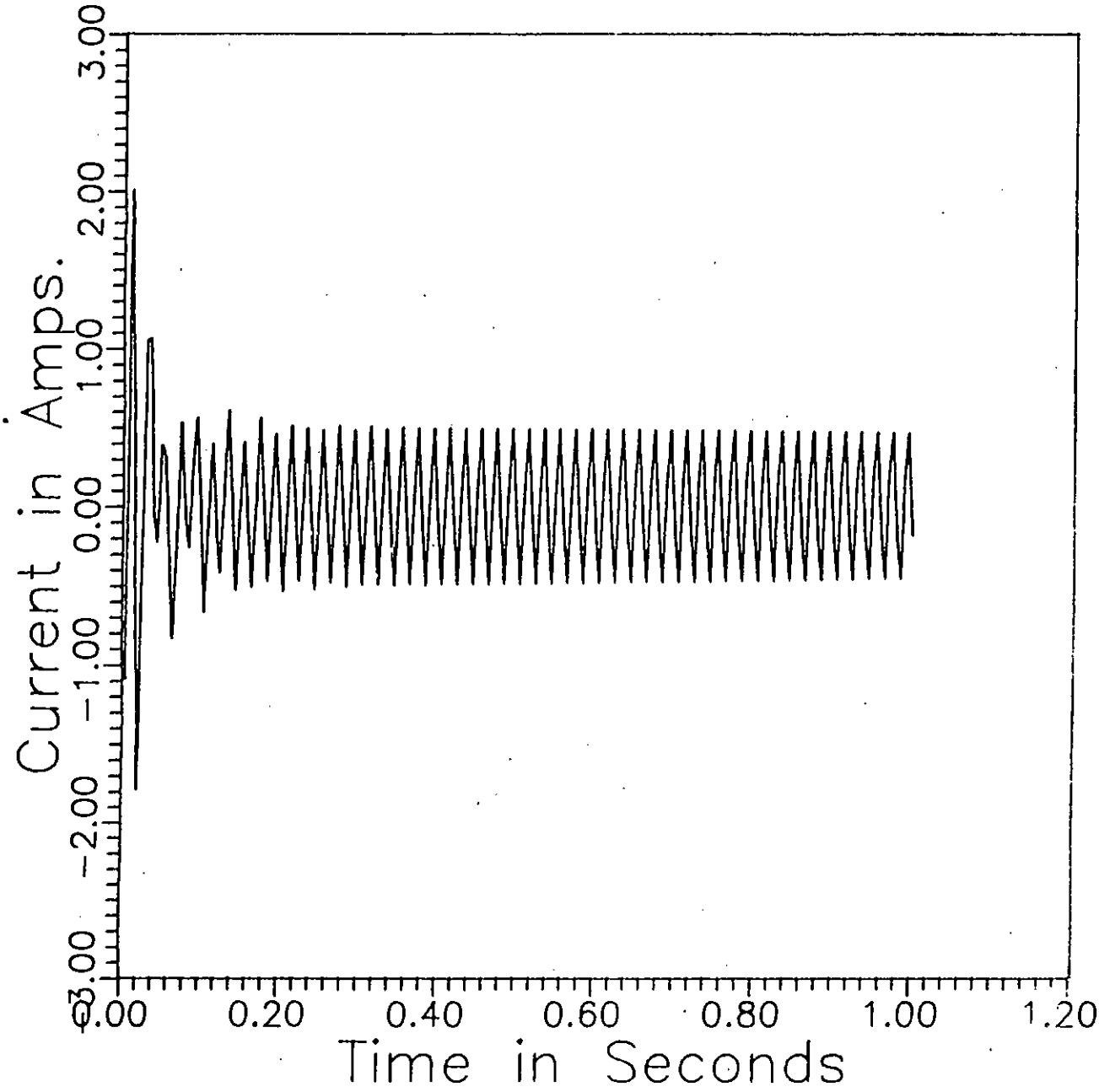

Fig. 3.2 b) Current vs. time characteristic of induction machine for sinusoidal input (time domain analysis).

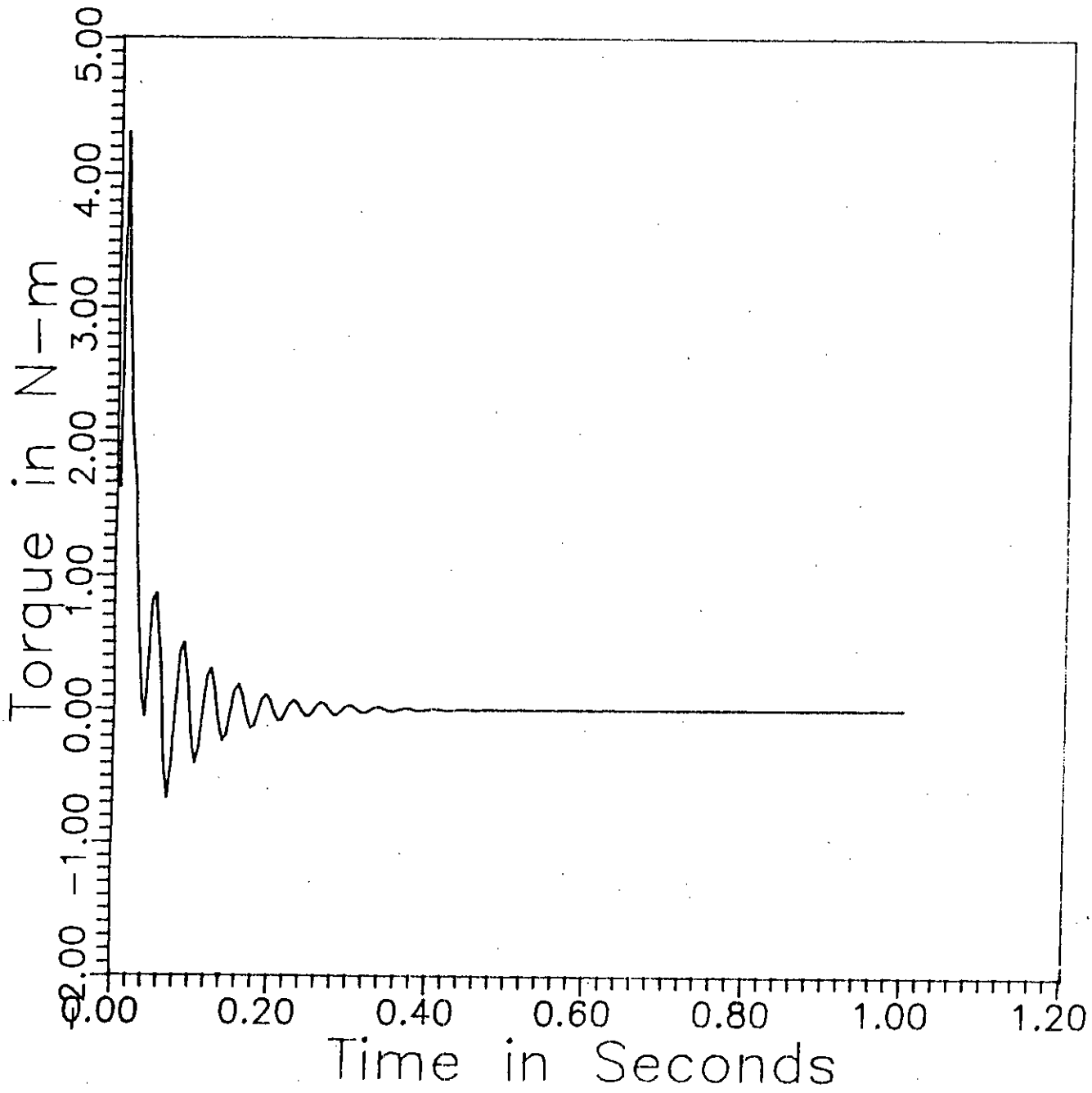

Fig. 3.2 c) Torque vs. time characteristic of induction machine for sinusoidal input (time domain analysis).

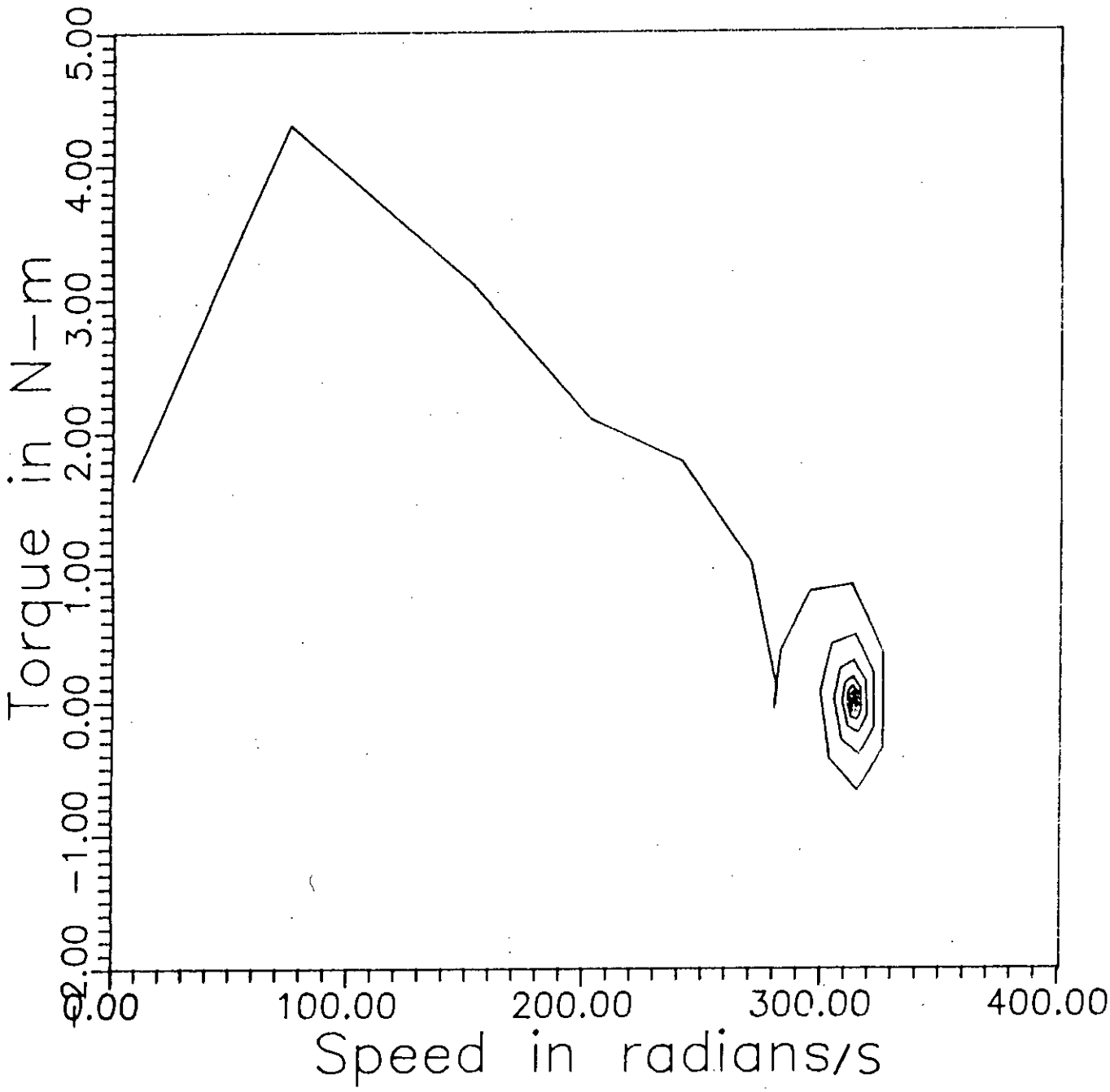

Fig. 3.2 d) Torque vs. speed characteristic of induction machine for sinusoidal input (time domain analysis).

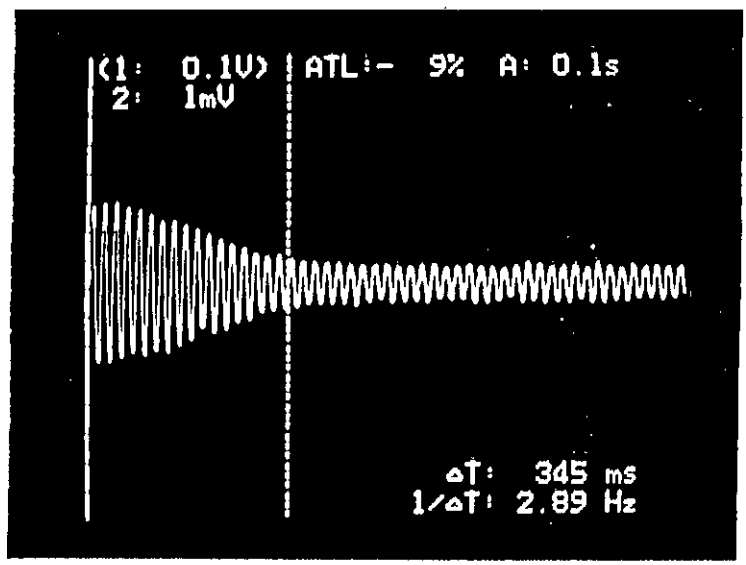

Fig. 3.3 Starting current of induction machine for sinusoidal supply ($\frac{1}{4}$hp, 400v l-l induction machine.

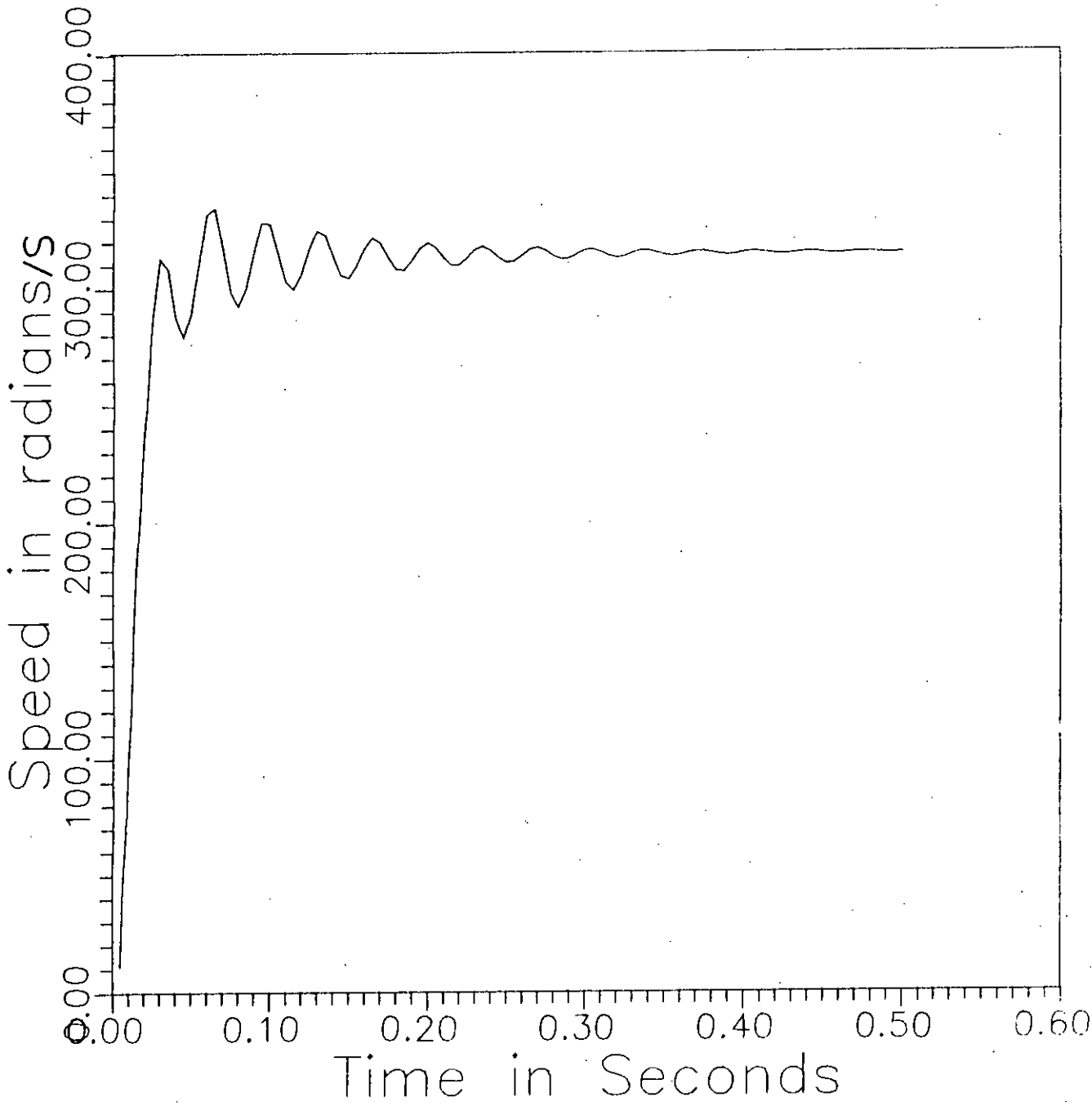

Fig. 3.4 a) Speed vs. time characteristic of induction machine for square-wave input (frequency domain analysis).

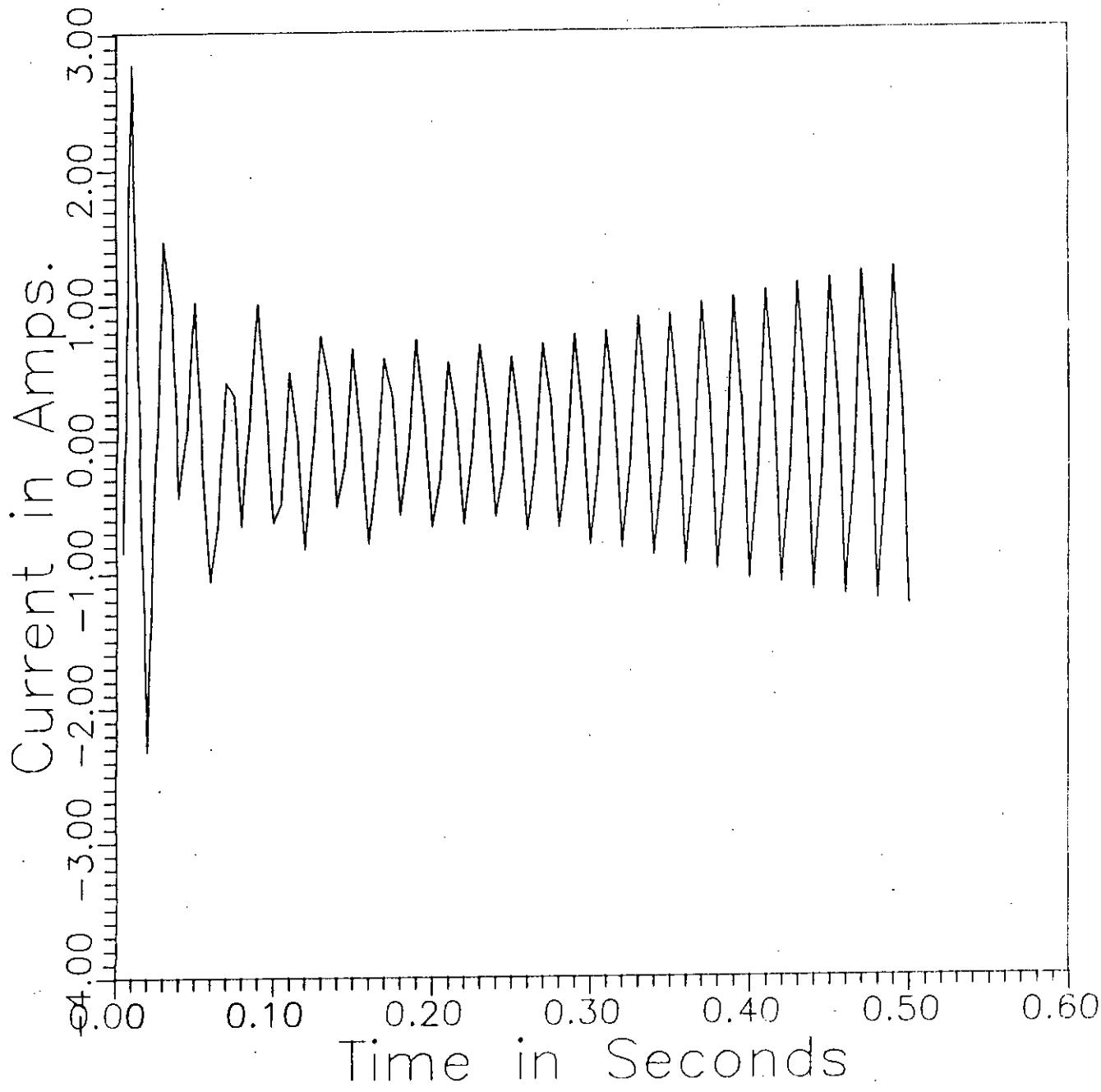

Fig. 3.4 b) Current vs. time characteristic of induction machine for square-wave input (frequency domain analysis).

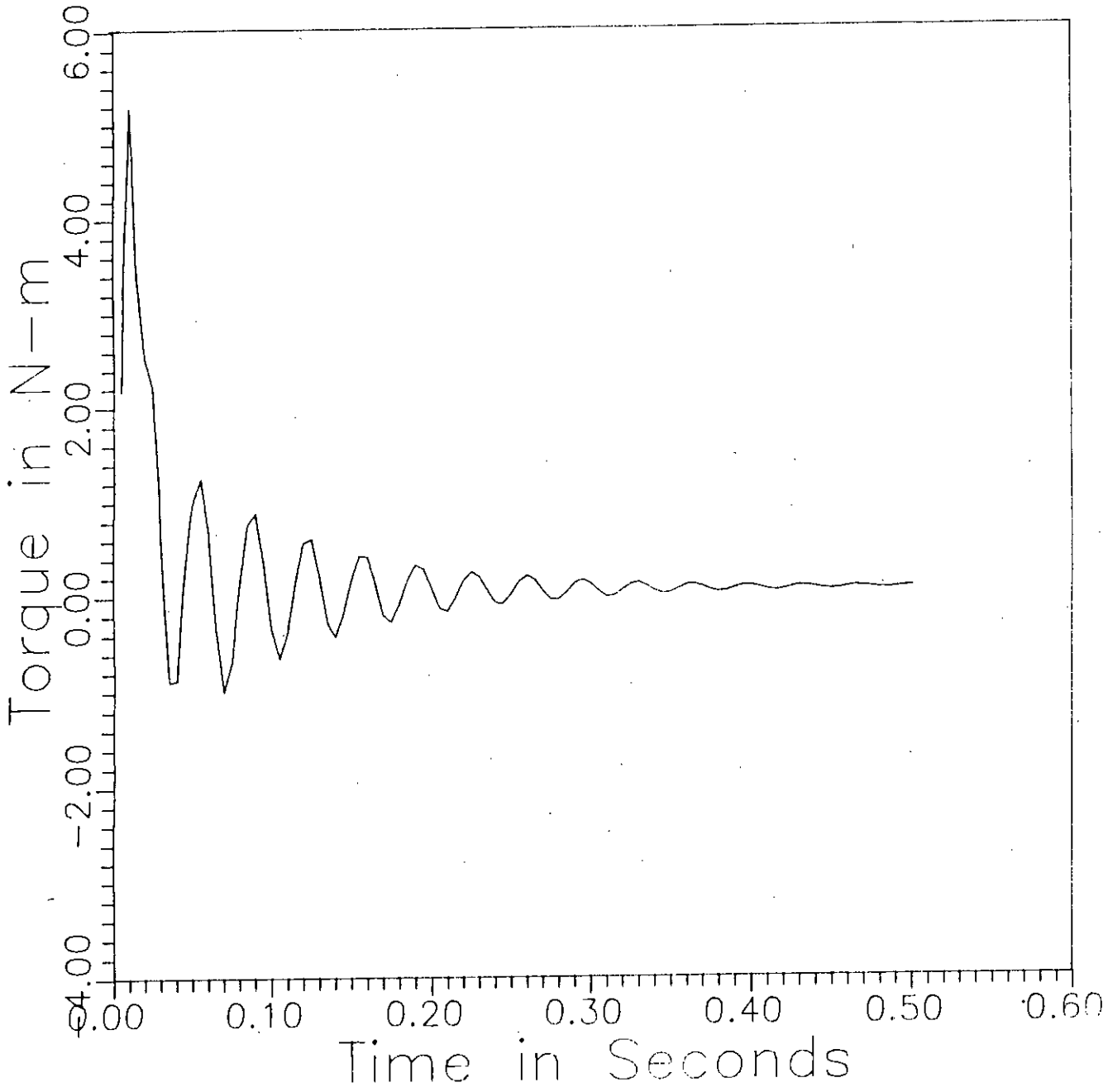

Fig. 3.4 c) Torque vs. time characteristic of induction machine for square-wave input (frequency domain analysis).

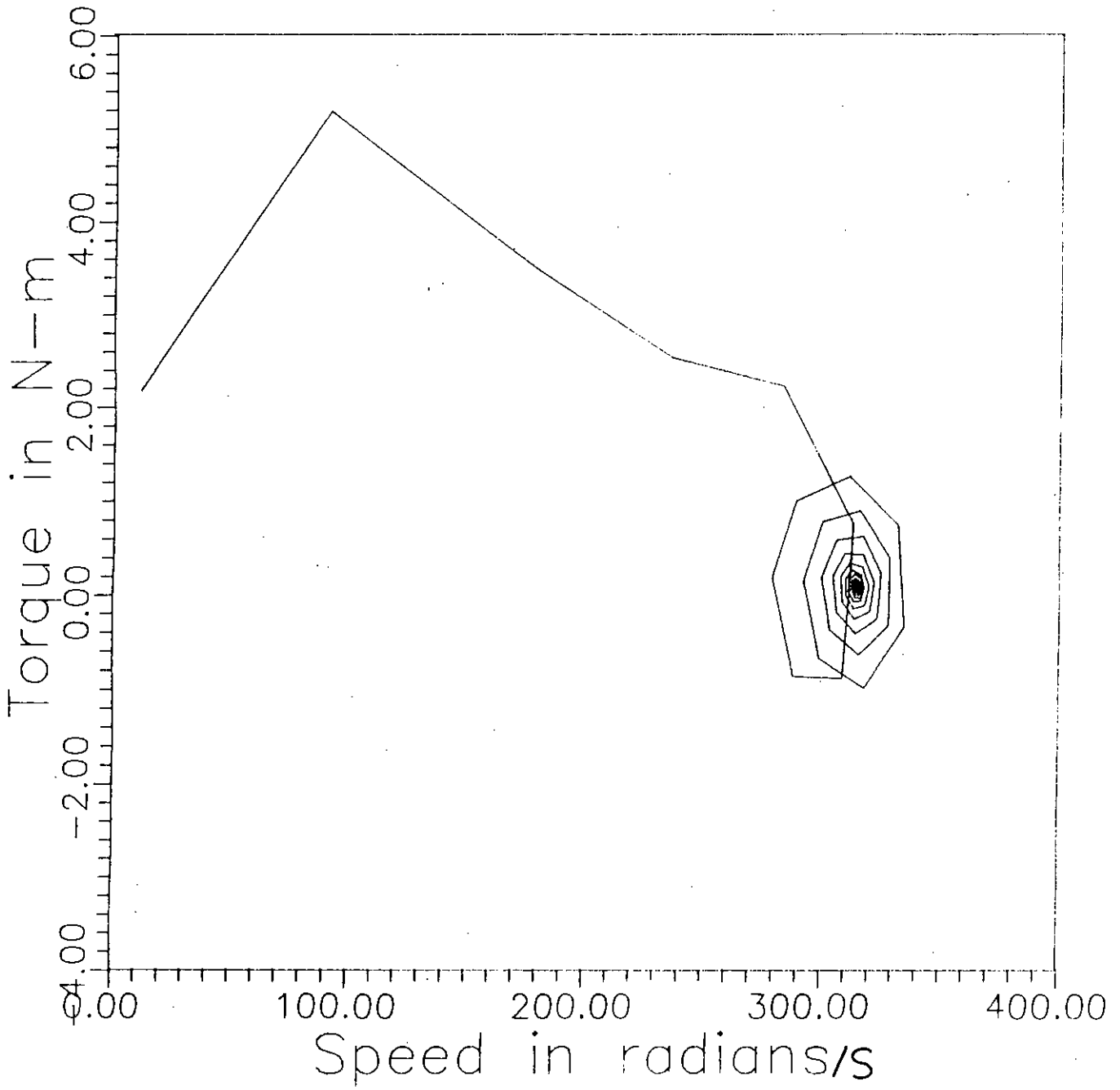

Fig. 3.4 d) Torque vs. speed characteristic of induction machine for square-wave input (frequency domain analysis).

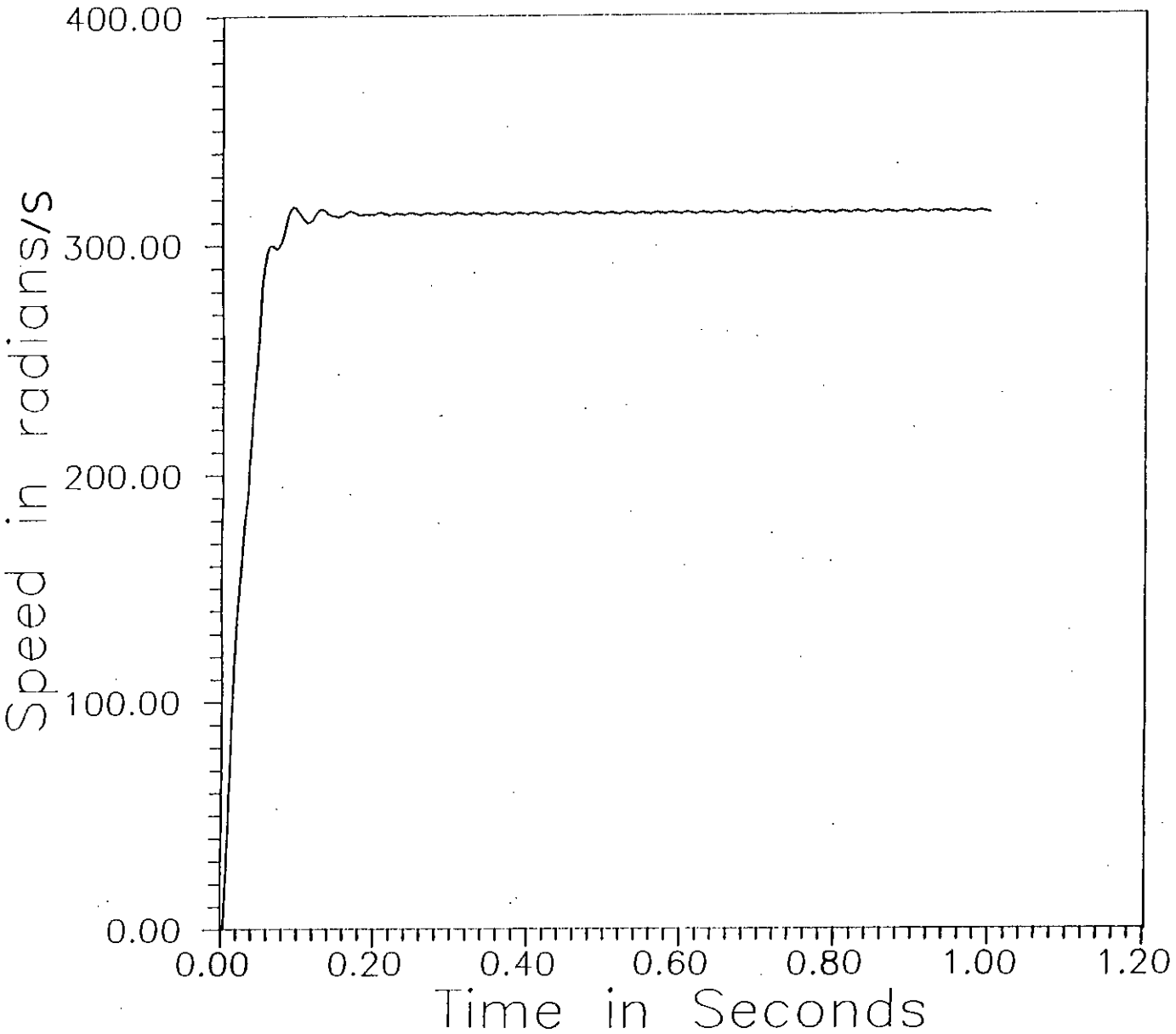

Fig. 3.5 a) Speed vs. time characteristic of induction machine for SPWM input (m=0.6, N=13) (time domain analysis).

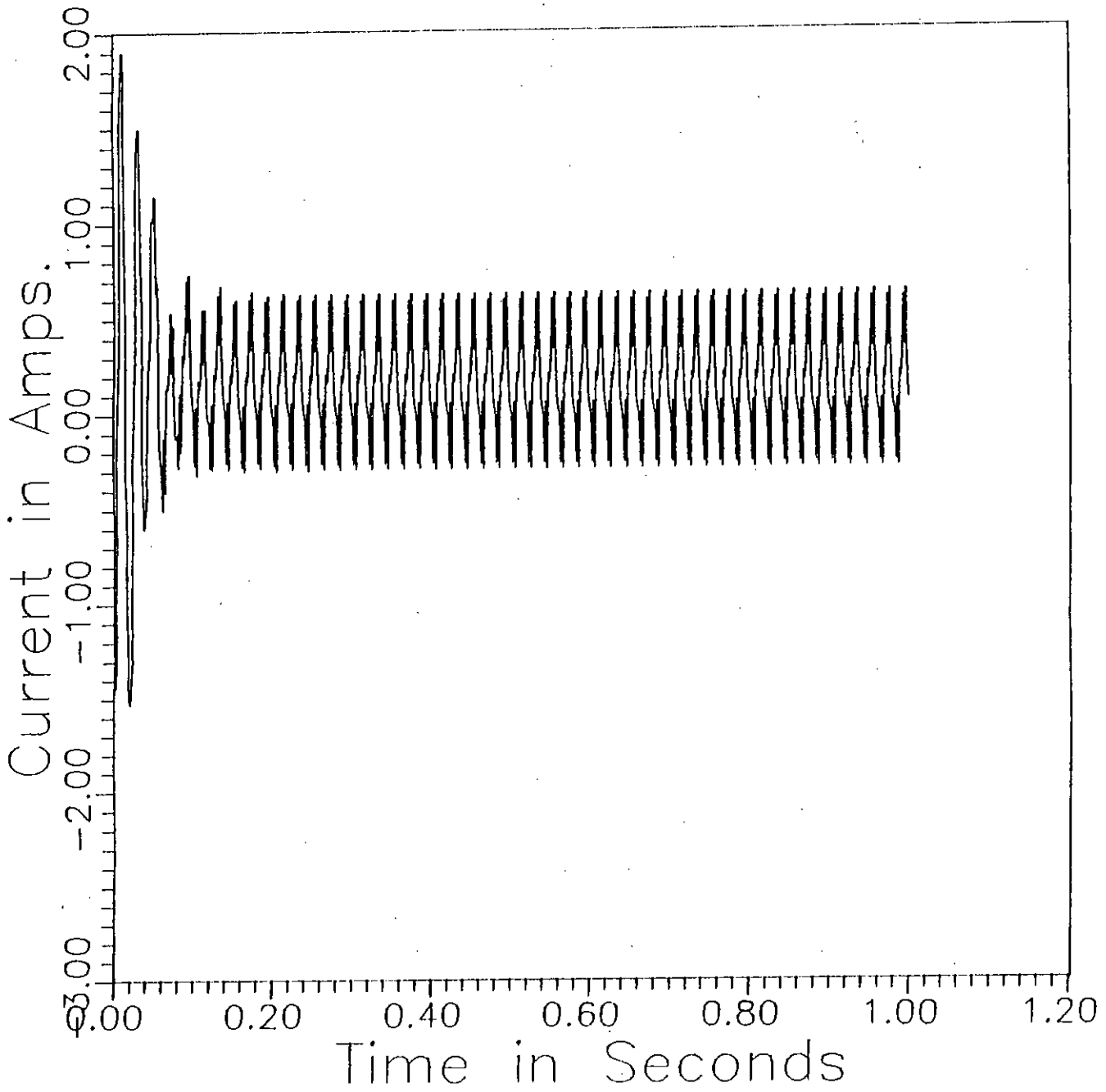

Fig. 3.5 b) Current vs. time characteristic of induction machine for SPWM input (m=0.6, N=13) (time domain analysis).

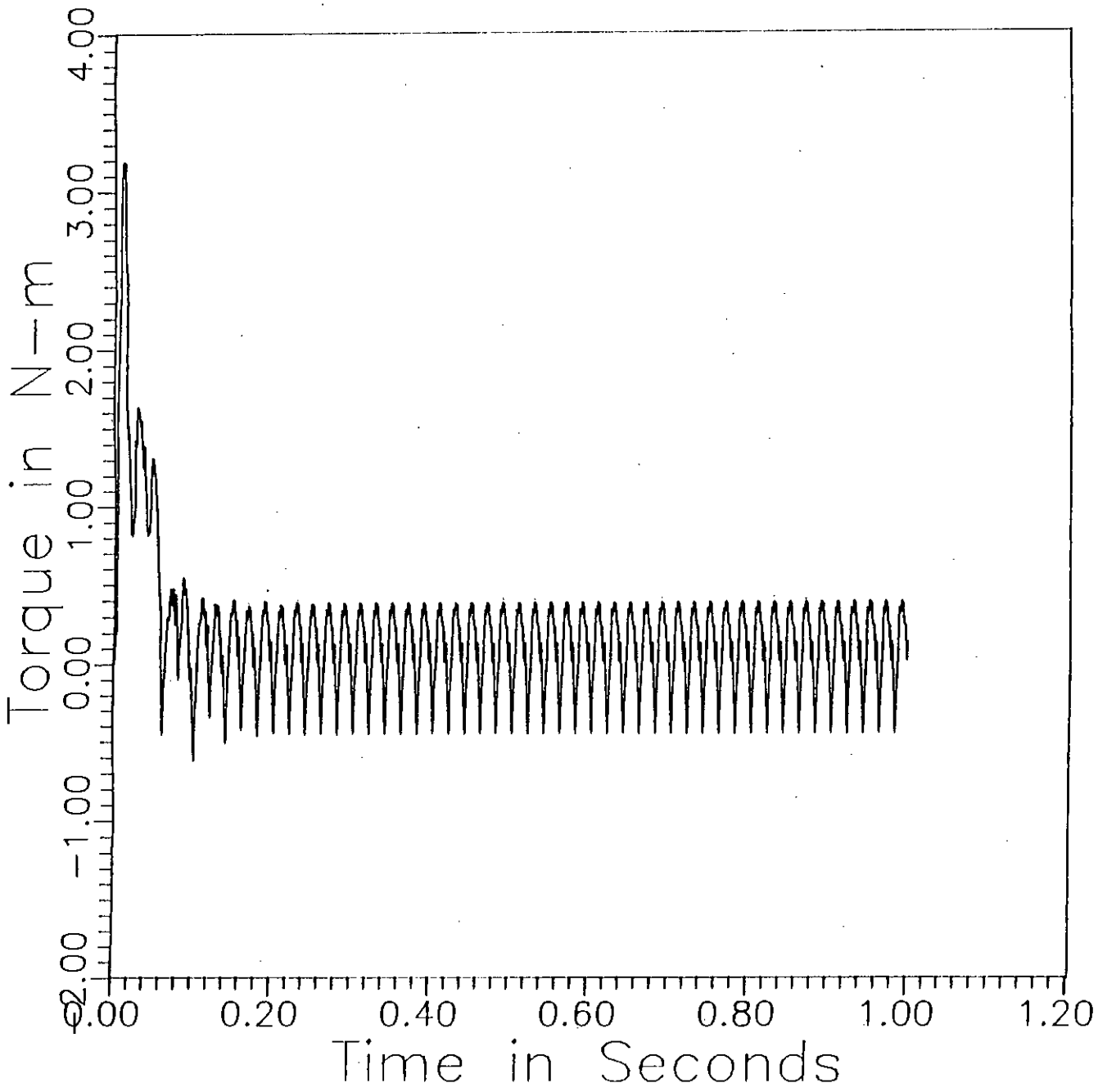

Fig. 3.5 c) Torque vs. time characteristic of induction machine for SPWM input (m=0.6, N=13) (time domain analysis).

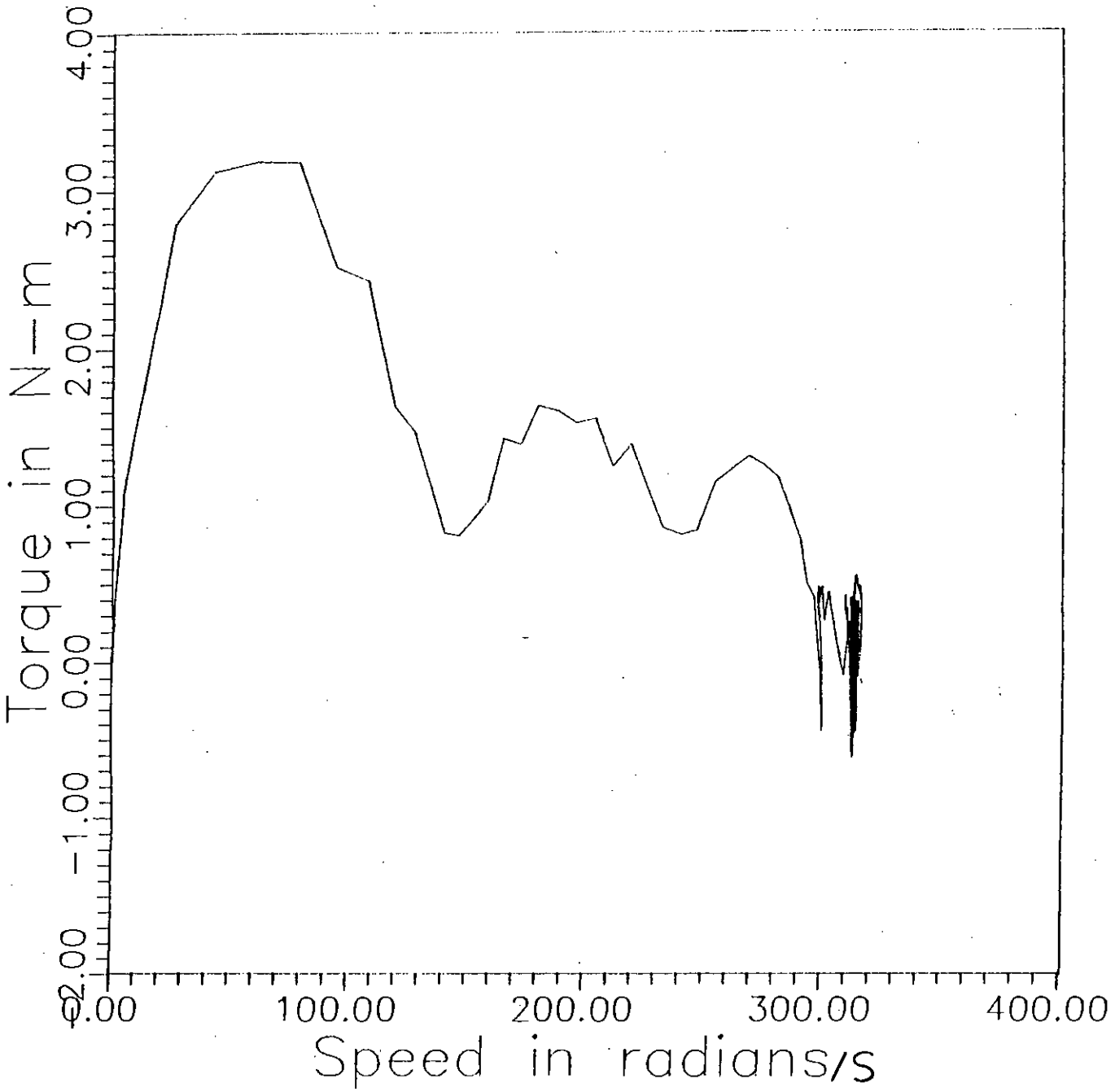

Fig. 3.5 d) Torque vs. speed characteristic of induction machine for SPWM input (m=0.6, N=13) (time domain analysis).

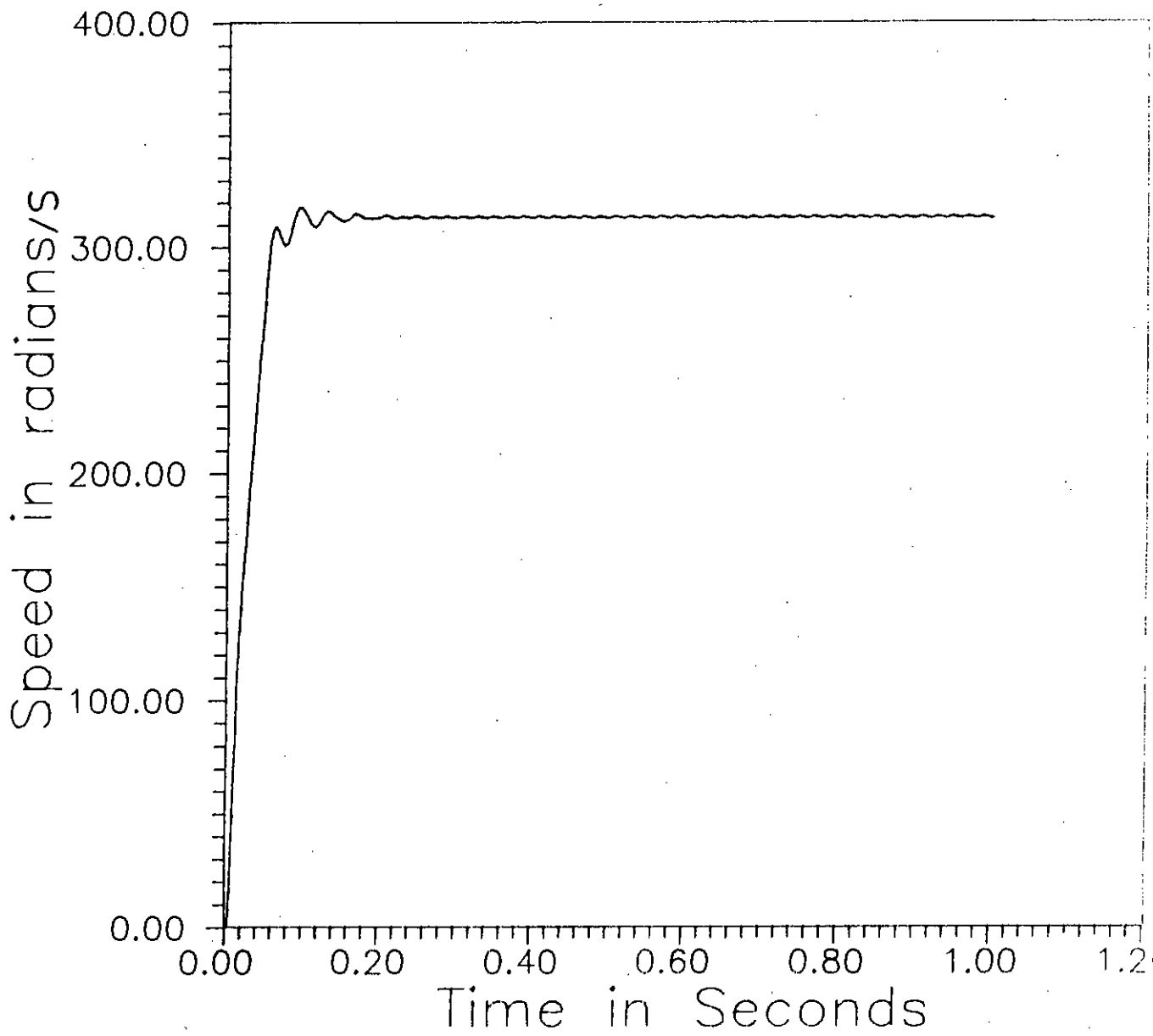

Fig. 3.6 a) Speed vs. time characteristic of induction machine for SPWM input (m=0.7, N=13) (time domain analysis).

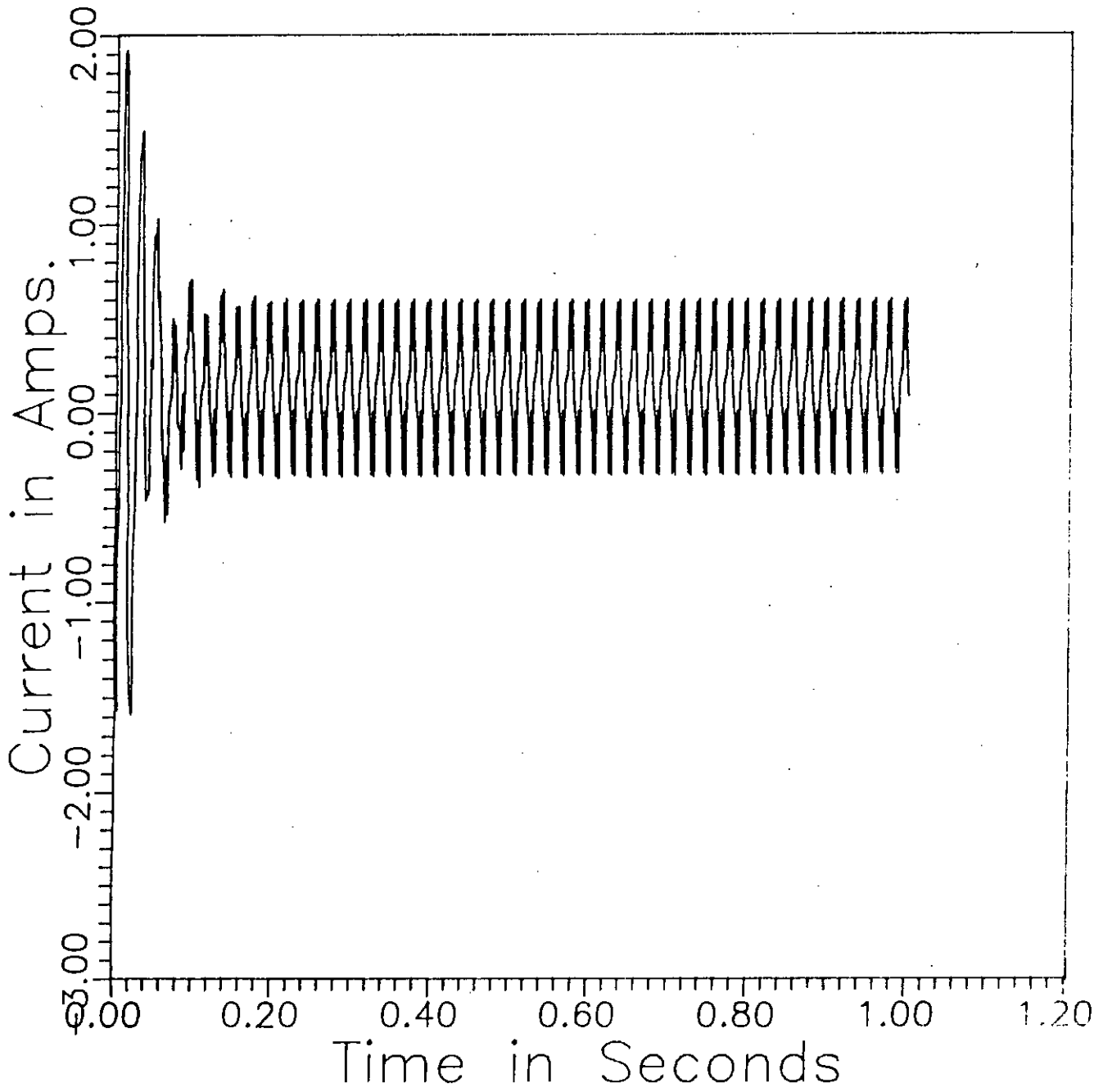

Fig. 3.6 b) Current vs. time characteristic of induction machine for SPWM input (m=0.7, N=13) (time domain analysis).

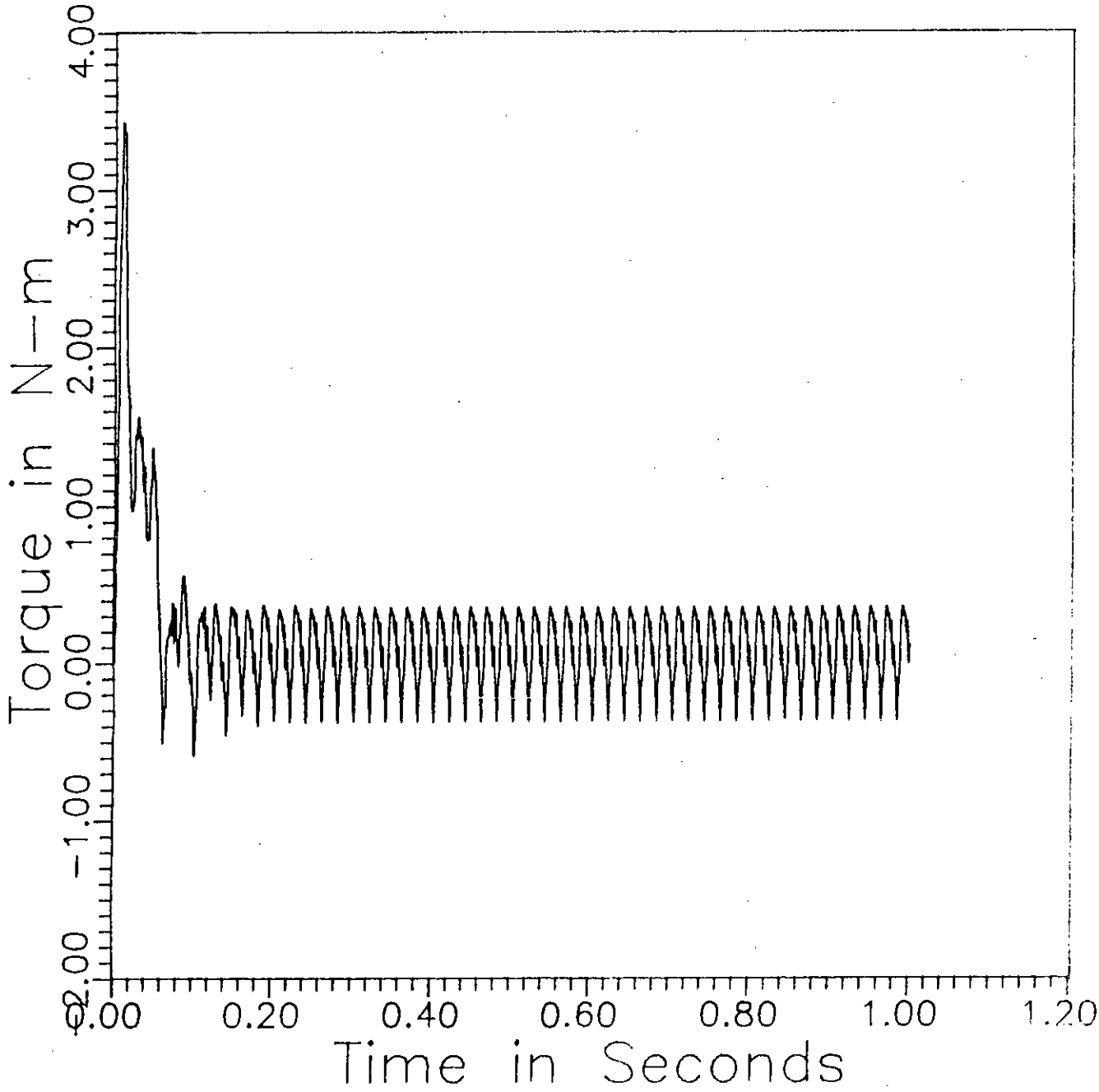

Fig. 3.6 c) Torque vs. time characteristic of induction machine for SPWM input (m=0.7, N=13) (time domain analysis).

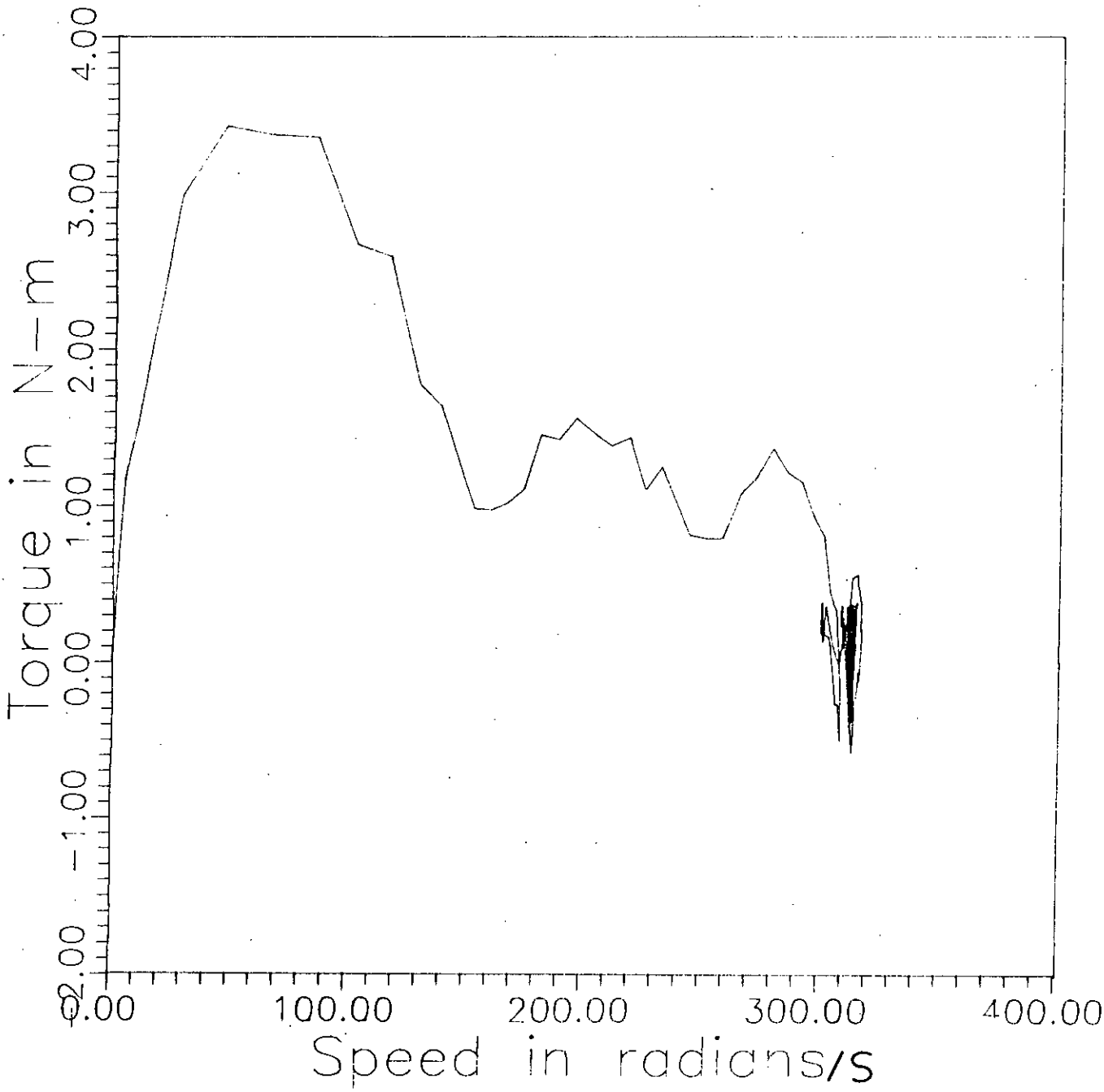

Fig. 3.6 d) Torque vs. speed characteristic of induction machine for SPWM input (m=0.7, N=13) (time domain analysis).

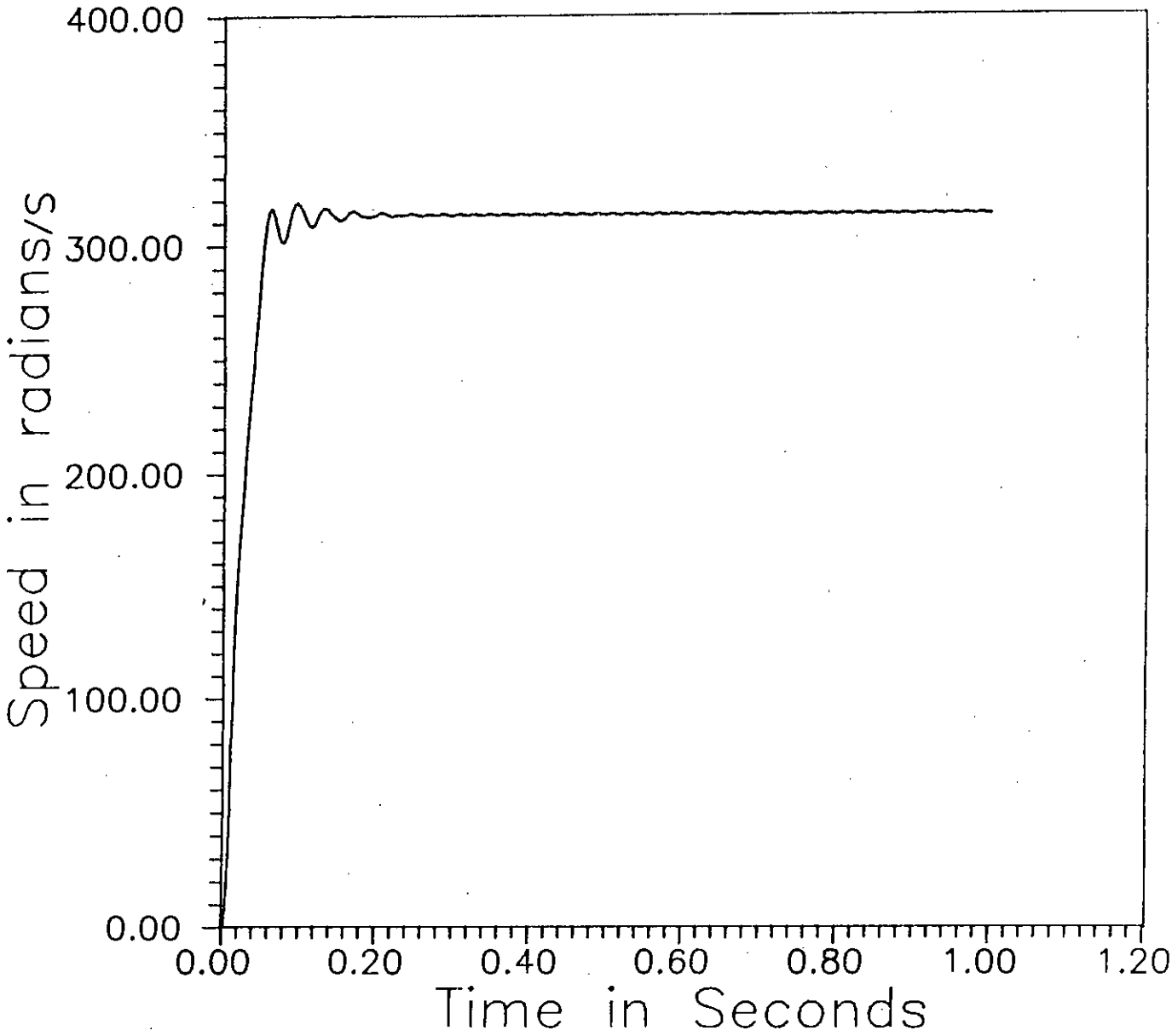

Fig. 3.7 a) Speed vs. time characteristic of induction machine for SPWM input (m=0.8, N=13) (time domain analysis).

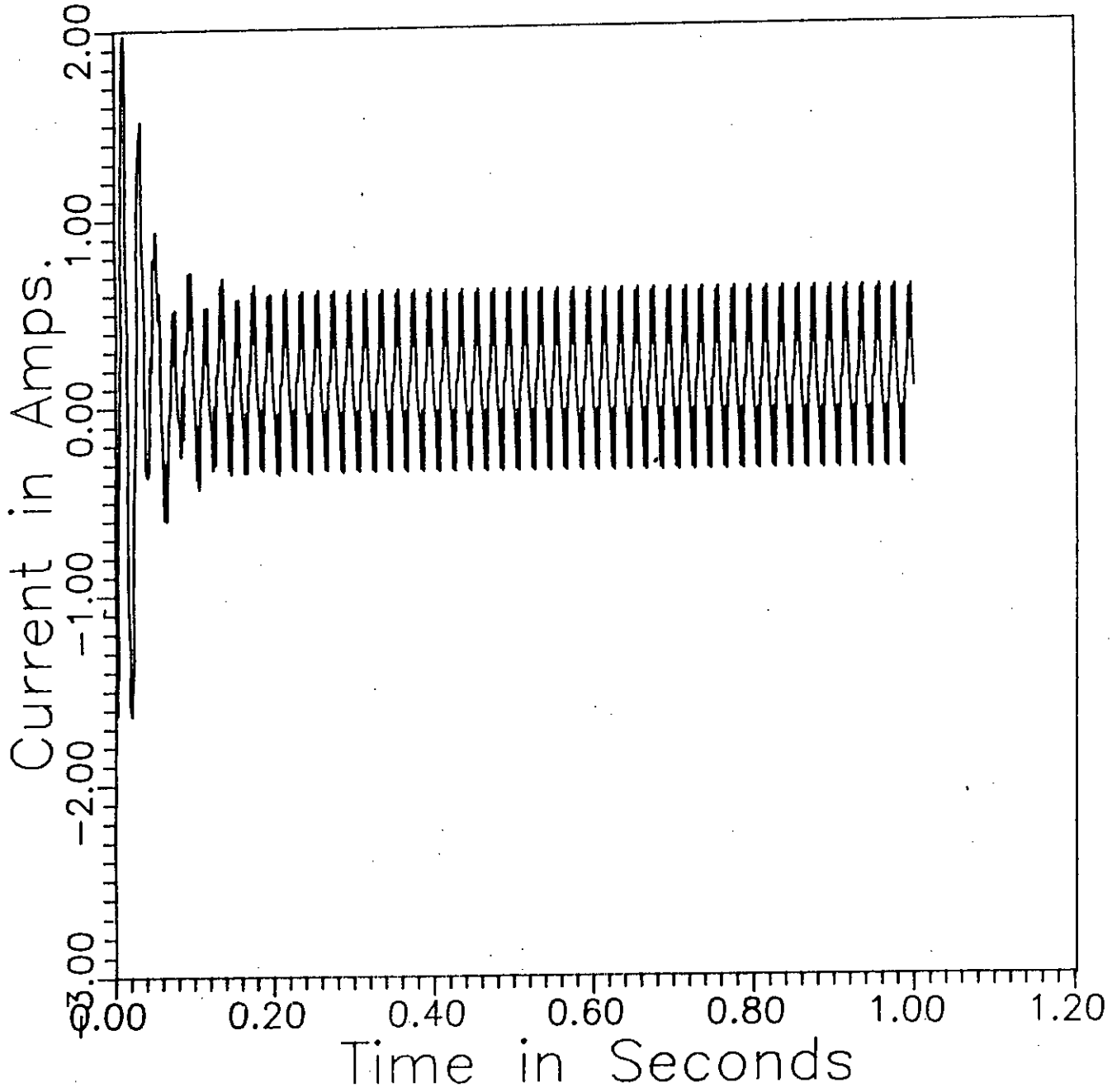

Fig. 3.7 b) Current vs. time characteristic of induction machine for SPWM input (m=0.8, N=13) (time domain analysis).

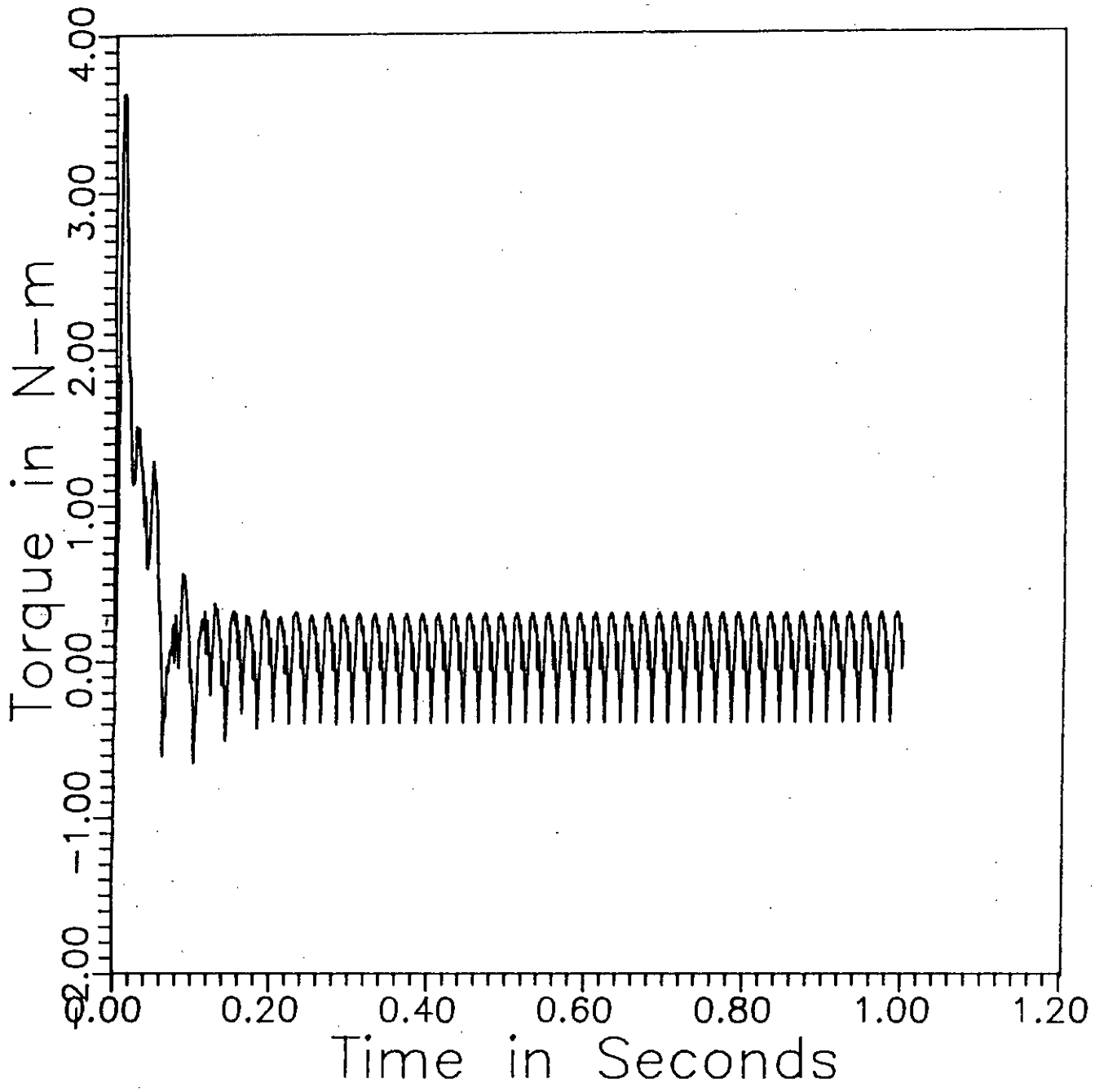

Fig. 3.7 c) Torque vs. time characteristic of induction machine for SPWM input (m=0.8, N=13) (time domain analysis).

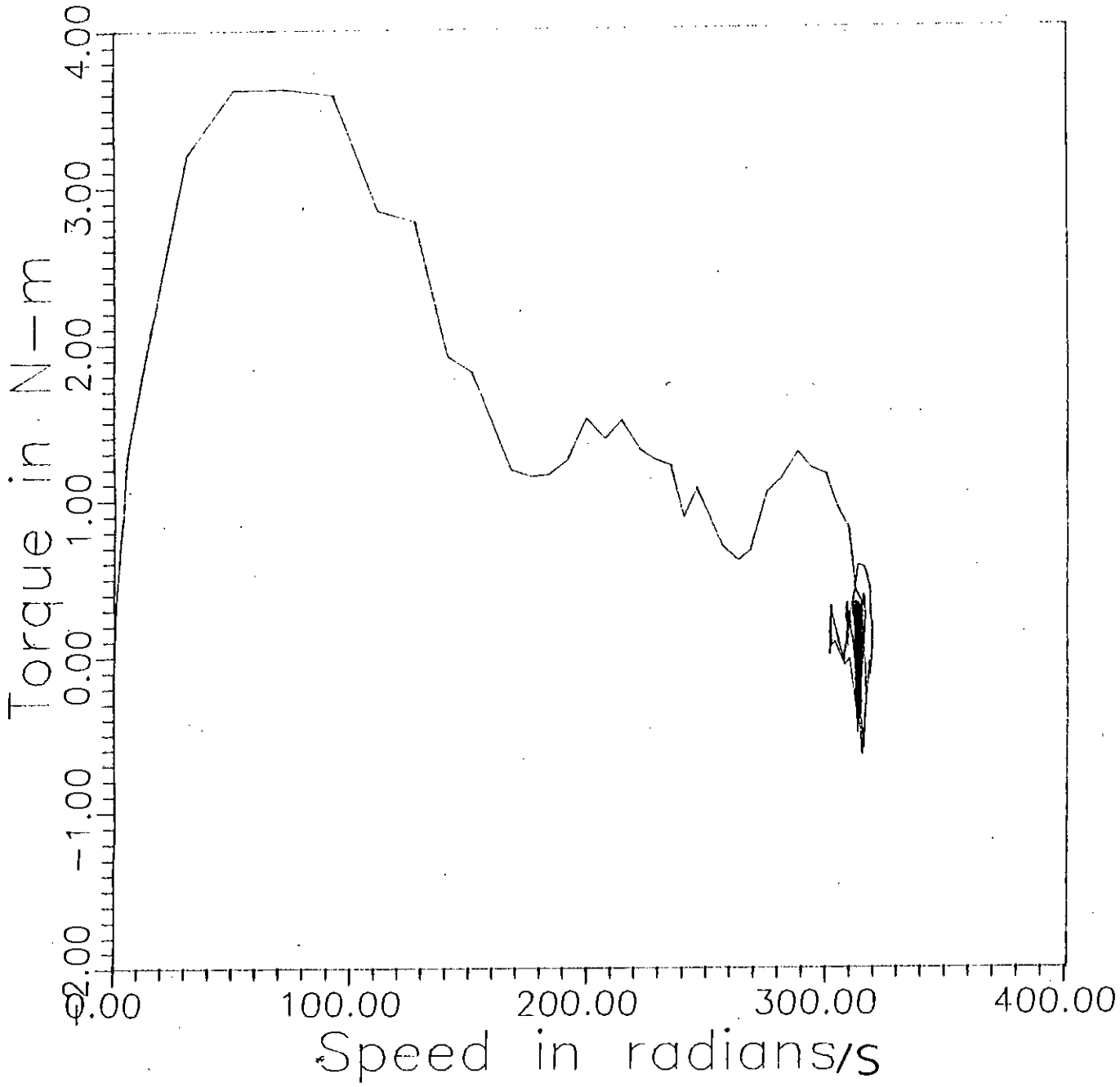

Fig. 3.7 d) Torque vs. speed characteristic of induction machine for SPWM input (m=0.8, N=13) (time domain analysis).

is due to high resistive component of the winding. The current vs. time response is experimentally verified in the laboratory on a $\frac{1}{4}$ hp machine and is shown in fig. 3.3 (Oscilloscope trace). The experimental setup is shown in appendix-C. Starting performance of the same machine was also studied for square wave and SPWM wave inverter inputs. The square wave fed motor's starting performance was studied by Fourier series analysis of input voltage and evaluation of frequency domain response of speed, current and torque. In the study, the series was truncated after 100th harmonics. During a numerical solution the computational time required was quite large (10 minutes for a 486 DX-33 MHz machine) and the results as presented in figs. 3.4 (a)-(d) are not satisfactorily accurate. This is evident from the current vs. time trace which shows that when the machine is supposed to be in steady state condition after settling from transient overshoot, the current is increasing . To overcome these difficulties, in this thesis as mentioned earlier, for PWM inverter-fed induction machine, time domain analysis was carried out. Typical results of SPWM inverter-fed machine at various modulation index are presented in figs. 3.5 (a)-(d) to figs. 3.7 (a)-(d). During solution by computers, it was observed that time required for evaluating starting performances by time domain analysis was very small [about 15-30 seconds depending on number of pulses per cycle in the same 486 DX-33MHz machine]. It is also evident from the current trace that the method is free from errors in contrast to that shown for square wave inverter-fed solution by frequency domain analysis. Since there was no approximation in the representation of voltage waveforms and parameters of the motor model are not dependent on frequency, it is believed that this method is an accurate solution technique for evaluating transient responses. However, it was unfortunate that the results could not be substantiated practically due to failure of the available SPWM inverter in BUET power electronics laboratory. It is left to the future researcher to experimentally validate the theoretical results.

The starting performance results presented in this thesis for various modulation index will in fact give an insight to designer the scope of using PWM inverter as an starter (mechanical and electrical both). It is a well known fact that during start with line voltage, normal induction machines take $7-10$ times their rated currents. Usually this high starting currents are limited by low voltage starters. PWM inverter have advantage of variation of voltage by modulation index. Hence during start, automatic control of modulation index and frequency of the modulating wave would maintain a constant v/f ratio to the motor input. The low voltage start will reduce starting current preventing electrical breakdowns and low frequency start will limit sudden speed up of the motor preventing mechanical breakdown. Characteristics of low current drawn by motors during inverter operation at reduced modulation index (causing small available voltage) are evident from current vs. time responses of figs. 3.5(b), 3.6(b) and 3.7(b).

3.5 DISCUSSIONS

Starting performance analysis of an induction motor fed from utility, square wave and PWM inverter supplies have been carried out in this thesis. For utility supply and PWM inverter fed induction machine time domain analysis have been carried out, whereas, for square wave inverter-fed machine frequency domain analysis using Fourier series technique was used. It has been shown that inverter fed induction machine performance analysis can be done if inverter voltages can be represented in time domain. Such analysis are free from truncation error of frequency domain analysis arising from truncation of Fourier series. The computational time required in time domain analysis of inverter-fed machine is less compared to frequency domain analysis. Starting performance analysis can easily be extended to evaluate

steady state performance of the machine by setting time derivatives in machine equations zero. Also PWM inverter can be considered as automatic starter, as well as speed controller. Further investigation into these areas may be the subject of future studies.

CHAPTER 4

CONCLUSIONS

4.1 CONCLUSIONS

Analyses of inverter-fed ac machines in the past were based on Fourier series analysis. In the frequency domain analysis, the accuracy of performance predictions are limited the by number of terms of Fourier series. Fourier series method also fails to detect subharmonics in PWM wave. These subharmonics are not multiple of fundamental frequency and appear in PWM waves. As a result the PWM inverter waveforms are prone to presence of subharmonics which cannot be determined by ordinary Fourier series method. In this thesis induction motors starting response has been studied using time domain analysis of motor and inverter voltage equations. Since inverter voltages are defined precisely in time domain, it eliminates the errors encountered in frequency domain analysis. Time domain analysis of PWM waveforms have been performed from knowledge of switching points of modulated wave. To make the study comprehensive, a complete study of PWM inverter waves

have been made through synthesis and harmonic analysis by FFT. Swithcing points of PWM waves were determined by a newly proposed transcendental equation and were used in waveforms definition for harmonic analysis. Results of this harmonic analysis provides selection criterion for modulation index and carrier frequency during the operation of the inverter. The results may also be used for frequency domain motor performance analysis if necessary. In this thesis frequency domain analysis has been carried out for square wave inverter-fed induction motor for comparison purpose only. The frequency domain motor's starting performance study has proved that the method is inaccurate and computationally time consuming. Subsequently a time domain analysis method of induction motor fed from PWM inverter voltages has been presented in this thesis mainly with theoretical results. Experimental results could not be made available due to failure of the PWM inverter in the power electronics laboratory. The time domain analysis presented in this thesis to find transient inverter-fed motor performance are more accurate and requires less computational time than its counterpart, the conventional harmonic analysis method.

Start up performance study of induction motors are important to find ways to limit their electrical and mechanical stresses. Static inverter supply may provide means to mitigate both stresses by limiting initial voltage and frequency of the motor input thereby reducing motor breakdowns due to these two reasons. Also inverters during their normal operations allow motors to adjust to load by variation of speed and hence maintain desirable efficient operation of motors and appliances. Results of waveform synthesis, harmonic analysis of inverter waves and starting behavior of line voltage of an inverter fed induction machine have been presented in the thesis.

4.2 RECOMMENDATIONS FOR FUTURE WORK

In this thesis practical results could not be incorporated due to reasons already stated. In future studies a detailed experimental verification can be undertaken. There are several other modulation techniques and some of them may prove advantageous to presently used SPWM technique. Hence future research work may include study of inverter fed induction machines using these techniques. As suggested in this thesis, inverters may be advantageously used as electrical and mechanical starter for an induction machine. Future investigation may include automatic v/f control in their theoretical and practical studies. Also transient during operation and the stability analysis of inverter fed induction machines can be incorporated. Such study may include closed loop facilities of inverter-fed machines such as hysteresis current control and flux control method in the performance study of closed loop control schemes.

REFERENCES

[1] Van Wyk, J.D., Skudelny, H.-ch. and Muller-Hellmann, A.,'Power electronics, control of the electromechanical energy conversion process and some appliations', IEE Proc., vol. 133, part B, no.6, November 1986, pp. 369-399

[2] Choudhury, M.A., 'An analysis of Delta moulated inverters with applications to submersible motors', Ph.D. dissertation, Memorial University of Newfoundland, Canada, December 1988

[3] Legg, L.V., 'Submersible pump selection, part-1', Oil and Gas Journal, July 9, 1979, pp. 127-131

[4] Legg, L.V., 'Submersible pump selection, part-2', Oil and Gas Journal, July 23, 1979, pp. 60-63

[5] Legg, L.V., 'Submersible pump selection, part-3', Oil and Gas Journal, August 6,1979, pp. 95-102

[6] Legg, L.V., 'Submersible pump selection, part-4', Oil and Gas Journal, August 27, 1979, pp. 105-110

[7] Hoestenbach, R.D., 'Large volume high horsepowerr submersible pumping problems in water source well.', Journal of Petroleum Technology (JPT), October, 1982, pp. 2397-2400

[8] Anderson, H.H., and Crawford, L., 'Submersible pumping plant.', Proc. IEE, November 1959, pp.127-140

[9] Anderson, H.H., 'Modern developments in the use of large single entry centrifugal pump.', Proce.IMC, 1955, vol. 169, pp.141-152

[10] Coltharp, E.D., 'Submersible electrical centrifugal pumps.', JPT, April 1984, pp.645-652

[11] King, K.G., 'Variable frequency thyristor inverters for induction motor speed control', Direct Current, February, 1965, pp. 125-132

[12] Kirnick, A. and Heinrick, 'Static inverters with neutralization of harmonics', AIEE transactions, vol.81, May, 1962, pp.59-68

[13] Turnbul, F.G., 'Selected harmonic reduction in static dc-ac inverterrs', AIEE transactions, vol. 83, July, 1964, pp.374-378

[14] Schonung, A. and Steinmmler, H., 'Static frequency changer with subharmonic control in conjunction with variable speed ac drives', Brown Boveri Review, August/September, 1964, pp. 555-577

[15] Nonaka, S. and Okada, H., 'Methods to controls pulse width of three pulse inverters', Journal of IEE, Japan, vol.86, July, 1972, pp.71-79

[16] McMurray, W., ' A comparative study of symmetrical three phase circuits for phase controlled ac motor drives', IEEE trans. on IA, vol. IA-10, May/June,1974, pp. 403-411

[17] Lipo, T.A., ' The analysis of induction motors with voltage control by symmetrically triggered Thyristors', IEEE trans. on PAS, vol. PAS-90, April/May,1971, pp. 515-525

[18] Locke, R., 'Design and application of industrial solid state contractors', IEEE/IAS conference record, 1981, pp.501-505

[19] Dubey, S., 'Classification of commutation methods', IEEE/LAS conference record, 1981, pp. 895-909

[20] Mapham, N.W., 'The classification of SCR inverter circuits', IEEE international convention record, part 4, 1964, pp. 99-105

[21] Bird, B.M. and King, K.G. 'An introduction to power electronics', Willey, 1983

[22] Gyo, C. and Park, S.B., 'Novel six step and twelve stepped CSI with dc side commutation and energy rebound', IEEE trans. on LA, trans, September/October, 1981 pp. 524-530

[23] Bose, B.K., 'Adjustable speed ac drives: A technological status review', Proc. IEEE, vol. 70, no.2, February, 1982, pp. 116-135

[24] Kliman, G.B, 'Harmonic effects in PWM inverter induction motor drives', IEEE/LAS conference record, 1972, pp. 783-790

[25] Klingshrin, E.A. and Jordon, H.E., 'Polyphase induction motor performance and losses on non-sinusoidal voltage source', IEEE trans. on PAs, pas-87, NO.3 mARCH/1968, PP.624-631

[26] Robertson, S.T.D. and Hebber, K.M., 'Torque pulsation in induction motorswith inverter drives', IEEE trans. on LA, March/April, 1971, pp.318-323

[27] Krause, P.C. and Thomas, C.H., 'Simulation of symmetrical induction machinery', IEEE trans. on PAS, vol. PAS-84, 1965, pp. 1038-1053

[28] Krause, P.C., and Lipo, T.A., 'Analysis and simplified representation of a

rectifier inverter induction motor drive', IEEE trans. on PAS, vol-PAS, no 88, May, 1969, pp. 588-596

[29] Kuntz, G., 'Advantage of submersible motor pumps in deep sea mining' - JPT, December, 1980, pp.2241-2246

[30] Smith, J.R., Stronach, A.F. and Goodman, K.A., 'Prediction of dynamic response of marine systems incorporating induction motor propulsion drives', Proc. IEE, vol. 127, pt. B, no. 5, September, 1980, pp. 308-315

[31] Bowes, S. R.,'New sinusoidal pulse width modulation inverters', Proc. of IEE, vol. 122, pt. B, no. 11, 1975, pp. 1279-1285

[32] Dickinson W.D., ' Micro computer control of variable drives using submersible motor as an instrument', IEEE trans. on IA, vol. IA-18, no. 4 July/August, 1982, pp. 373-381

[33] Alcock, D.N., 'The equipment for the economics of variable flow well pumping', IEEE trans. on Industrial Applications (LA), vol. LA-16, no.1, Jan./Feb., 1980, pp. 144-153

[34] Yaucey, F.R. and Khanis, A.G., 'Submersible pumping Long Beach unit of East Wilmington fields. -a 17 year review.', JPT, August, 1984, pp. 1321-1325

[35] Way, A.R. and Hewett, M.A., 'Engineers evaluate the North Sea field', Petroleum Engineers Interrnational, July, 1982, pp. 92-112

[36] Motierrman, S.J., 'Accelerated development planned for the Beatrice.', Petroleum Engineers International, January, 1970, 1979, pp.66-69

[37] Kilvington, L.J. and Gallivan, J.D., 'Beatrice Field: Electrical submersible pump and reservoir performance, 1981-183.', JPT, November, 1984 pp.1934-1942

[38] Ryall, M.L. and Grant, A.A., 'Development of ne high reliability down hole pumping system for large horsepower', JPT, November, 1983, pp.1707-1718

[39] Kuntz, G., 'The technical advantage of submersible motor pumps in deep sea technology and the delivery of manganese nodules.', Ocean Technology Conference (OTC) record, 1979, pp.85-91

[40] Ogawa, Kitno, S., and Takahashi, M., 'Commutatorless propulsion for deep sea submersible research vessels', Report on the commutatorless propulsion motors of ocean engineering R and D division, Kawasaki Heavy metal Industries Ltd, Japan, 1979

[41] Kuntz, G., 'Submersible motor pumps, a modern solution for offshore and on-shore technology.', paper C-129/76, pump and compressor for offshore oil and gas conference, University of Aberdeen, June 29 - July 1, 1976

[42] Alcock, D.N., 'Application of variable frequency drives to deep well submerrsible pumps', Petroleum Engineers International, March 15, 1980, pp. 37-44

[43] Alcock, D.N., 'Production operration of submerrsible pump with closed loop adjustable speed control', IEEE trans. on LA, vol. LA-17, no.5, Sept./Oct., 1981, pp.481-489

[44] McClung, W.J., and Johnson, J.A., 'Electric submerrsible pump applications

and operration in small opne-hole completion', JPT, November, 1983, pp. 1719-1729

[45] Baily, M.C., 'ESP - electrical submerrsible pumps, part-1', Petroleum Engineers International, August/1982, pp. 98-103

[46] Baily, M.G., 'ESP - electrical submersible pumps, part-3', Petroleum Engineers International, November, 1982, pp.33-40

[47] Patel H. and Hoft R., ' Generalized technique of hermonic elimination and voltage control of thyristor inverters , part-1', IEEE trans. on IA, vol. IA-9, May/June, 1973, pp. 310-317

[48] Bozdzer, A. and Bose, B.K., 'Three phase ac power control using power transistor', IEEE trans. on LA, vol. LA-12, September/October, 1976, pp. 490-505

[49] Mathlab software, Mathwork Inc. U.S.A.

[50] Bose, B. K.,'Power electronics and ac drives', Prentice Hall, 1986

99

APPENDIX A

Machine Parameters

The machine parameters obtained by different tests for the machine under test are given below

$X_s = 17.55\ \Omega$/phase
$X_r = 17.55\ \Omega$/phase
$X_m = 455.19\ \Omega$/phase
$r_s = 40\ \Omega$/phase
$r_r = 45.2\ \Omega$/phase

$L_s = 0.0559$ H/phase
$L_r = 0.0559$ H/phase
$L_m = 1.45$ H/phase

$L_1 = L_s + L_m = 1.505$ H/phase
$L_2 = L_r + L_m = 1.505$ H/phase

Turns ratio = 100 : 1

APPENDIX B

Program Flowchart

The flowchart of computer program to simulate the transient response of machine is shown below.

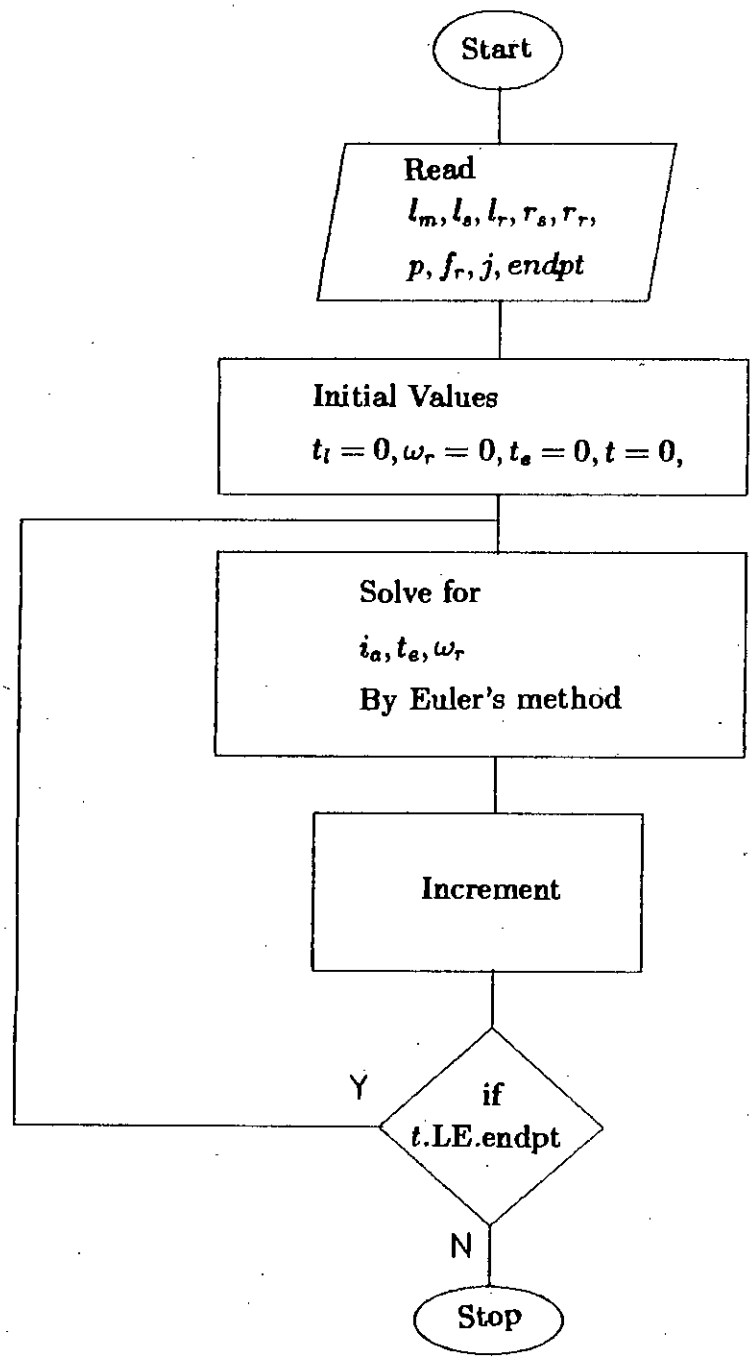

APPENDIX C

Experimental Setup

The experimental setup of the test done in laboratory is shown below.